

NEW SOLAR RADIATION PRESSURE MODELS FOR GPS SATELLITES

Y. Bar-Sever, D. Jefferson, and L. Remans

Jet Propulsion Laboratory/California Institute of Technology

The mismodeling of solar radiation forces is currently the largest error source in the precise orbit determination of GPS satellites. Consequently, it is a dominant error source in many precise applications of the GPS, such as, geodesy, determination of Earth orientation, and low Earth orbiter tracking. We have developed a new approach to the problem of modeling the solar radiation forces on GPS satellites that significantly improves the quality of the model. The approach is aiming to replace the conventional re-launch design phase of solar pressure and heat reradiation models by a more accurate post-launch phase. The approach is also suitable for many other Earth-orbiting satellites.

The current GPS constellation of Block II and Block 11A satellites was used as a prototype for developing and validating our approach. We used the daily JPL GPS precise ephemerides over a period of 9 months to adjust a parametrized model of the solar pressure so as to obtain best fit. The resulting model proved to be significantly more accurate than the standard solar pressure model for GPS satellites (Bar-Sever, 1997). For example, 4-day orbit prediction accuracy has increased by 63% for non-eclipsing GPS satellites, and by 28% for eclipsing satellites. The new models will be made available to all IGS Analysis Centers.

References

Bar-Sever, Y. E., New and Improved Solar Pressure Models for GPS Satellites Based on Flight Data, Final Report, Prepared for Air Force Materiel Command SMC/CZSF, April 12, 1997.

A LOOK AT THE IGS PREDICTED ORBIT

J. F. Zumberge

Jet Propulsion Laboratory, California Institute of Technology
Pasadena, CA 91109 USA

SUMMARY

The quality of the IGS predicted orbit has been assessed by comparing it to the IGS final orbit. For each satellite and day during the 6-week period beginning November 16, 1997, the 3-D rms difference over the day between the predicted and final orbit was computed. The distribution of this quantity is shown in Figure 1. Each count corresponds to one satellite and one day.

The median 3-D rms is 57 cm, which is approximately a factor of seven smaller than the corresponding number for the broadcast ephemeris. However, the high-end tail in Figure 1 – 8.5% are above 3 m – limits the use of the IGS predicted orbit. It would be beneficial to identify problematic satellites when the prediction is published.

It was found that poorly performing satellites are not well correlated with either (i) the smoothness of the broadcast ephemeris or (ii) time. There is, however, some correlation with pm, as indicated in Figure 2. For example, predictions of prn14 and prn23 are consistently poor. Although not indicated in Figure 2, the eclipse status is also a consideration, at least for some satellites. For example, the predictions for prn10 are typically worse when that satellite is in shadow.

With additional work, one might be able to develop a not-too-complicated algorithm using prn and shadow/sun status to flag many of the problematic satellite-days in the IGS predicted orbit. To realize the full potential of the IGS predicted orbit, however, one probably needs to use near-real-time data to flag the outlier satellites and days.

Acknowledgment The research described here was carried out by the Jet Propulsion Laboratory, California Institute of Technology, under a contract with the National Aeronautics and Space Administration.

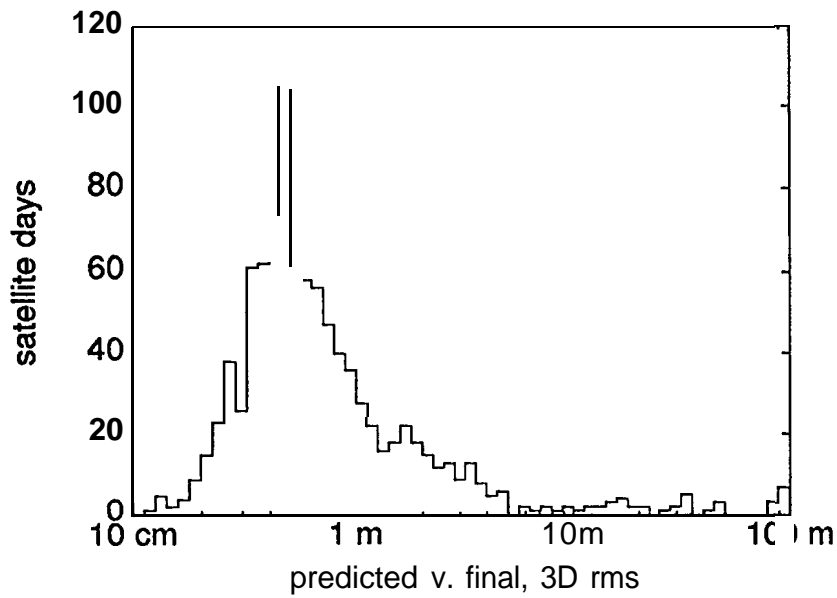


Figure 1: Distribution of the daily 3D-rms difference between the IGS predicted and final orbits.

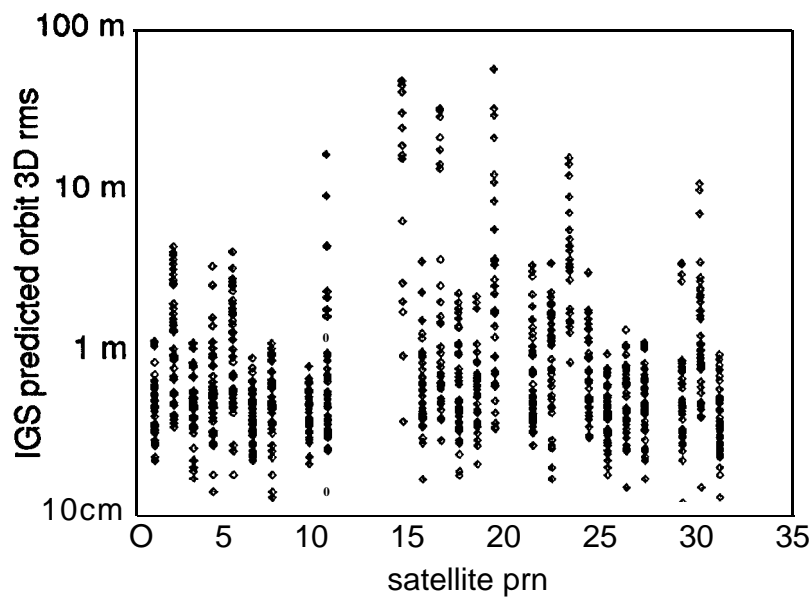


Figure 2: Correlation of predicted performance with pm.

REAL TIME EPHEMERIS AND CLOCK CORRECTIONS FOR GPS AND GLONASS SATELLITES

M.M. Romay-Merino, J. Nieto-Recio, J. Cosmen-Shortmann, J.R. Martin-Piedelobo
GMV, Isaac Newton 11, P.T.M. Tres Cantos, E-28760 Madrid, Spain

ABSTRACT

Algorithms computing clock and ephemeris corrections for GPS and GLONASS satellites as the basis for GIC (Ground Integrity Channel) and WAD (Wide Area Differential) services constitute one of the most important part of the EGNOS (European Geostationary Navigation Overlay Service) system. Using the GPS/GLONASS broadcast data it is not possible to compute the user position with the desired accuracy and integrity for high demanding users, such as aeroplanes. To achieve the desired user positioning requirements some corrections should be applied to the broadcast data. These corrections must be computed in real time, and they will be transmitted to the user via a geostationary satellite. Corrections can be divided in ephemeris or orbit corrections, satellite clock corrections, and ionospheric corrections. These corrections shall be valid in the regional area to be analysed, Europe in this case.

This paper summarises the results obtained using the most promising algorithms, based on the use of a state of the art orbit determination algorithm (BAHN developed at ESOC/OAD). These results have been obtained using real data from a dedicated campaign. Eight GPS and GLONASS receivers have been deployed in Europe to evaluate the performances of the algorithms to compute ephemeris and clock corrections. The use of orbit and clock corrections allows to determine the user position in real time with an accuracy about one meter, which fully satisfy the EGNOS performances requirements.

INTRODUCTION

Europe's primary contribution to GNSS - 1 will involve signal relay transponders carried on geostationary satellites, and a network of ground stations. They are intended to provide a regional augmentation service for GPS and GLONASS signals over Europe. Thus improving considerably the positioning accuracy of a user located in the coverage area. This augmentation is called an "overlay", and the European programme is known as EGNOS (European Geostationary Navigation Overlay Service).

Using the current GNSS systems, user positioning accuracy of about 100 meters (for GPS satellites) can be achieved when no augmentation system is used. The following figure illustrates the typical user positioning errors when GPS data is used:

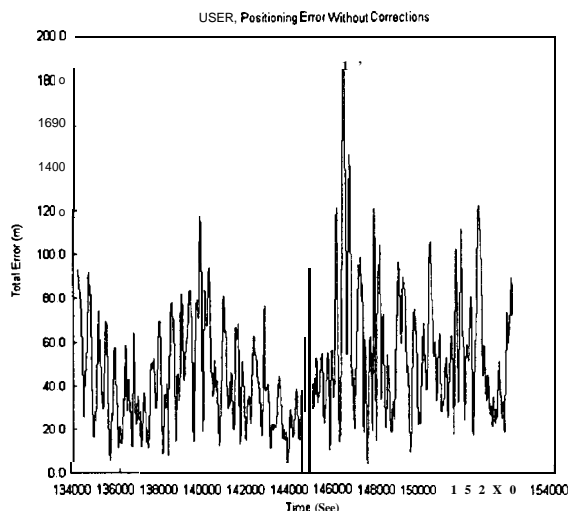


Figure 1 GPS Typical user positioning errors

EGNOS is expected to improve considerably the user positioning accuracy. EGNOS will reach its Advanced Operational Capability in 1999, when it can be used as primary source of navigation and positioning for applications such as aircraft landing approaches

EGNOS provide the backbone for three essential navigation services: ranging, integrity monitoring and wide-area differential corrections.

Ranging service. The ranging service will enable the EGNOS transponders to broadcast GPS-like navigation signals. As a result, these satellites become two more sources of space-based navigation data for users. This is important because neither GPS nor GLONASS systems can guarantee that the minimum number of six satellites required for safety-critical applications is in view at all time and all locations world-wide.

Integrity service. Range errors estimates for each GPS, GLONASS, or EGNOS navigation signal are broadcasted. The EGNOS integrity service will enable users to known within 10 seconds whether a navigation satellite signal is out of tolerance, allowing action to be taken before any critical situation arises.

Wide area differential correction service. Correction signals to improve the precision of satellite navigation are broadcasted to the users. With the wide area differential service, the satellite navigation precision will dramatically increase to 5 to 10 meters well above the approximate] y 100 meters for the currently available non-encrypted signals from GPS.

This paper describes the algorithms to be used to provide the Wide Area Differential (WAD) ephemeris and clock correction service. The most promising technique is analysed to some extent, and the results obtained when using this algorithm are presented.

ALGORITHMS SELECTION AND DESCRIPTION

Three different types of algorithms can be considered to perform an accurate orbit determination:

- . Dynamic methods
- Geometric methods
- . Reduce dynamic methods

The algorithm used to compute clock corrections is the same for all above mentioned algorithms, Once the ephemeris corrections have been computed the clock corrections will be computed from the measurement's residuals.

Dynamic methods. These methods are based in the integration of the equations of motion:

$$m \frac{d^2 x}{dt^2} = \sum_{i=1}^n F_i$$

Where F_i account for all perturbation acting on the satellite, like: gravitational perturbations, surface force perturbations, tidal perturbations, manoeuvres, etc.

Combining dynamic with observations:

$$y = Hx + \varepsilon$$

it is possible to improve the knowledge of the state variables, and therefore the satellite orbit determination. The major problem of the dynamic methods is the required computational time. A significant amount of computational time is required to compute the ephemeris corrections, thus they are in principle not suitable for real time operations. In the other hand they are able to compute accurate predictions. The state equations can be used to propagate the satellite ephemeris into the future, and the propagated ephemeris can be used in real time to compute the ephemeris corrections.

Once the satellite ephemeris corrections have been computed, satellite clock corrections can be easily computed. To estimate satellite clock corrections, the satellite must be at least visible for two reference stations simultaneously.

It can be concluded that it is possible to use dynamic methods for real time applications if it is possible to compute accurate predictions. Preliminary analyses, using globally distributed data show that predictions over 24 hours have an accuracy (rms) of about one

meter, this will be sufficient to provide accurate ephemeris and clock corrections to the EGNOS users.

Precise orbits for the GPS satellites can be computed operationally at regular time intervals. The objective of this operational orbit determination process will be to determine the GPS orbits in the past and to produce accurate orbit predictions for the future.

The objective of the tests to be performed here will be to evaluate the possibility of computing accurate GPS/GLONASS orbits using only tracking data from the dedicated ground stations. The possibility of using external data from IGS stations will be considered.

Geometric methods. These methods do not make any use of information coming from the dynamics. They are also identified as inverse GPS methods. The position of the reference stations is accurately known, therefore if four or more than four stations are simultaneously tracking the satellite, the satellite position and clock error can be estimated. To apply these methods station clocks must be synchronised. This is normally done by using common view techniques. Station clocks synchronisation failures will severely influence the accuracy of the satellite ephemeris and clock corrections. These methods do not aim to provide real ephemeris corrections. They provide corrections that are valid for the region of interest, therefore the extrapolation of the correction to other areas may not be possible.

Reduce dynamic methods. These methods are a combination of the two previously described methods. They combine dynamical information with geometric information coming from the measurements. These methods can provide more accurate corrections than the dynamic or geometric methods, but as they are using relatively simple dynamic models, they can not provide accurate orbit predictions. Reduce dynamic methods are using dynamic models, therefore a significant amount of computational time is still required to evaluate the perturbations coming from those models, and they will not be able to operate in real time. These methods will not be considered in this analysis. Some examples have been performed by considering Keplerian propagation, no significant improvement was obtained with respect to the kinematic propagation.

DATA CAMPAIGN DESCRIPTION

A dedicated GPS/GLONASS campaign has provided the required data in order to evaluate the performances provided by the different algorithms to compute ephemeris and clock corrections.

The objective of the GPS/GLONASS Measurement Campaign was to provide a consistent dataset from widely distributed sites in Europe, with suitable equipment including dual-frequency GPS, single frequency GLONASS receivers, Atomic Frequency

Standards and meteorological logging devices. The location of the deployed receivers is represented in the figure below:

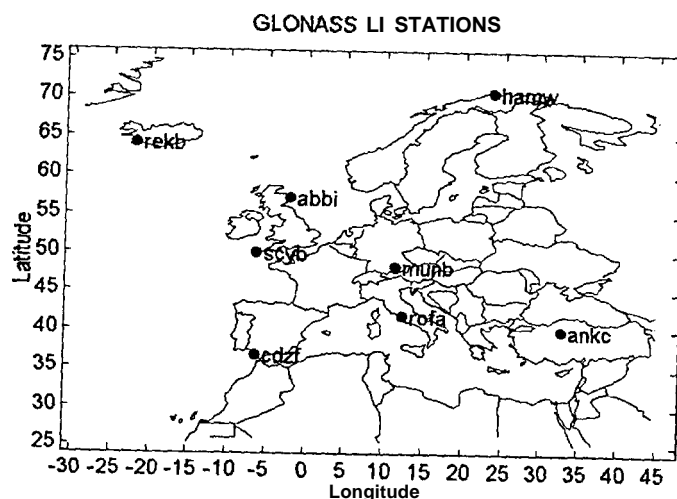


Figure 2 Ground stations used during the analysis

ALGORITHMS EVALUATION APPROACH

In order to evaluate the performances of the algorithms, to compute ephemeris and clock corrections, some already developed software packages have been integrated with some new developed software packages in a single tool.

Five different algorithms to compute ephemeris and clock corrections have been considered:

1. Dynamic algorithm, using the at ESOC developed GPSOBS and BAHN software packages.
2. Snapshot algorithm based in single differences
3. Snapshot algorithm based in double differences.
4. Snapshot and Kalman filter algorithm based in single and double differences
5. Clock correction algorithm common to all ephemeris computation algorithms

The implemented tool covers the following functionalities:

- Data generation
- Data pre-processing
- Computation of ephemeris and clock corrections
- User positioning determination

Standards and meteorological logging devices. The location of the deployed receivers is represented in the figure below:

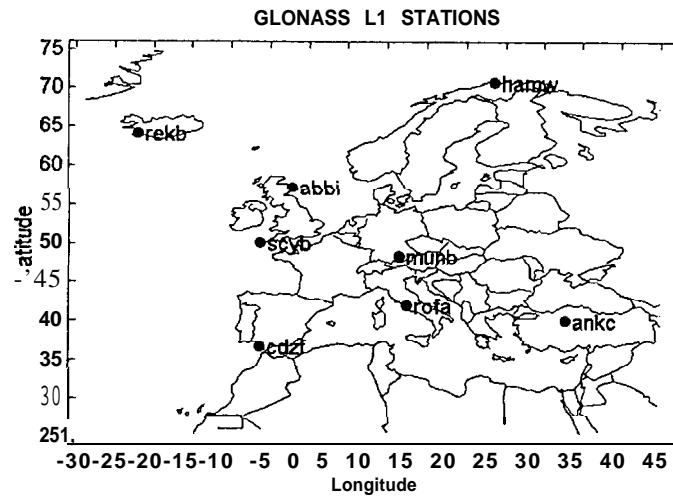


Figure 2 Ground stations used during the analysis

ALGORITHMS EVALUATION APPROACH

In order to evaluate the performances of the algorithms, to compute ephemeris and clock corrections, some already developed software packages have been integrated with some new developed software packages in a single tool.

Five different algorithms to compute ephemeris and clock corrections have been considered:

1. Dynamic algorithm, using the at ESOC developed GPSOBS and BAHN software packages.
2. Snapshot algorithm based in single differences
3. Snapshot algorithm based in double differences.
4. Snapshot and Kalman filter algorithm based in single and double differences
5. Clock correction algorithm common to all ephemeris computation algorithms

The implemented tool covers the following functionalities:

- . Data generation
- . Data pre-processing
- . Computation of ephemeris and clock corrections
- User positioning determination

with the data from the dedicated campaign to try to determine accurate GLONASS orbits and to establish the best orbit determination strategy for those satellites, as no accurate orbits are available for those satellites. Unfortunately a very limited amount of SLR data was available, so very precise orbits could not be computed. The availability of SLR data during the month of June 1996 is summarised in the table below:

<i>Satellite</i>	<i>Number of SLR observations</i>
GL-63	421
GL-66	137
GL-67	1031

Table 1 GLONASS SLR data available

Meteorological data are required in order to remove tropospheric delays from the measurements. Some facilities to generate RINEX files from the campaign data have also been implemented.

GPSOBS. GPSOBS is a state of the art GPS data pre-processing software package developed at ESOC. This program is used at ESOC to pre-process RINEX files, the output of this module is directly usable by the orbit determination package BAHN.

As it has been mentioned before, BAHN has been used to compute accurate GPS and GLONASS orbits. Unfortunately GPSOBS is not able to handle GLONASS data, therefore GLONASS data have not been processed to the same extent as GPS data.

GPSOBS has been used to generate double differences of carrier phase and pseudorange measurements from the ESA GNSS - 1 campaign, from the at GMV installed receiver, and from some IGS stations.

Data from all satellites have been generated. Antenna corrections and ionospheric corrections have been applied to those data. Cycle slips have been removed, and eclipses perturbations have been modelled. The interval between observations has been selected as 6 minutes, and a minimum elevation of 20 degrees has been selected. Initial values for clock parameters are computed.

Pre-processing for real-time algorithms. This module is not really part of the algorithms to compute ephemeris and clock corrections, but it is required in order to perform those corrections, and in order to compute the user position.

The pre-processing is valid for real (GPS and GLONASS) and simulated measurements, but the methods used depend on which case is considered. This algorithm is intended to provide a iono-free, tropo-free, carrier phase smoothed pseudorange to the algorithms working in real time.

Ephemeris computation algorithms. Different algorithms have been used to compute accurate ephemeris corrections to the GPS and GLONASS satellites.

The core of the dynamic algorithms is the general utility orbit determination program BAHN. BAHN is a state of the art package developed at ESA/ESOC over the last

decades, This package has been extensively used to compute precise orbits for many different types of satellites and using different types of tracking data systems. In particular ESOC is actively participating as an Analysis Centre and Operational Data Centre in IGS. In the scope of this analysis BAHN has been extensively used to compute accurate orbits for GPS and GLONASS satellites.

Geometric algorithms have been implemented, those algorithms use pre-processed data, the position of the satellite can be computed if four or more stations are simultaneously tracking the satellites. Some of the implemented methods use a Kalman filter to smooth the computed corrections.

User Positioning Algorithm. This algorithm is intended to provide the user position using GPS or GLONASS measurements. Pre-processed measurements for the selected user, and ephemeris and clock corrections generated by any of the algorithms are used to obtain the position of the user.

The analysis of the user positioning errors is required in order to assess the performances of the algorithms. The accuracy of the ephemeris corrections for GPS satellites can be evaluated just by comparing with accurate IGS orbits. For clock corrections no accurate solutions are available. To have an estimation of the errors associated with the clock estimation the user position errors are estimated, and from those values an upper limit of the contribution of the clock corrections to the total UERE (User Equivalent Range Error) can be estimated.

ALGORITHMS EVALUATION TESTS RESULTS.

The performances of the different algorithms to compute accurate ephemeris and clock corrections have been evaluated using real data from the dedicated tracking data campaign. One of the stations of the campaign will be used to simulate the user performances in terms of positioning errors. This section summarises the results obtained in terms of accuracy of the ephemeris and clock corrections, and also in terms of the accuracy of the user positioning.

Geometric algorithms.

The following table represents for all satellites and algorithms the rms in meters of the ephemeris corrections errors. All stations (eight) have been used to compute the solutions. Due to the large correlations between ephemeris and clock corrections similar errors may be expected for clock corrections, as it was concluded from the tests based on simulated data

	Single Differences Snapshot	Single Differences Kalman Filter	Double Differences Snapshot	Double Differences Kalman Filter
TOTAL	489	524	101	112

Table 2 RMS of the ephemeris corrections in meters

From the above results the following conclusions can be addressed:

- For single differences algorithms different behaviour has been observed for different satellites. Corrections for low elevation satellites are worse than corrections for high elevation satellites,
- Almost the same results are obtained for **all** satellites when using double differences algorithms (ephemeris errors around 100 meters).
- Algorithms based in **Kalman** filters are providing worse performances than snapshot algorithms.
- Ephemeris corrections errors computed using double differences algorithms are significantly smaller than when using single differences algorithms. Although they are bigger than the typical ephemeris broadcast errors.

The use of geometric algorithms to solve for the satellites ephemeris and clocks represents the inverse GPS problem. The position of some reference ground stations is accurately known, and the unknown is the satellite position and clock. The concept of DOP (Dilution of Precision) needs to be redefined as in this case the user is the satellite, and the “satellites” are the reference ground stations. Therefore the “inverse DOP” is computed. The precision of the ephemeris and clocks computed using geometric methods will depend on the “inverse DOP” value and the measurements errors. The satellite position errors can be represented as the product of the “inverse DOP” by the measurements errors. This is basically the same concept applied to the user in the typical GPS case, but now applied to a satellite.

The figure below represents the “inverse DOP” values for two satellites and for the reference geometrical configuration (eight stations):

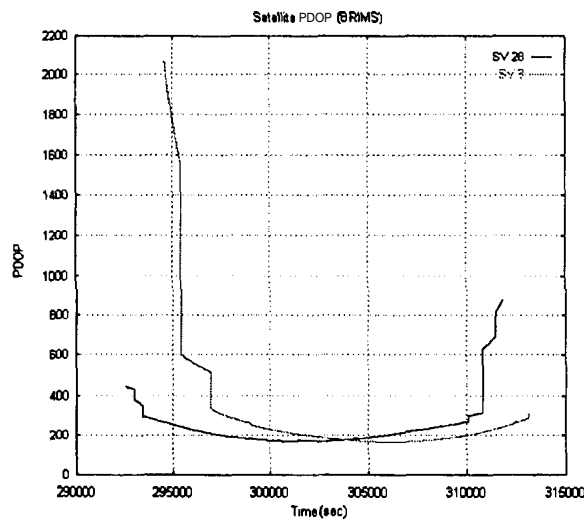


Figure 4 Inverse GPS DOP values

This explains the large ephemeris errors obtained. Maximum PDOP values can be up to 2000, and in optimal geometrical conditions they are about 200. This is certainly worse than for a typical GPS user where those values are typically between 2 and 5. This is

mainly due to the bad geometrical conditions, distances between stations are smaller than distances between satellites.

Measurements errors of about 50 cm will address to ephemeris errors among 100 and 1000 meters. These measurements errors can be considered as realistic for a low elevation satellite. These errors are slightly smaller for a higher elevation satellite.

It can be concluded that using geometric algorithms it is only possible to compute accurate ephemeris if the measurements were almost perfect.

Performances have also been evaluated from the user point of view. For all the cases the user positioning errors will be represented as the total error divided by the PDOP, this represents an indication of the total UERE.

The accuracy to be achieved for a user located at Rome without transmitting any correction is:

	User Error (m)
UERE	23.0

If ephemeris and clock corrections based in geometric algorithms are applied the user position accuracy change to:

	Single Differences Snapshot	Single Differences Kalman Filter	Double Differences Snapshot	Double Differences Kalman Filter
UERE (m)	0.80	2.86	0.52	0.73

This relatively good results, despite of the large ephemeris errors, have been obtained because clock corrections are compensating ephemeris corrections. This compensation may not be valid for all user locations. A theoretical analysis shows that this compensation is higher for a user located close to centre or the area covered by the stations. For a user located far from this location the user position errors will increase with the ephemeris corrections errors. For a user close to the borders of the investigated area (ECAC) this degradation has been estimated as a 10-15 % of the ephemeris errors.

To analyse the influence of the user location. The same tests have been repeated for a user out of the area covered by the stations. Reykjavik has been selected as user. Only one algorithm has been selected to perform this test: snapshot single differences.

The table below represents the user position errors:

	User Error (m)
UERE	5.04

- It can be concluded that the performances of the geometric algorithms are severely depending on the user location. Ephemeris errors are compensated with clock errors for a user close to the centre of the area covered by the stations, but this is not valid when the user is relatively far from this location.

- The situation will not improve by increasing the number of stations, or by modifying the location of the stations. This will only modify the location where clock corrections compensate ephemeris corrections.
- The only way to improve the performance is reducing the correlation between ephemeris and clock corrections by reducing the errors in the computed ephemeris corrections.

Dynamic algorithms.

Dynamic algorithms have been used to compute the orbits of the GPS satellites. The orbit determination package BAHN (developed at ESOC/OAD) has been used in combination with data from the eight stations involved in the dedicated tracking data campaign. The computed orbits were compared against the very accurate IGS orbits in order to have an estimation about the accuracy of the determined orbits. It shall be indicated that only data from a European network of stations has been used, while to compute the IGS orbits data from a world-wide network have been used.

GPS orbits with an accuracy of about 1.11 meters have been computed.

Some effort has been devoted to compute ephemeris corrections in a well-defined reference frame, in particular in the ITRF-93 reference frame. The success is demonstrated by the small values obtained for the seven parameters defining the transformation between the computed orbits and the IGS orbits. The translations are at the 1 cm level, rotations at the 1 mas level, and the scale factor is about 0.1 parts per billion. The accuracy of the orbit predictions, which is defining the accuracy of the ephemeris corrections to be transmitted to the user, is presented below as a function of the prediction length:

prediction interval	Total rms
3 h	3.14
6 h	3.42
12 h	3.43
24 h	4.71

Table 3 Orbit predictions accuracy in meters

The influence of the number of stations and their location in the orbit prediction accuracy have been evaluated. It can be concluded that better results are obtained when the eight stations are used, but still acceptable results can be obtained if only four stations are used. Orbits are computed using as observable double difference carrier phase measurements. So the addition of an isolate station out of Europe will not improve the results. Some improvements have been observed when two stations located in USA have been added (to perform this tests real data from IGS stations have been used).

Correlations between ephemeris and clock corrections can mask the results, because the performances of the algorithms are usually validated from the user point of view. It was already mentioned when evaluating geometric algorithms that wrong ephemeris

corrections can be compensated by clock corrections. This compensation is expected to be high for a location close to the centre of the configuration defined by the stations. Different conclusions may be obtained by considering different user locations. The following figure represents the percentage of the non compensated ephemeris errors as a function of the user location. The horizontal plane represents the ECAC area, and the vertical axis the percentage of non absorbed ephemeris errors:

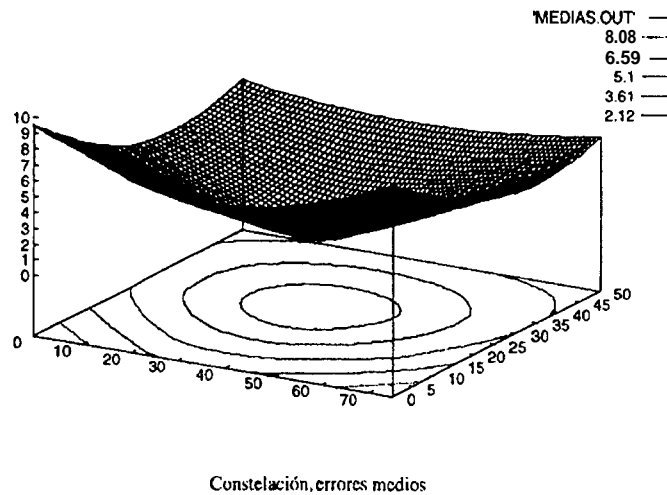


Figure 5 Percentage of the non compensated ephemeris errors as function of the location

From the above figure it can be observed that for a user located close to the corners of the ECAC zone the non absorbed ephemeris errors can amount up to a 10 % of the total ephemeris errors. Other tests performed using different orbit errors suggest that those values are never bigger than 15% for the mean values. The worst location user is at the corners of the area covered by the stations. In these tests the selected user location is close to the centre, to extrapolate the conclusions to the worst user, a 15% of the total ephemeris error will be added to the UERE value. Figures below represent the computed ephemeris and clock corrections

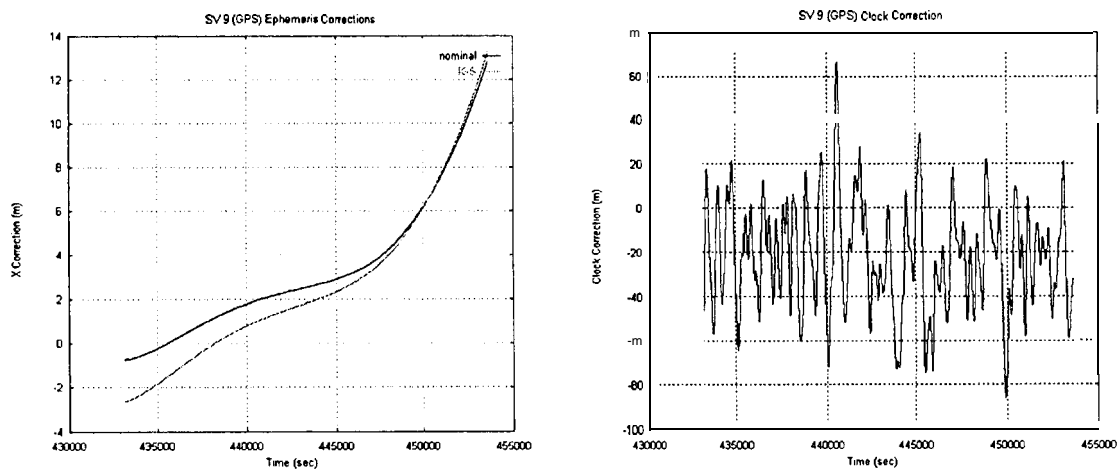


Figure 6 Estimated ephemeris and clock corrections

The performances of the dynamic algorithms have also been evaluated from the user point of view, the obtained results are represented in the table and figure below:

UERE (m)	0.51
----------	------

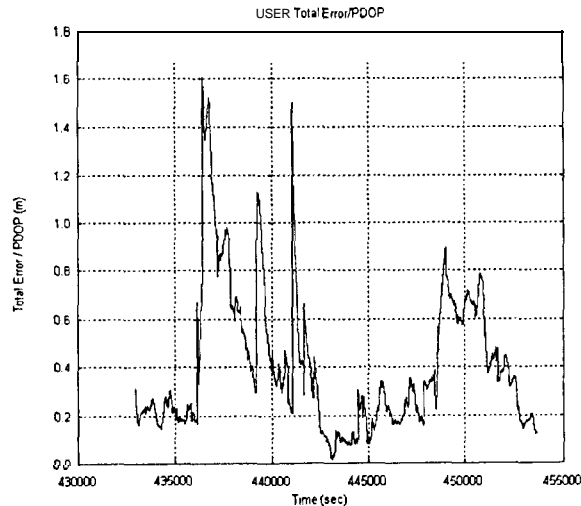


Figure 7 UERE after applying of corrections based in dynamic algorithms

The following conclusions can be addressed:

- Dynamic algorithms are able to provide accurate user positioning. Also ephemeris and clock corrections are quite accurate.
- The estimated UERE value for a user at a central location is about 0.5 meters.
- Similar behaviour are observed for the horizontal and vertical components of the user positioning errors

Another central location (Munich instead of Rome) has been selected as user to confirm the results from the previous test. The time interval selected to perform the test is different, as data from a previous day have been used. The orbits used to perform this test have relatively high orbit errors, about five meters.

The results obtained are presented in the table below:

UERE (m)	0.46
----------	------

To analyse the sensitivity of the algorithm to different user locations several tests modifying the user location have been performed. It should be considered that the station selected as user has not been used to compute ephemeris and clock corrections. Ephemeris and clock corrections have been computed for each of the cases. The results will be affected by the different geometrical conditions associated to each of the cases.

These results can be compared with the results obtained when the user was located at Rome.

The table below summarises the obtained results for the different cases:

	Ankara	Reykjavik	Hammerfest
UERE (m)	0.56	0.58	0.41

It can be concluded that the performances of the dynamic algorithms from the user point of view are less sensitive to the user location than the geometric algorithms.

Some tests have been performed for **GLONASS satellites**. **No accurate ephemeris are available for these satellites, so it has not been possible to get an estimation about the orbit determination accuracy achieved in this case. In addition to that no accurate pre-processor for GLONASS data was available, so the orbit determination was based in pseudorange measurements, The computed orbits are believed to have an accuracy of a few meters. In addition to that** clock corrections have also been computed for GLONASS satellites.

The performances of the algorithms to compute ephemeris and clock corrections have been evaluated from the user point of view, and the obtained results are summarised in the table below:

Error	Without corrections	Clock & Ephemeris corrections
UERE (m)	7.20	2.98

The table above represent the user position errors for a user located at Rome with and without corrections. The following conclusions can be addressed:

- The positioning user errors obtained without corrections are in agreement with the expected performances of the GLONASS system.
- The user positioning errors are substantially reduced when applying corrections. The non availability of accurate GLONASS orbits makes difficult to conclude anything about the quality of the computed ephemeris corrections, although from the results of these tests it seems that the computed ephemeris corrections are not very accurate.
- The user positioning errors obtained are mainly due to the large noise of the measurements, and not only due to errors in the clock estimation.

CONCLUSIONS

A complex infrastructure has been specifically developed, this has made possible the evaluation and assessment of different algorithms. The following items related to the developed infrastructure and the way the experiment has been conducted are highlighted:

- . Geometric and Dynamic algorithms to compute ephemeris and clock corrections have been evaluated.
- . Algorithms have been evaluated using different sources of data, namely: simulated, ESA GNSS-1 campaign, GMV GPS receiver, IGS, and SLR.
- Dynamic algorithms have been evaluated for GPS and GLONASS satellites. Geometric algorithms have been only evaluated with GPS data.
- . The results obtained are affected by the applied pre-processing and the quality of the data used.

It can be concluded that **dynamic algorithms are providing better performances than the geometric algorithms. Geometric algorithms can not be considered as a valid alternative for the EGNOS system.**

From the results of this experiment, the UERE (1 σ value) associated to the ephemeris and clocks correction is estimated in about 0.65 metres. However the reduced amount of data used in the experiment as well as the fact that additional ionospheric errors could appear for high solar activity. A **risk margin of 15%** could be considered to account for those effects.

REFERENCES

B. Hoffman-Wellenhof, H. Lichtenegger and J. Collins. Global Positioning System, Theory and Practice.

Global Positioning System. Standard Positioning Service. Signal Specification. GPS NAVSTAR.

Yeou-jyh Tsai et al. Evaluation of Orbit and Clock Models for Real Time WAAS. Standford University. ION-95.

Changdon Kee, Bradford W. Parkison, Penina Axelrad. Wide Area Differential GPS. Navigation Journal of The Institute of Navigation, Vol. 38, No. 2, 1991.

J.M. Dow, T.J. Martin Mur, M.M. Romay ESA's Precise Orbit Determination Facility, Merino. ESA bulletin, number 78, may 1994.

GLONASS Interface Control Document, 1995.

P.N. Misra, R.I. Abbot, E.M. Gaposchkin. Integrated use of GPS and GLONASS: Transformation between WGS 84 and PZ-90. ION GPS-96

Minimum Operational Performance Standards for Sensors Using Global Positioning System/Wide Area Augmentation System, RTCA Paper No. 240-95/SC 159-664, April 20.1995.

M.M. Romay Merino et al. Experiment 2.2a Test Report. Evaluation of Real Time Integrity and Differential Correction Algorithms for WAD Systems, ref.: GMVSA 2170/96

POTENTIAL USE OF ORBIT PREDICTIONS AND RAPID PRODUCTS IN THE GRAS PROGRAMME

Pierluigi Silvestrin

Earth Observation Preparatory Programme

Directorate of Applications Programmed

European Space Agency

ESTEC, NL-2200AG Noordwijk, The Netherlands

BACKGROUND

The European Space Agency (ESA) is currently developing instrumentation and data analysis tools for atmospheric sounding by radio occultation (**RO**). The GNSS Receiver for Atmospheric Sounding (GRAS) is a space instrument based on the use of RO technique with global navigation satellite systems such as GPS and GLONASS (collectively indicated as **GNSS**) as sources of opportunity. The final program objective is to provide data products of a specified quality for operational meteorology, climate monitoring and prediction, and studies of atmospheric processes and space weather physics.

The RO method is widely considered a mature technique for atmospheric remote sensing. It benefits from a long scientific and technical heritage from planetary exploration experiments, starting with the Mariner IV mission in 1964. Concepts for RO measurements of GPS signals to probe the Earth's atmosphere have been published since 1987 [**Gurvich** and **Krasilnikova**, 1987]. Since then, the quality of derived data products has been proved to be, in several respects, superior to that of current observation techniques, such as spaceborne radiometry or in situ monitoring by e.g. **radio-sondes** [see e.g. Melbourne et al., 1994, **Kursinski** et al., 1997; **Rocken** et al., 1998].

Within the ESA programmed, theoretical and simulation-oriented studies included a validation of error analyses using data from the GPS-MET experiment and the development of improved calibration and retrieval algorithms [**DMI** et al., 1995; **CRI** et al., 1998]. Combined with the GRAS instrument development, these activities enabled European meteorologists and climatologists to propose a dedicated space program, the 'Atmospheric Profiling Mission' within the Earth Explorers framework [ESA, 1996]. The mission proposal, consisting of a constellation of 12 small satellites each carrying a GRAS instrument and the required ground segment, was partly successful since it resulted in the decision to embark GRAS as a co-passenger instrument in all suitable Earth Explorers. It is planned to launch these satellites at two years intervals starting in 2004.

Meanwhile, the European Organisation for the Exploitation of Meteorological Satellites (**Eumetsat**) has added GRAS to the payload of the MetOp satellites for meteorology and climatology. These satellites are being developed by ESA for **Eumetsat**, which will take over the operations and the data exploitation. Each satellite carries a set of instruments including a wind **scatterometer**, an imaging radiometer, three temperature and humidity sounders, an ozone monitoring instrument and **telecom** equipment for data dissemination. The orbit will be a sun-synchronous frozen orbit at 820 km altitude, with a 5 days repeat period and local solar time at the descending node of **9:30** a.m. The on-going MetOp- 1 development is on schedule for a launch in 2003, to be followed by the **MetOp-2** launch in 2007 and **MetOp-3** in 2011.

THE GRAS INSTRUMENT

GRAS provides measurements of the code and carrier phases of signals from both GPS and GLONASS at the **L1** and **L2** bands. Both descending (set) and ascending (rise) occultation signals are observed through two antenna arrays placed on the anti-velocity and velocity sides of the spacecraft, respectively. Each array features 15 antenna elements and provides **~12 dB** gain in a field of view which includes the atmosphere in an azimuth range of +/- 53°. This allows some 1000 occultation profiles per day to be observed, assuming full operation of both GPS and GLONASS. A conventional zenith-looking antenna receives signals for real-time navigation and precise orbit determination (POD).

GRAS uses 16 dual-band channels, of which 6 are reserved for **GPS-based** POD. Its Ultra-Stable Oscillator (**USO**) has an overall stability better than 10^{-12} over 0.1 s - 100s observation intervals, enabling the use of a **single-differencing** approach in the ground processing of occultation measurements. This minimises the number of required ground stations and improves performance by reducing thermal noise, **multipath** and tropospheric scintillation errors.

The main observable for occultation processing will be carrier phase and amplitude measurements at 50 Hz sampling rate. Amplitude measurements with a precision of 0.2 dB will be used mainly for diffraction correction processing. The preliminary requirements for the signals undergoing an occultation have been established on the basis of analyses and simulations of the retrieval process. The main carrier phase requirements are outlined in Table 1. Measurements of the L2 band signals are not required when crossing the lowest height region ($h < 12$ km). In this case, the instrument operation will take advantage of the possibility to make ionospheric corrections based on extrapolated ionospheric **doppler** (or refraction angle) and of the strong signature by refraction in the troposphere on the **L1** signal phase.

Height region	Measurement error (rms)	Observation bandwidth
$h > 30$ km	< 1 m m	> 10Hz
$30 \text{ km} > h > 12$ km	$< 3 + (12-h)/9$ mm	10 to 25 Hz
$1 \text{ km} < h < 12$ km	$< 30 + 27(1-h)/11$ mm	>25 Hz

Table 1: GRAS Carrier Phase Measurement Requirements

The space qualification and reliability/availability requirements mandate the use of **radiation-tolerant** components, which are being tested in GRAS prototypes. Earlier receiver breadboards

were used to validate the basic design [Riley et al., 1995]. Flight equipment production will start in 1999. A similar instrument, the GPSOS (GPS Occultation Sensor) is being designed for the U.S. National Polar-orbiting Operational Environmental Satellite System (NPOESS) programme by the same European industrial consortium developing the GRAS. It is also planned that the instrument functionality be extended to measure signals reflected by the sea surface so as to derive scatterometric information [Martin-Neira, 1993].

OBSERVATION REQUIREMENTS AND DATA PRODUCTS

The observation requirements for a GRAS-based system have been compiled by a Science Advisory Group including numerical weather prediction (NWP) experts. They are formulated separately for the three application domains, namely operational meteorology, climate monitoring and prediction, and space weather, as detailed in Tables 2-4 for a **MetOp-type** mission. In the tables, the horizontal resolution indicates the mean distance of individual soundings over the specified time window (defined as the time required to achieve global coverage). The timeliness requirements are referred to the time of observation. For operational meteorology, these stringent requirements have top priority and drive the design of the ground processing subsystem. On the other hand, the main performance requirements (accuracy, vertical domain) are slightly relaxed compared to the performance achievable with the most sophisticated retrieval algorithms.

	Temperature	Humidity	Refraction angle
Geographic coverage	global	global	global
Horizontal resolution	<1000 km	< 1000 km	< 1000 km
Vertical resolution	0.5-1.0 km	0.5 km	< 0.5 km
Vertical range	500 hPa to 10 hPa (5-30 km)	surface to 300 hPa (0-10 km)	surface to 80 km
Time window	< 12 hours	c 12 hours	c 12 hours
Absolute accuracy	< 1.0 K	< max{10 %, 0.2g/kg}	< max{1 prd, 0.4 %}
Timeliness	3 hours	3 hours	2.25 hours

Table 2: Observation Requirements for Operational Meteorology

	Temperature	Humidity
Horizontal domain	global	global
Horizontal resolution	< 1000 km	< 1000 km
Vertical domain	surface to 1 hPa (< 50 km)	surface to 300 hPa (< 10 km)
Vertical resolution	0.5 km/1.0 km (Troposphere/Stratosphere)	0.5 km
Time domain	> 10 years	> 10 years
Absolute accuracy	< 0.2 K (monthly average)	< 3 % (monthly average)
Long term stability	< 0.1 K/decade	< 2 %/decade
Timeliness	1-2 months	1-2 months

Table 3: Observation Requirements for Climate Monitoring and Prediction

	Ionospheric monitoring, modelling and prediction		E layer analysis	Plasmaspheric analysis and modelling
	large-scale	meso-scale		
Horizontal domain	global	global	global	global
Horizontal resolution	< 1000 km	< 1000 km	< 1000 km	< 5000 km
Vertical domain	100- 800 km	100- 800km	90- 130km	103-2 10 ⁴ km
Vertical resolution	10 km	5km	0.5 km	500-5000 km
Time domain	> 1 year	> 1 year	> 1 year	> 1 year
Time window	< 12 hours	< 12 hours	< 12 hours	c 12 hours
Accuracy: TEC	0.5-5%	0.1-5%	0.5-5%	2-20%
electron density	1-20%	1-10%	1-10%	10-30%
Timeliness	3 hours	1 - 2 months	1-2 month	1 - 2 months

Table 4: Space Weather Observation Requirements

The currently assumed architecture for the MetOp space and ground systems is outlined in Fig. 1 (where PCDA = Polar Command and Data Acquisition; PDIF = Polar Data Ingestion Facility; PSCC = Polar Satellite Control Centre). Two high-latitude ground stations will be used, e.g. in Kiruna and Fairbanks, so ensuring a data **downlink** at each orbit.

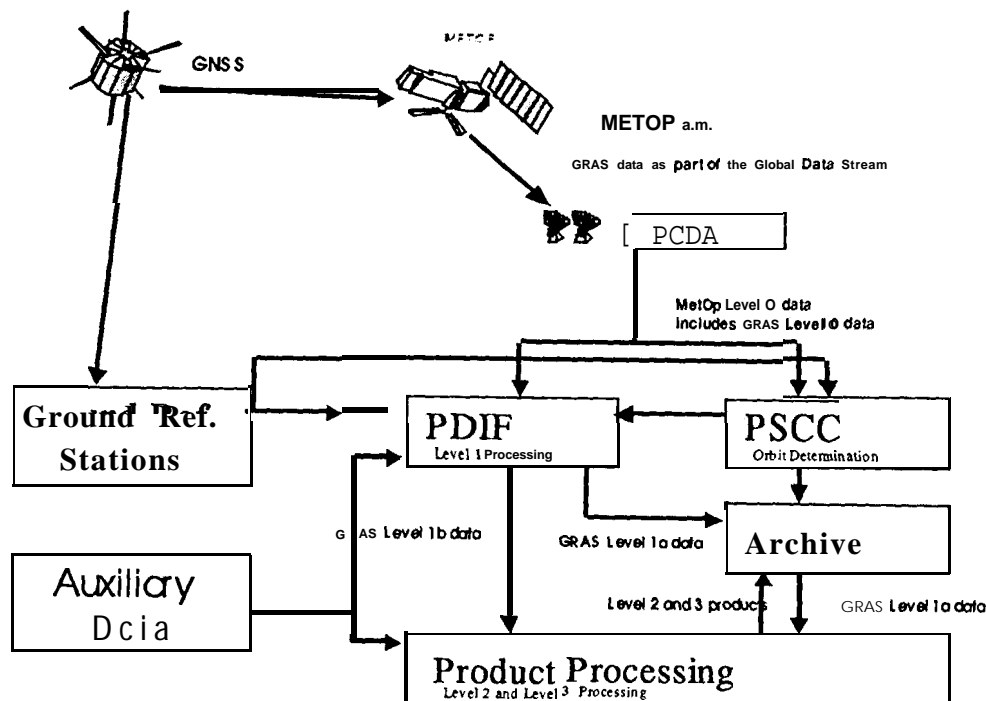


Figure 1: Space/Ground Segments Architecture

Following the CEOS (Committee for Earth Observation Systems) guidelines, the GRAS data products have been defined for various processing levels:

- Level 1a: tracking and occultation data (code and carrier phases, amplitudes), ground station tracking data (for occultation processing), ancillary spacecraft and ground station data;
- Level 1b: GRAS POD data, GNSS POD data, L1 and L2 excess phase and amplitude data, L1 and L2 refraction angles (functions of the ray impact parameter);
- Level 2: refractivity profiles, temperature, pressure and humidity profiles, total electron content and electron density profiles;
- Level 3: profiles (1D), images (2D) and fields (3 or 4D) of atmosphere parameters.

A simplified outline of the data processing (from level 1a to levels 1b and 2) is given in Fig. 2. Level 1b data should be available to users within 2.25 h and level 2 data within 3 h. Apart from the POD step, the other processing steps to derive level 1b and level 2 data (referred to as the occultation processing) are not computationally demanding and can be performed well within the timeliness requirement. This applies also when advanced retrieval methods based e.g. on the Fresnel transform for diffraction correction are applied [CRI et al., 1998].

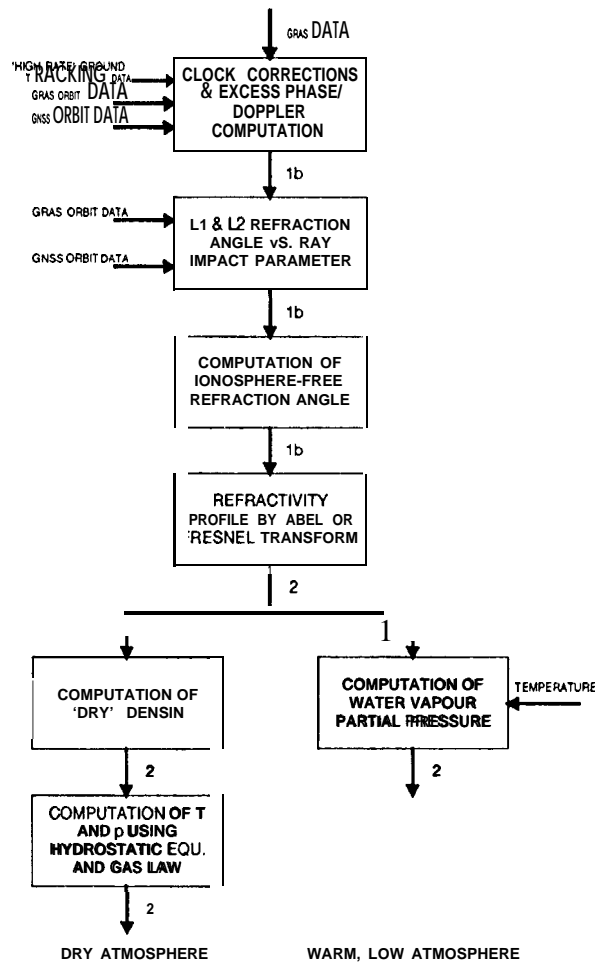


Fig. 2: Data processing from 1a to 1b and 2

PROCESSING REQUIREMENTS

GRAS and GNSS POD data is required in the first processing step (computation of the excess phase delay and **doppler** shift caused by the atmospheric refraction) and in the second step (computation of refraction angles). Ground tracking data is also required in the first step to derive single differences (SD) of carrier phases, which remove GNSS oscillator instability errors. It is expected that ionosphere-free refraction angles will be the preferred input to NWP systems for data assimilation [Eyre, 1994].

The ground tracking data will be taken from a set of -10 reference stations properly distributed over the globe. These stations must be equipped with high-availability **geodetic**-class GNSS receivers and clocked by high-performance USO. The data retrieval must occur at least as often as the orbital period. About 12 to 15 stations would be needed if the processing were based on the use of double-differences, with some increase in the operation costs.

The POD requirements for both the GRAS-carrying satellite and the GNSS satellites have been assessed using a software simulator. The EGOPS (End-to-end GNSS Occultation Performance Simulator) tool is used to perform sensitivity analyses with respect to several

parameters of both the 'model world', which include detailed models of the signal propagation and of the observing system, and the retrieval system (i.e., the ground processing chain) [CRI et al., 1998]. The **EGOPS** retrieval system can accept an input of simulated data or real data. This feature was used to validate the tool, GPS-MET phase measurements being reproduced within the 'model world' to mm-level precision. Atmospheric parameters were also retrieved from **GPS-MET** data and successfully compared with in situ measurements and with the results of analyses using NWP systems.

The POD position accuracy for both GNSS and GRAS affects only the determination of the measurement geometry. The accuracy needed for the ray impact parameter and the ray perigee is related in general to the maximum refractivity gradients found during a tropospheric occultation. If it is insufficient, the error on the height level attributed to a given temperature or humidity measurement can exceed the vertical resolution of the RO technique. However, for operational meteorology a vertical resolution of 0.5 km is acceptable, hence the position determination accuracy can be fairly relaxed. A formal requirement for POD of GRAS and GNSS of 1 m rms has been set, which is expected to be feasible without special developments.

The velocity estimation accuracy is the 'driving' requirement, since a velocity error maps directly in the excess **doppler** shift in the first processing step. The **doppler** error is proportional to the projection of the velocity estimation error on the ray path, therefore, because of the occultation geometry, the main error components are the along-track one for GRAS and the radial one for GNSS. The challenging requirement is on the velocity estimation accuracy of the low-orbiting GRAS. Analyses and EGOPS simulations agree that a GRAS along-track error of 0.05 mm/s, corresponding to -0.2 K error in the temperature retrieval under average conditions, should be the goal. For operational meteorology, a 1 K error at 30 km implies a maximum along-track velocity error of 0.2 -0.3 mm/s, assuming the system is designed in such a way as to make the other error contributors negligible in comparison. The velocity estimates are also used in the computation of the refraction angles from excess **doppler** shifts, but the impact on the final accuracy is negligible if the velocity error is at the sub-mm/s level.

USE OF PREDICTED GNSS ORBITS AND RAPID PRODUCTS

GPS rapid orbits and orbit predictions are now established IGS products of high quality. Efforts are underway to improve them further, in particular to continuously ensure predicted orbits at the decimeter level. This will exceed what is needed for the GPS POD data in the data processing to level 1b. As regards the prediction of velocities, thermal errors obtained by comparing predicted GPS orbits with GPS precise orbits have been computed and found to remain below 0.05 mm/s over a 24 hours prediction period. The accuracy of GPS predicted orbits, both in terms of position and velocities, is therefore not considered critical. No results are yet available about the performance of GLONASS POD or orbit predictions.

For the MetOp satellites, the current baseline assumes that the dedicated ground network needed for occultation processing is used also for POD. Previous experience suggests however that the required POD (velocity) accuracy will be reached only after augmenting the network to at least -20 reference stations properly distributed in the northern and southern hemispheres. Considering that, in this initial approach, the POD must be performed in near-

real time (within -20 minutes from downlink of GRAS data), this scenario is particularly demanding for both data transmission and computation time.

A possible alternative consists in taking advantage of the IGS rapid orbit products to perform POD and precise orbit predictions for the MetOp satellite or other low Earth orbiter (LEO). Recent results obtained at the Delft Institute for Earth-Oriented Space Research (DEOS) indicate that the accuracy to which the orbit of an ERS-class LEO can be predicted may suffice for occultation processing [Visser et al., 1996]. The DEOS work included a comparison between ERS-2 predicted orbits and precise orbits for April 1996. The GEODYN software was used for both POD and orbit prediction, the POD being based on laser ranging data. The predicted radial position rms accuracy was found to deteriorate from about 14 cm for the first day to about 54 cm for the fifth day. For the predicted along-track velocity, the rms accuracy was about 0.06 mm/s over the first day and 0.09 mm/s over the second day. The caveat is of course that these results have been obtained in a low solar activity period, i.e. a favorable situation for air density prediction. For future LEOS, continuous tracking with GPS which will improve the POD accuracy, while prediction accuracy will benefit from better dynamic models.

A timeline for this processing scenario is sketched in Fig. 3. Assuming that rapid combined orbit/clock products are available at sub-daily intervals, e.g. every 6-12 hours, with clock data at relatively high rate (30 s period or less), the LEO POD can be performed after each rapid product delivery using the rapid products and all the GRAS tracking data available at the end of the period of validity of the rapid products (period no. 1 in Fig. 3; here all the GRAS tracking data up to retrieval m together with the rapid products delivered at the end of period 2 can be used for POD). The POD is followed by a precise orbit prediction over a period of e.g. 48 hours. The process is repeated when new rapid products are delivered. The occultation processing following a generic retrieval n of the GRAS data and of the ground tracking data will therefore use predicted orbits for both GPS and LEO. Only the occultation processing will be performed after each GRAS data retrieval, hence at the LEO orbital rate. Two benefits are obtained, namely the time needed for the LEO POD becomes much less critical and the need to augment the dedicated ground network to cater also for LEO POD is removed.

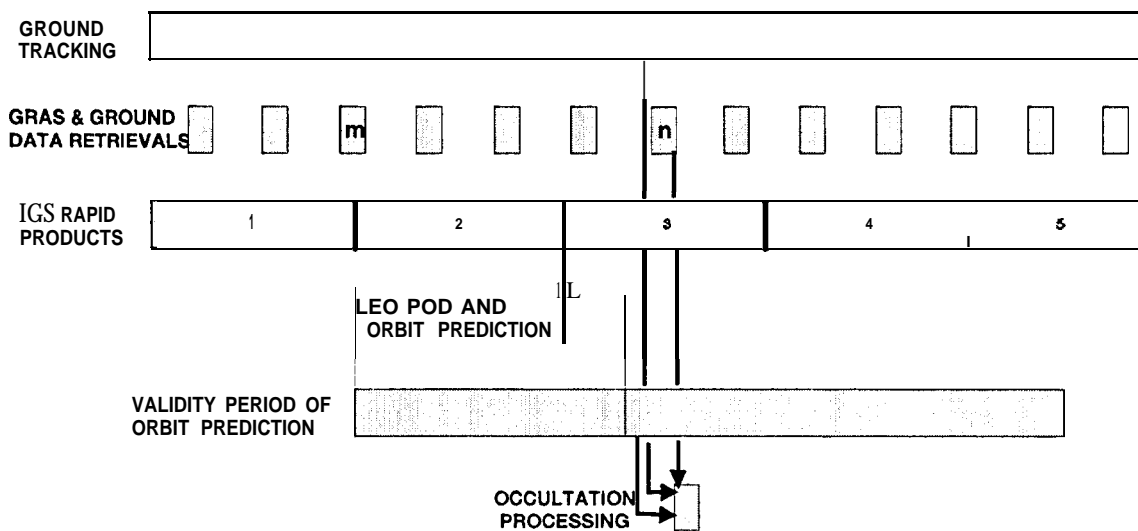


Figure 3: Timeline for Ground Processing using Rapid Orbit and Clock Products

A critical aspect is given by the delivery rate of the rapid products, which equals the rate at which the LEO orbit predictions are updated. It remains to be investigated whether delivery of rapid products every 12 hours (with 12 hours latency, as assumed here) is sufficient for accurate orbit predictions also with high solar activity. On the other hand, since the GPS tracking data from the dedicated ground network will be available anyway, it should also be investigated whether these can be used to correct the predicted LEO orbits with limited computational effort.

CONCLUSIONS

The GRAS programme aims at providing atmospheric soundings for operational meteorology and other applications. The operational use of the data products puts severe constraints on delivery time and consequently drives the complexity and cost of the ground data processing. A possible approach relying on the availability of precise GPS orbit predictions and of combined orbit/clock rapid products has been outlined. To be useful for this application, the rapid products should be provided at a sub-daily rate and include 'high rate' clock solutions based on tracking data from ground stations with reference clocks.

Acknowledgements: discussions with P. Visser of Delft University of Technology and G. Kirchengast of Graz University are gratefully acknowledged.

REFERENCES

- CRI et al., 1998, Using Global Navigation Satellite Systems (GNSS) for Operational Meteorology and Climatology, Final report of ESA Contract 11930, ESA Publication Division, ESTEC, Noordwijk, The Netherlands
- DMI et al., 1995, Derivation of Atmospheric Properties using a Radio Occultation Technique, Final report for ESA Contract 11024, ESA Publication Division, ESTEC, Noordwijk, The Netherlands
- ESA, Atmospheric Profiling Mission, 1996, SP-1 196(7), ESA Publication Division, ESTEC, Noordwijk, The Netherlands
- Eyre, J.R., 1994, Assimilation of Radio Occultation Measurements into a Numerical Weather Prediction Model, ECMWF Technical Memorandum 199, ECMWF, Reading, UK
- Gurvich, A. S., T.G. Krasilnikova, 1987, Navigation Satellites for Radio Sounding of the Earth Atmosphere, in *Issled. Zemli Kosmosa*, 6, pp. 89-93, March 1987
- Kursinski, E.R, et al., 1997, Observing Earth's Atmosphere with Radio Occultation Measurements using Global Positioning System, in *Journal of Geophysical Research*, 102, no. D19
- Martin-Neira, M., 1993, A Passive Reflectometry and Interferometry System (PARIS): Application to Ocean Altimetry, in *ESA Journal*, Vol. 17, pp 331-355

Melbourne, W.G., et al., 1994, The Application of Spaceborne GPS to Atmospheric Limb Sounding and Global Change Monitoring, JPL Publication 94-18, JPL, Pasadena, USA

Riley, S., et al., 1995, A Combined GPS/GLONASS High Precision Receiver for Space Applications, in *Proc. of ION-GPS International Technical Meeting*, Palm Springs, USA

Rocken, C. et al., 1998, Analysis and Validation of GPS/MET Data in the Neutral Atmosphere, to appear in *Journal of Geophysical Research*

Visser, P. N.A.M., et al., Operational Orbit Computation of ERS- 1 and -2 at DEOS, presented at AGU Fall Meeting, San Francisco, December 1996

Topic 3: IGS Reference Frame Realisation and Contributions to ITRF

IGS REFERENCE FRAME REALIZATION

J. Kouba

Geodetic Survey Division, **Geomatics Canada, NRCan**
615 Booth Str., Ottawa, Canada KIA OE9
e-mail: kouba@geod.emr.ca

J. Ray

Earth Orientation Dep., U.S. Naval Observatory
3450 Massachusetts Ave, NW, Washington, DC 20392-5420 USA
e-mail: jimr@maia.usno.navy.mil

M.M. Watkins

Jet Propulsion Laboratory (**JPL**)
M/S 238-600,4800 Oak Grove Drive, Pasadena, Cal. 91109 USA
e-mail: mmw@cobra.jpl.nasa.gov

ABSTRACT

The current set of 13 ITRF94 stations and the **IGS** approach to **ITRF** realization are no longer adequate for high precision frame reference definition. A new set of 52 Reference Frame (RF) Stations has been identified and is proposed to be used for a new IGS realization of **ITRF**. The new approach of **ITRF** realization is based on a nearly rigorous accumulated combination of weekly GNAAC SINEX solutions for station positions and EOPS of the current week. The **orbit/clock** solutions can then be obtained by an approximation of back substitution. This way the consistency of all IGS products, including the future IGS **SINEX** products, is enforced. It is proposed that this new, **nearly** optimal IGS realization of **ITRF** should be implemented preferably by June 28, 1998, but not later than January 3, 1999. The ITRF96 station coordinates and velocities for the set of 52 RF stations were evaluated and compared to an accumulated combination of GNAAC **SINEX** solutions, resulting in an rms agreement of a few mm horizontally and less than 10 mm vertically. For an interim and immediate improvement of the **IGS** realization of **ITRF**, it is suggested that a large subset of 47 **ITRF96** station positions and velocities be selected and used, starting as early as March 1, 1998. This new set of **ITRF96** stations is to replace the current 13 **ITRF94** station set.

INTRODUCTION

The prime objective of **IGS** is to provide a global **IGS** reference system, including realization, maintenance, and easy accessibility for all **IGS** users and GPS applications.

“A global IGS reference system” here is used in a broad sense. It encompasses not only a traditional reference system (with its **imbedded** reference frames, e.g. **ITRF**, **ICRF**, etc.), but also the standards and calibrations for ionosphere, troposphere and other, yet unforeseen, **GPS-related** information. Such a reference system, in addition to traditional theory, constants, conventions, documentation and monitoring, can be realized and represented in discrete and/or model forms. As with any global reference system, the IGS reference system must strive for global coverage and the utmost accuracy and consistency, both internally and with respect to the internationally adopted standards (e.g. **IERS**, **BIPM**, etc.). This is precisely what the IGS Terms of Reference imply. Even the components which contribute to the IGS reference system are listed, giving the specific IGS products for its realization, namely, orbits, EOP, station coordinates, clocks, along with (global) tropospheric and ionospheric information. The first four components (**orbits/EOP/station coordinates/clocks**) are fundamental in nature, although only the first three are generally considered to be absolutely essential, thus requiring the utmost precision to support IGS users. However, the recent precise point positioning approach (**Zumberge et al., 1997**) and the precise time transfer initiative (Ray, 1998) make the IGS clock product component equally important and fundamental in nature. Thus, the IGS quadruplet **orbits/EOP/station coordinates/clocks** must all be consistent and highly accurate. They should include GPS (and possibly **GLONASS**) satellites only and about 200 (polyhedron) stations. Not all possible (e.g. LEO) satellites and not all possible stations computed by ACS /AACs or observed by IGS users should or need to be included in the above IGS (reference system) product components. The **tropospheric/ionospheric** delay products should also be global (i.e. with global resolution), highly accurate and consistent within the IGS reference system. For more discussions on **clock/orbit** consistency and possible product additions and/or enhancements, see the other position papers and presentations at this workshop (e.g. Springer et al., 1998; Ray, 1998; Gendt, 1998; **Schaer and Feltens, 1998**).

The stability of the underlying reference frame (ITRF), realized by the global GPS network, **is crucial and an** integral part of, perhaps the basis of the whole IGS reference system as described above. However, the current IGS realization of ITRF has been gradually degrading due to the decrease in quality and availability of some of the 13 **ITRF** stations that are used for the current **IGS** realization of **ITRF94**. More specifically, the **ITRF94** realization is obtained by constraining the 13 **ITRF** station coordinates and velocities (**Kouba and Mireault, 1997, p. 56**). More and better ITRF station **position/velocities** and new approaches are required to solve this urgent problem. The future IGS reference frame realization should not only be precise, robust, consistent, and stable but it should also take advantage of the **GNAAC** station combinations (**G-SINEXes**). Furthermore, the **IGS** reference **frame** realization should ensure a high product consistency, in particular for the core products, viz., the IGS orbit, EOP, station coordinate (**G-SINEX** and **P-SINEX**) and clock combinations. The new ITRF96, which was recently released, can contribute significantly to the IGS reference frame realization, thus it is also discussed here.

CONSISTENCY OF IGS REFERENCE SYSTEM AND IGS PRODUCTS

Some constants and models defining a reference frame may not be accurately known, however the reference system should always be consistent, i.e. all the derived constants and reference system components must be consistent with these, albeit not accurately known, constants. Then transformation and relations to a new and improved reference system can be realized with greater precision and ease. The same is true for the underlying reference frames (i.e. positioned, oriented and scaled coordinate systems). A good example of the importance of reference system/frame consistency is the case of the core **IGS** products. The **IGS** orbit and IGS station solutions imply two realizations of **IGS** reference **frame**; i.e. they imply two sets of reference frame positions, orientations and scales that are not necessarily identical. Furthermore, the **IGS** EOPS imply an orientation for the reference **frame**. Clearly the implied reference frames should all be the same so that **IGS** users, when using any combination of the core products, will not detect any conflicts and (statistically speaking) will obtain the same results. For example, users of the new precise point positioning approach (**Zumberge** et al., 1997) realize the **ITRF** implied by the IGS orbits and clocks rather than a mixture of the two reference frames implied by stations and orbits, which is the case for more traditional GPS positioning approaches. This example also demonstrates the importance not only of the IGS orbits, EOPS, and stations but also clock solutions must be consistent with the other **IGS** products. It should be mentioned that the consistency of orbits and EOPS has been attempted from the very beginning, as evident from the fact that the initial **IGS** orbit combination enforced **orbit/EOP** consistency by rotating submitted orbits to adopted IERS (Bull. A and B) EOPS prior to the IGS combinations (**Beutler** et al., 1995). This was later abandoned in favor of separate orbit and EOP combinations as the AC orbits and EOPS were (and still are) considered to be sufficiently consistent (**Kouba** and **Mireault**, 1997). The need for **EOP/station** consistency, i.e. the need to include EOP in the **SINEX** station solutions, has also been recognized at an early stage (**Blewitt** et al., 1994). However, so far, less than half of ACS include EOPS in their **SINEX** submissions and the **SINEX** submissions for most ACS are not consistent with the **orbits/EOPs** submitted to IGS and the AC EOPS submitted to **IERS!** This is clearly unacceptable and a serious deficiency, which should be corrected as soon as possible!

The need for **clock/orbits/EOP/station** solution consistency is nowadays quite accepted, as it became evident thanks to the modern precise point positioning mentioned above. This will be **even** more accentuated with the time transfer project. However, that the tropospheric and ionospheric **IGS** products must also be consistent with the **IGS** core products is not as widely appreciated, but the same condition applies to these two atmospheric products. Specifically, tropospheric delays require the corresponding station solutions and (radial station error) corrections prior to the IGS tropospheric delay combinations (**Gend**, 1996). Clearly, **IGS** tropospheric delays should be harmonized (refer to) the **IGS** station coordinates (combined), or the adopted station solutions. Similarly for the ionospheric delay combination, the crucial component here is the (L1 -L2) calibration delay for both satellite and station hardware. This is important not only for single frequency (**L1**) users who use the ionospheric delay information for improved position

determinations (largely free of the ionospheric effects) (Huot et al., 1998), but it also has significant implications for precise time transfers. All the IGS clock products (be it the current satellite clock or the **future** station clock products) have the **L1/L2** delays imprinted in them; consequently the **L1/L2** calibrations are required and need to be applied when compared to external (time transfer) measurements at the ns and sub-ns level. Clearly, the **L1/L2 station/satellite** biases and **L1/L2** satellite and station clock corrections, be they implied or externally corrected for independent clock **comparisons/time** transfer such as in the proposed pilot project (Ray, 1998), must be precise and consistent (preferably the same, in this case). So we also have a strong “connection” of ionospheric and clock products and in turn a strong connection between clocks and the **orbit/station** position products (the station positions are required for receiver clocks, too).

REVIEW OF CURRENT STATUS OF IGS REFERENCE FRAME REALIZATION

Since the official start of IGS, the IGS reference frame realization has been accomplished by simply fixing, constraining or aligning **IGS/AC** solutions to the adopted ITRF coordinates of the same 13 stations: ALGO, FAIR, GOLD, HART, KOKB, KOSG, MADR, SAINT, **TIDB, TROM**, WETI', YAR1, YELL (see Figure 1). All the 13 stations have, or have had multi-technique (in most cases **VLBI**) collocations. Since January 1994, three official versions of **ITRF** have been used (**ITRF92, ITRF93** and **ITRF94**). Changes of ITRF versions introduced apparent station coordinate discontinuities that can reach up to 3 cm, in particular the changes to and from **ITRF93**, which was differently aligned by up to 1 mas with respect to the other **ITRFs** (Boucher et al., 1994). For more details and the specific estimates of transformation parameters between different **ITRF** versions used by IGS, please consult the Analysis Coordinator Report in the 1996 IGS Annual Report (Kouba & Mireault, 1997). Consult also the **IGSMail#1391** (<http://igs.cb.jpl.nasa.gov/igs.cb/mail/mess.1391>) which gives the information about a simple program facilitating the transformation of the current **IGS** sp3 orbit files to and from one of the above **ITRF** versions. In order to aid its users and prevent possible misuse and confusions connected with the past and future **ITRF** changes, IGS should consider transforming all past products based on previous **ITRF** realizations into the currently adopted **ITRF**. Even better, IGS should consider implementing, at the DC level, a simple user interface, e.g. based on the transformation program mentioned above, which would allow users to get all the **IGS** core products in an **ITRFyy** of their choice. However, it should be noted here that all such **ITRF** transformations of **IGS** products are only approximate due to limitations of the past and current ITRF realizations as discussed below.

Due to systematic errors in **ITRF** and GPS solutions, as well as the limited number, distribution and precision of the 13 (**ITRF94**) stations, the **station** position errors are mapped into the constrained **IGS/AC** solutions (and the implied reference frame). The distortions and reference frame variations vary amongst ACS and also in time, with possible small, periodical systematic and random effects. Even when a more optimal

approach, such as applying minimum datum constraints to unconstrained (“fiducial free”) AC solutions (see e.g. Heflin et al. 1997; Jefferson et al., 1997), the **ITRF** and GPS systematic errors as well as changes in station geometry and of processing approaches cause systematic reference frame variations (errors). For example, the current deficiency of the (13) **ITRF** station distribution is responsible for an increased noise and a decrease of the stability of **IGS** and AC solutions for PM y especially (Springer, 1998 personal comm.). More recently, the problems have been magnified since at least two or three **ITRF** stations have become unusable (e.g. **TROM**, **MADR**), leaving at times only 9 or even 8 **ITRF** stations available and usable as **fiducials**. Such a low number of stations can compromise all the **IGS/AC** products as reference frame errors can easily exceed the formal errors. The situation is particularly acute for the **IGS Rapid** products where timely availability of data is critical.

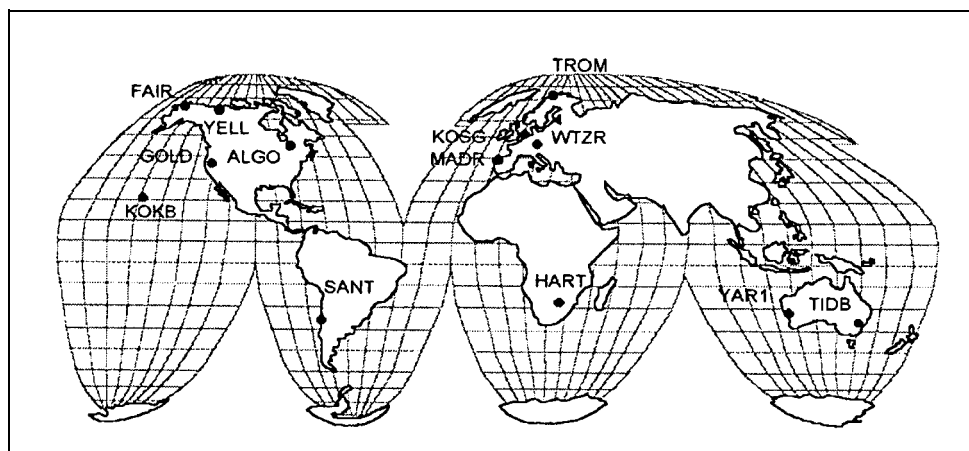


Fig. 1. The set of the 13 **ITRF** stations used by **IGS** for the current **ITRF94** realization

Clearly, a much larger number of **ITRF** stations and more consistent set of **ITRF** station coordinates than the currently adopted **ITRF94** coordinate/velocity set are urgently needed. That is why a search for a new much larger set of **ITRF** station was initiated during the AC Workshop held in March 1997 at JPL. An initial set of about 50, well distributed global stations, was identified as potential candidates at the workshop and the discussions continued by e-mail until August 1997 when a more definitive set of 52 stations was identified and agreed upon by all ACS (Figure 2). All the 52 stations survived a rigorous test and criteria of GPS data and solution quality, consistency and timeliness. Unlike for the 13 **ITRF** station selection, good multi-technique and **ITRF** coordinates, though important, are not as essential as long as there is a sufficient number of multi-technique stations remaining in the station set. This is so because there is already a sufficient number of **GPS-only** stations with a very high level of internal consistency which can effectively and reliably interpolate/realize **ITRF** even when some of the few crucial **ITRF** stations are missing, thus mitigating the current reference frame problems discussed above. Accordingly, this new set is termed reference **frame** (RF) station set, rather than an **ITRF** station set - the term used for the current 13 (**ITRF/multi-technique**) station set. For more details on the RF station list, the selection criteria as well as the individual station “performance”, please refer to Appendix I.

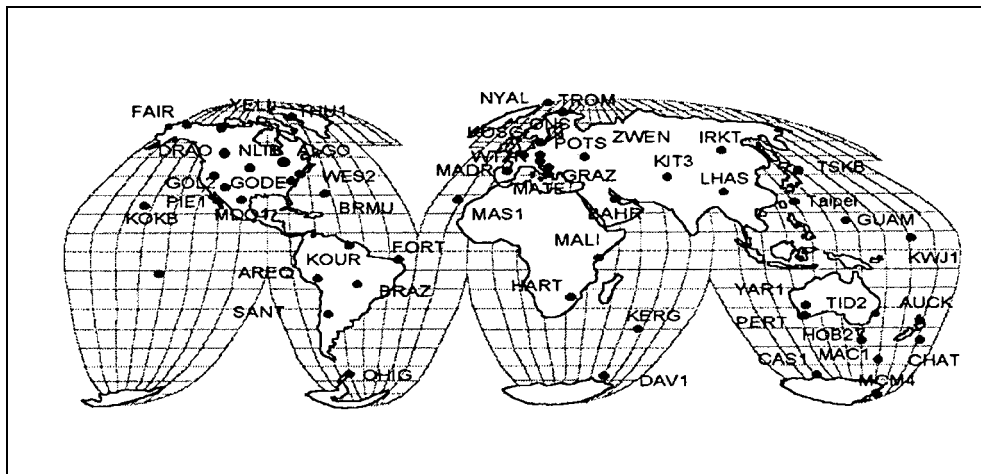


Fig. 2. The Proposed set of 52 Reference Frame (RF) stations for future ITRF realization of IGS

Currently **IGS** does not produce any official (combined) IGS station coordinate product, though it is well positioned to do so thanks to the significant effort invested into the **ITRF** **Densification** Pilot Project (e.g. Kouba, 1997) which is nearing maturity. Based on the earlier discussions here, it is essential that there is also an official IGS station **position/velocity** product (after all it is one of the four “core” products!) which is consistent with the current IGS products (**orbits/EOP/clocks**). Actually the **SINEX** approach developed and perfected in the **ITRF** **Densification** project may significantly enhance IGS **ITRF realization/maintenance**, and even provide the IGS contribution to **ITRF** (see the following sections for more detailed discussions on this subject).

INTERIM (IMMEDIATE) IMPROVEMENTS OF IGS REFERENCE FRAME (ITRF) REALIZATION

During the selection and discussions of RF stations it was contemplated that an a **GPS-only** solution, with properly positioned, oriented and scaled reference frame, would be used for the new IGS **ITRF** reference frame realization. With the release of an improved version of **ITRF (ITRF96)** in August 1997 it became clear that the new **ITRF** version is indeed internally quite consistent with precision comparable to the best **IGS** station position solutions and can be used in place of the 13 **ITRF** stations. Note that, unlike the previous **ITRF** (yearly) realizations of **IERS**, the **ITRF96** datum (i.e. frame positioning, orientation and scale) is supposed to be (at least nominally) the same as that of **ITRF94 (Boucher, 1997, personal comm.; Ray, 1997)**. The final version of **ITRF96**, released in December 1997, has corrected a small misalignment and the time evolution (with respect to **ITRF94**) as well as a few **outliers** contained in the preliminary (August 97) **ITRF96** version (**Altamimi, 1997, pers. comm.**). At the IAG Rio97 Meeting in September 1997 the IERS Directing Board officially accepted **ITRF96**.

A relatively fast and efficient resolution of the current IGS reference frame “crisis” is to replace the 13 ITRF stations with **ITRF96** station coordinate/velocity set for most if not all the selected 52 RF stations. This is only an interim step as it does not address nor incorporate the **ITRF Densification** project and its potential impact and improvements in IGS ITRF realization. Before using the RF station ITRF96 coordinates and velocities they must first be evaluated and tested for precision and consistency. That indeed the new **ITRF96** version is highly consistent with ITRF94 is evident from Table 1, where the **ITRF96/ITRF94** alignment and coordinates/velocities for the 13 **ITRF** stations are compared. As one can see in Table 1, both **ITRF94** and **ITRF96** are almost identical in translation and orientation with the exception of small misorientations (of about -0.2 mas) in **R_x** and **R_z**, which are barely statistically **significant** (the formal sigmas are about 3 mm, 0.1 mas, 0.4 ppb). Even more encouraging is that the rates are practically zeros (equal or less than the formal sigmas of about 1 mm y⁻¹, 0.03 mas y⁻¹, 0.2 ppb y⁻¹). In the second part of Table 1, the alignment of each ITRF94 & 96 is checked with respect to NNR NUVELIA (McCarthy, 1996), using only the respective ITRF station velocities. Also shown are position/velocity rms after the transformations, Both **ITRF** solutions are well aligned in velocity, with nearly zero rates. The differences between ITRF96 and ITRF94 rates in the last line of Table 1 compare quite well to the relative transformation rates in the second line. The formal sigmas for these NNR alignments are about the same as above, i.e. 1 mm y⁻¹, 0.03 mas y⁻¹ and 0.2 ppb y⁻¹. This should be no surprise as **ITRF94** and **ITRF96** time evolution should, by definition, be consistent with the NNR NUVELIA (Boucher, 1990).

Table 1: Transformation ITRF94 to ITRF96 (using the 13 ITRF station positions/velocities)

Epoch	T _x	T _y	T _z	R _x	R _y	R _z	S _{cl}	rms (mm)		
	mm	mm	mm	mas	mas	mas	ppb	dN	dE	dH
Param 1997	0.1	0.5	0.8	-0.190	-0.005	-0.230	-0.5	8.2	8.4	10.5
Rate ./y	-0.5	-0.2	-0.6	0.018	0.033	-0.002	-0.01	2.4	1.3	2.9
Rates with respect to NNR Nuvelia, computed from the velocities of 11 of the 13 ITRF stations; SANT & GOLD excluded due to plate margin effects .										
	mm/y	mm/y	mm/y	mas/y	mas/y	mas/y	ppb/y	rms (mm/y)		
ITRF96	-0.6	-1.8	-0.3	-0.03	0.02	0.02	0.00	1.6	2.2	2.7
ITRF94	0.2	-1.2	-0.6	-0.03	0.00	0.01	0.12	1.7	1.5	2.5
ITRF96-94	-0.8	-0.6	0.3	0.00	0.02	0.01	-0.12			

The **ITRF96** station coordinates of the newly selected 52 RF station set are evaluated in Table 2 and Fig. 3 where the **ITRF96** solution is compared to a combination of more than 100 GNAAC **SINEX** weekly combinations (GPS Weeks 830-933). The weekly GNAAC (**G-SINEX**) files are routinely produced by the three **GNAACs** (i.e. MIT, NCL and JPL) as a part of the **ITRF Densification** Project (Herring, 1997; Davies and **Blewitt**, 1997; **Heflin** et al., 1997). Remi **Ferland** of **NRCAN AC** (formerly EMR) kindly produced this “IGS **SINEX**” combined solutions (labeled here as **IGS97P05**), using his **SINEX** combination

software. As seen from Table 2 and Fig. 3, both **ITRF96** and IGS station positions are highly consistent and precise, at least for the 52 RF station set and for the epoch of 1997.0. The station position rms agreement (after a 14-parameter transformation) is at the 2-mm and 7-mm level for horizontal and vertical directions, respectively. Even for a more representative and useful epoch of 1998.0 the rms agreement is still at about 4-mm horizontal and about 10-mm vertical precision levels, which is significantly better than the **ITRF94/ITRF96** position agreement (see Table 1). For completeness, position rms values for epoch 1999.0 are also shown in Table 2 and Fig. 3. Individual station position residuals are listed in the Appendix II. It is expected that, except for one or two questionable **ITRF96** station velocities, the rms increases for the 1998 and 1999 epochs are largely due to weaker station velocities for the **IGS97P05** solution, since they are based on less than two years of GPS data. This can be seen in Fig. 3 but also in Table 3 where the **ITRF96** and **IGS97P05** station velocity solutions are compared to the NNR **NUVEL1 A** plate motion model.

Table 2: ITRF96 and combined (**IGS97P05**) station coordinates residuals for 52 RF stations at 1997.0 (**IGS97P05-ITRF96**) after 14-parameter transformation.

	Dx	Dy	Dz	dN	dE	dH	Epoch	Excluded from means & sig.
	mm	mm	mm	mm	mm	mm		
Mean	0.4	-0.7	0.1	-0.2	-0.3	0.0	1997	none
Sig	4.9	5.2	5.5	1.6	2.3	7.2		
Mean	1.8	0.4	1.9	0.2	0.0	0.0	1998	AUCK , CHAT dE & MCM4 dH
Sig	7.0	7.8	11.3	3.7	4.2	10.8		
Mean	3.1	1.5	3.6	0.5	0.0	-0.1	1999	AUCK, CHAT dE & MCM4 dH
Sig	10.3	12.6	19.1	6.0	7.2	17.4		

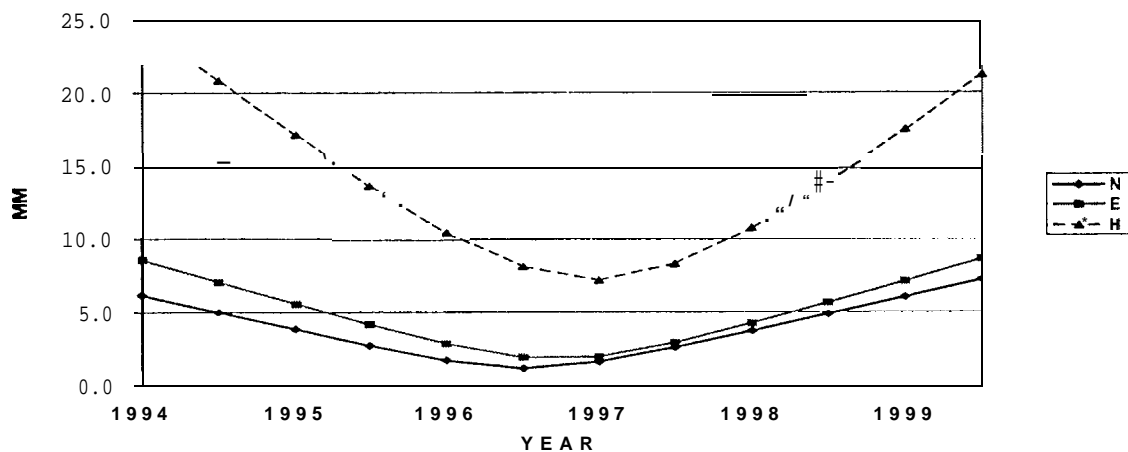


Fig.3: ITRF96 and combined (**IGS97P05**) station coordinates rms for 52 RF stations after a 14-parameter transformation.

While the IGS97P05 horizontal velocities compare equally well to NNR NUVEL1A, the vertical velocities show considerably worse agreement than ITRF96 (i.e. assuming the zero vertical motion which is implied by NNR NUVEL1 A). However, two ITRF96 station velocities (for AUCK and CHAT) appear to be anomalous (see the Appendix III, where individual station velocity residuals are listed), thus likely cannot be included in the new ITRF station coordinate/velocity set. Also, two Antarctic stations (MCM4 and CAS 1) appear to have erroneous vertical ITRF96 velocities. Thus the stations AUCK, CHAT, MCM4 and CAS 1, together with BHR, which has rather large ITRF96 residuals, were not recommended for inclusion into the new ITRF96 station set. Altogether 47 RF stations has been recommended for the new ITRF96 station set (Altamimi, 1998). IGS97P05, in addition to the same two Antarctic stations above, has additional problems with the vertical velocities at stations GRAZ, TROM, NYAL and LHAS (see Appendix III).

Table 3: ITRF96 and IGS97P05 differences from NNR NUVELIA (EURA, NOAM, AUST, ANTA, SOAM Plates) for RF stations (see the Appendix III for specific station exclusions to mitigate plate margin effects on the means and sigmas below).

STATION	PLATE	IGS97P05 - NNR NUVEL1A			ITRF96 - NNR NUVELIA		
		N (mm/y)	E (mm/y)	H (mm/y)	N (mm/y)	E (mm/y)	H (mm/y)
Mean	EURA	1.75	-2.18	3.81	1.37	0.36	0.52
Sigma	EURA	3.50	2.74	9.53	1.89	2.05	1.98
Mean	NOAM	-1.09	0.04	-0.63	-1.07	0.82	-0.52
Sigma	NOAM	1.45	1.80	4.85	1.07	1.52	2.34
Mean	AUST	2.53	-3.93	-3.74	-0.75	4.70	-1.40
Sigma	AUST	2.43	1.91	3.72	3.10	0.74	1.60
Mean	ANTA	-0.98	-3.17	0.75	-4.36	0.05	10.27
Sigma	ANTA	1.97	4.49	17.40	3.77	6.21	10.84
Mean	SOAM	1.12	1.73	3.18	-0.70	2.53	-2.50
Sigma	SOAM	0.57	2.38	4.97	1.42	3.08	6.64

It would be very useful if all ACS compare their best station **position/velocity** solutions to the ITRF96 coordinates/velocities of the 52 RF stations above, in particular for the problematic station solutions in both ITRF96 and/or IGS97P05 solutions. It is hoped that exclusions of stations (e.g. AUCK, CHAT, MCM4, CAS 1, BHR) from the new ITRF96 station set could be finalized at the workshop so that the new RF set of 47 stations could be adopted by IGS and used instead of the ailing 13 ITRF94 stations. It is proposed that this finalized RF station set, with the ITRF96 coordinates/velocities, together with the official **igs.snx** (SINEX Header template of antenna heights), is then used, starting as early as March 1, 1998, as an interim IGS realization of ITRF96. Since some small discontinuities

of about 0.2 mas are expected, it is essential that, as in the past, all ACS and the IGS products make this **ITRF96** change at the same time. Also note that it would be preferable that all ACS use minimum datum constraints (e.g. **Blaha**, 1971), based on this new **ITRF96** set, as recommended in the following sections. It is, however, recognized that, given the rather short time frame and the urgency, the usual (sigma) constraining should be acceptable. Besides, since the new set is highly consistent it is no longer so important (to apply the minimum datum constraints). In fact it may even be advantageous to apply sigma constraints, as the new **ITRF** set may be less prone to systematic effects (biases) than individual, minimally constrained AC and IGS solutions. This is applicable and important to IGS and AC Rapid solutions. Note that **all** stations of the new RF set, including some stations with possibly questionable **ITRF96** collocations, can be used for the new and nearly optimal IGS **ITRF** realization proposed in the next section because the new RF set is so internally consistent. Thus the IGS **ITRF96** realization will be defined by the adopted **ITRF96** positions/velocities of a large subset (47) of the RF stations, together with the current **igs.snx** template containing the antenna heights and offsets, The **igs.snx** file is maintained and available at the following **IGSCB** WWW site:

ftp:/ /igsb.jpl.nasa. gov/igsb/station/general/igs.snx

The adoption of the new **ITRF96** station set should result in significant improvements of stability and precision of all IGS core products and EOPS, in particular.

PROPOSED IGS REFERENCE FRAME REALIZATION AND MAINTENANCE

As already discussed above, it is essential that all **IGS** reference system components, i.e. all IGS combined products, be consistent and precise. In an ideal case this can be accomplished when all the submitted AC solutions are combined in a single rigorous (**SINEX**) adjustment of **all** the **IGS** products as unknown parameters. However this is not possible both for theoretical as well as practical reasons. Namely, strictly speaking, GPS global analyses cannot be (rigorously) subdivided into overlapping portions of networks (stations). In addition, it is very difficult to parametrize global adjustments and yet allow different and innovative approaches, For example, satellite state vectors are generally incompatible amongst ACS unless identical models and (stochastic) error models are employed, and yet satellite **ITRF** positions are largely independent of the modeling effects and thus are better suited for exchange, comparisons and combinations. Only approximations to an ideal and rigorous method are possible. There are several possible approaches, each with varying degrees of **complexity** and approximation.

It is important to free the **IGS** products from changes and errors in the fiducial stations set. These changes can occur either **from** upgrades in **ITRF** or the RF station set, which involved improvement of the relative site positions, or from errors either due to blunders at the AC's or due to unplanned configuration changes at fiducial sites. All of these have occurred in the last few years with the 13 **ITRF** stations, Therefore it is suggested to ACS and to GNAACS that always only minimum constraints (not "sigma constraints") are used

in the final solutions. The ITRF frame is then realized from a Helmert transformation of unconstrained solutions with proper outlier detection in the computation of the transformation parameters. This means a site by site review of station residuals after the transformation, and editing out any outlying site, and re-computing the transformation. This makes it possible to reduce or remove the “warping” like effect of an anomalous site. As seen from the above discussion, it is essential for precise, robust solutions in a consistent reference frame to have a large set of highly consistent RF station set.

Another relatively simple but well proven approach is an extension to the IGS combination of the “fiducial free” method which has been developed and used at JPL for a number years (see e.g. Jefferson et al., 1997). Here “fiducial **free**” orbit solutions are requested and then combined, resulting in a “fiducial free” **IGS** orbits **and** clocks. Then using a sufficiently large and well-distributed subset of **IGS** stations with the combined “fiducial **free**” orbits held fixed in a regular global analysis for “fiducial free” station positions and **other** pertinent parameters. In order to economize, the **new** precise point positioning approach can be used here, provided that the IGS clock information is precise, consistent and frequent enough. Finally, a reference frame is attached, **i.e. the** “fiducial free” combined orbits are transformed according to the transformation between the “fiducial free” station positions and the adopted set of **ITRF** stations. The advantage of **this** approach is the relative insensitivity to problems or changes of **ITRF** (i.e. “fiducial”) stations of the individual AC orbit solutions; i.e. the corresponding AC “fiducial free” station solutions need not to be used. However, the disadvantages are that the method does not use the valuable information contained **in AC station/EOP SINEX** solutions. The current orbit (and future station) reference frame consistency feedback to ACS, contained in the current **IGS** summary Tables 1, 2 and 4, would not be possible. Furthermore, the method relies on single software to provide the **station/orbit** datum connection, which could potentially result in a decrease of reliability and precision; and there is additional processing workload at the raw data level (even when the efficient point position method is used).

The approach highlighted here is based on a nearly rigorous (**SINEX**) combination of station **positions/velocities/EOP** (Blewitt et al., 1997). **It** is a method endorsed by the recent **IERS/ITRF** workshop held in October 1996 in Paris, Fr. (Reigber and Feissel, 1997). It was developed during the **ITRF densification** pilot project, thus it is fully compatible with the project. It also closely approximates a simultaneous adjustment of all the core IGS products, i.e. **orbits/EOP/clocks** and stations, while it maintains the core product consistency, as long as the submitted AC products themselves are consistent. The scheme is outlined below:

a. First, assume that **all** the submitted AC core solutions -- i.e. **orbits/clocks/EOP** (in SP3 and ERP files) and **A-SINEX** files also containing EOP -- are consistent, either unconstrained, or minimum datum constrained. For a detail description of the method of the minimum datum constraints see (e.g. Blaha, 1971; Vaníček and Krakiwsky, 1982, p.275). Note that this condition is not currently satisfied.

b. All the **A-SINEX** files (with **station/EOP**) are combined weekly by GNAACS and the resulting combinations (**G-SINEXes**) are then timely submitted (with **EOP!**) for a weekly **IGS** cumulative, unconstrained solution for station **position/velocities** and **EOP** (for the current week **EOP** only). This combination is called “accumulated kinematic solution” in **Blewitt et al. (1997)**. Note that the **A-SINEXes** could alternatively be used here, but this may not be optimal, as it would not take advantage of the **GNAAC** combinations, thus potentially it could be less robust and precise. This combination of **G-SINEXes** is, in fact, equivalent to a simultaneous **station/velocity** adjustment of all **A-SINEXes**, or all the GPS data accumulated **from** the start to the current week.

c. An ITRF reference frame is then attached to the unconstrained IGS combined SINEX solution of **station/velocity** and **EOP** (of the current week only). The reference **frame** attachment can be e.g. accomplished by minimum datum constraints, based on the soon to be finalized list of 47 RF stations with good ITRF96 positions/velocities. (See the previous section for detail discussions on the **ITRF96** station set). Altogether 14 minimum datum constraints are required (7 **Helmert** parameters and the corresponding rates). The values and sigmas used (derived at least from the **ITRF96** sigmas (or matrix) and the IGS matrix) should be entered in the **SINEX apriori** block, so that the original unconstrained SINEX file can be recovered. The above constrained file can be designated e.g. as **IGS(SSC/SSV/EOP)yyPww** (**yy-year; ww-the** week of the year), and considered the official (Final) IGS station/position and **EOP** product, and it would, in fact, represent the current and official **IGS** realization of **ITRF** as well. Note that **Blewitt et al. (1997)** also propose independent weekly combinations which, once ITRF is attached in a way which is consistent to the accumulated solution above, represent another type of IGS realization of **ITRF**. This discrete (weekly) realization should have a distinct **IERS** designation, e.g. **IGSyyPwww**, here **www** could stand for the GPS week.

d. Using the weekly **A-SINEXes** (the short (**SSC**) AC **SINEX** files would be preferred here) a 7-parameter transformation between the **IGSyyPww** above and each of the AC solutions is computed. The AC transformation parameters are then used to transform the submitted AC orbits and **EOP** (one transformation per each week and AC) to be consistent with the **IGSyyPww**. Furthermore, the AC orbits for each day are rotated according the AC PM differences between AC and **IGS EOP** (of step c, i.e. the **IGS(EOP)yyPww**), very much as it used to be done during the initial years for the IGS Rapid using **IERS Bull A** and the **IGS** Final using **IERS Bull B** orbit combinations (**Beutler et al., 1995**), Note that here, in place of or in addition to the daily PM rotations, full 7-parameter transformations can also be applied to AC orbit, while maintaining the history of transformation parameters in Tables 1 and 2 of the IGS (Final) combinations. This forms an important AC feedback on solution datum connections and consistency amongst orbit, **EOP** and station coordinate solutions. The check of consistency here is that the weekly mean PM **x, y** differences and the corresponding **Ry, Rx** rotations are statistically the same.

e. Finally, the transformed AC orbits (i.e. weekly by the 7-parameter transformations and daily by the AC PM **y,x** differences) are then combined into the consistent **IGS** orbits. Subsequently the AC clocks are corrected for the **AC-IGS** orbit radial differences as it is

already being done for the current IGS **orbit/clocks** combinations.

In this way, a new and unique official **IGSyyPww SINEX** product would be introduced which would also contribute to much higher consistency of the other IGS core products as **well** as more precise and stable **IGS ITRF** realization (through the **IGS** core products) than it is the case today. ACS would be well advised to use the **IGSyyPww station position/velocities** of RF stations for their ITRF needs, in particular for the AC and IGS Rapid solutions. In fact the above concept of ITRF realization is, due to its complexity and inherent delays, only practical for the IGS Final products. Timely (i.e. the weekly) **IGSyyPww station/EOP** solutions would greatly benefit all IGS users and the AC Rapid analyses and the **IGS** Rapid products generation in particular, including the **IGS** timely contributions to **ITRF**. When attaching a reference frame to the IGS Final **SINEX** “cumulative kinematic” solution it is important that the accumulation include weekly solution for geocenter and scale and this information is also entered into the in **IGSyyPww SINEX** file. This way a precise geocenter and monitoring is maintained as well as unique and exact (i.e. stable with no drift) reference frame attachment is enforced.

It should be noted here that the above “accumulated kinematic solution” (IGSyyPww) is optimal in terms of station positions/velocities only, as it uses all past and present GPS data in a rigorous way (Helmert blocking). While, the above proposed orbit solutions with minimum or no constraints (i.e. “fiducial free”) are, strictly speaking, sub-optimal as only GPS data from the current day or week is utilized in AC orbit solutions. The IGS (Final) orbit solution would be optimal only if the IGSyyPww position/velocity matrix (of the previous week) is used for constraining in the AC solutions (of the current week) in this way all data, including the past data are used in a rigorous way.

Although the AC solutions, constrained according to sigmas as it is currently done by most ACS, or according to the **IGSyyPww** matrix, can in principle, be used here, it is recommended that AC apply minimum or no datum constraints in all AC Final solutions. Currently, the sigma/matrix constraining can potentially introduce small reference frame inconsistency even when a highly consistent and precise station coordinate set such as the future **IGSyyPww** set is used. This situation, as discussed above, should change fairly quickly with proper and efficient feedback on AC **orbit/EOP** and station solution consistency and frame relative biases, That is why the proposed scheme of orbit combination (“back-substitution”) and the question of sigma/matrix versus minimum or no constraints in AC Final solutions, should be reviewed after several years of operation of the proposed scheme, or when AC Rapid solutions that use **sigma/matrix** become more precise and stable than the corresponding AC Final ones.

For the **AC/IGS** Rapid solutions, the **sigma/matrix** constraining of RF stations with **IGSyyPww** positions/velocities, could be quite acceptable or even desirable due to lack of data availability. Besides it is only meaningful to maintain and realize IGS realization of ITRF from more definite and also more precise **IGS/AC** Final solutions. By using the recent **IGSyyPww** station positions/velocity maximum consistency between **IGS** Rapid and Final products is ensured. Note that regardless of which method of constraining ACS

choose (unconstrained, minimum) to apply for their Final solutions, their **orbit/EOP/clocks** (i.e. SP3 and **ERP** files) must be transformed to be consistent with the corresponding weekly AC **SINEX/EOP** files.. This should not be a major effort, and in fact should have been enforced from the beginning, and besides, it has already been the case for some ACS for several years now! (See the Appendix VI for more detail information and practical suggestions on AC product consistency).

It is important that a unique (and official) IGS station polyhedron product is established, In that regard it would be preferable if the **GNAAC** polyhedron combinations (i.e. **P-SINEXes**) are used instead of **G-SINEXes** in the step *b* above, however the use of **P-SINEXes** would introduce delays of up to several weeks which may not be acceptable. Besides it is advantageous that RNAACS, as it is currently required, use the IGS Final **orbit/clock/EOP** products in their (**R-SINEX**) analyses. In this regard, it is far more efficient and convenient to obtain an official IGS station polyhedron product (**P-SINEX**) by a back substitution, using the above IGSyyPww global solution. The **IGSP-SINEX** products would then have the same IERS designation, i.e. **IGSyyPww**.

SUMMARY AND RECOMMENDATIONS

It is essential that all the **IGS** products are made highly consistent and in particular the **IGS** core products (i.e. **orbits/EOP/clocks** and station positions) must be consistent as they are used in various combinations for different applications or realizations of the **IGS** reference frame. This necessitates that all the AC core products submitted to IGS and IERS must be self-consistent, The urgent need for a larger and more precise **ITRF** station set than is the case for the currently used 13 **ITRF94** stations can quickly and sufficiently be met by adopting **ITRF96** positions/velocities of a new **ITRF** set of about 47 stations. This interim step should be adopted as early as March 1, 1998.

A new and nearly optimal **ITRF** realization should utilize the **GNAAC** combinations. It is nearly optimal in terms of station positions/velocities and EOPS; in fact it is the same approach recently recommended by IERS for simultaneous solutions of EOP and positions. In order to increase the IGS product consistency and to prepare ground for adaptation of the new approach of **ITRF** realizations, the following recommendations are offered for consideration to the workshop:

1. That IGS adopts **ITRF96** as early as March 1, 1998 to replace the currently ailing and problematic IGS realization of **ITRF94**, which currently is based only on less than 13 **ITRF** stations.
2. As an interim measure and to facilitate an immediate **ITRF** realization improvement it is recommended that the selection of the new **ITRF96** station positions and velocities for a large subset of the RF station is finalized at this workshop. This newly selected **ITRF96** set of the 47 globally distributed IGS stations is to be used for **ITRF96** realization in all IGS products beginning as early

as March 1, 1998. IGS realization of ITRF is then accomplished by the above ITRF96 station coordinates/velocities together with the current official **igs.snx**, which contains antenna offset and height information in the **SINEX** format.

3. That all weekly submitted AC **SINEX** solutions (A-SINEXes) contain the EOP of the current week and that the submitted AC orbits/clocks (**sp3**) and EOP (**erp**) files are consistent with the above A-SINEX solutions. This is essential not only for the increased **IGS** product consistency but also for the future (improved) ITRF realization and IGS products. It is recommended that this is implemented and ensured by all ACS by June 28, 1998.
4. That the **GNAAC** combinations retain (and adjust) the submitted AC EOP information of the current week in their **G-SINEX** combined products, along with the usual station position solutions. It is recommended to be implemented by June 28, 1998.
5. The **SINEX** extensions as outlined in the Appendix IV, allowing the minimum datum and transformation parameter constraints to be coded in the **SINEX format**, are accepted and used by IGS on or before March 1, 1998. Furthermore, that IGS submits the **SINEX** extension for acceptance to Prof. Tom Herring of **CSTG**, who is currently responsible for the **SINEX format**. This will provide a means and encouragement to ACS and other IGS users to use (minimum) datum constraints, as well as it allow an **efficient** and safe monitoring of geocenter and scale changes (e.g. Ray, 1997). It is further recommended that only the AC Final products, which are based on minimum or no datum constraints, be accepted for the **IGS Final orbit/clock/EOP/station** combinations after June 28, 1998. (See the Appendix V for more details and suggestions on coding the minimum datum constraints in the AC (A-SINEX) submissions).
6. That a (super) combination of **G-SINEXes** for station coordinates and EOP is researched and initiated on behalf of IGS. This EOP (**G-SINEX** combination) cumulative solution would replace the current IGS EOP combination and it would lead to an official **SINEX** station solution product (both for global as well as the polyhedron stations). The polyhedron **SINEX** solutions could be produced by back substitution when P-SINEXes are made available to produce the **IGS P-SINEX** products (station **positions/velocities** only). The implementation goal should also be by June 28, with the **official IGS SINEX (G and P)** products on or before January 3, 1999!

Remarks: The current **IGS orbit/clock** combination would require only minor modifications, i.e. the prior transformations based on one set of (up to 7) transformation parameters for each week and AC, and for each AC a pair of **daily PM x,y** difference rotations (and/or up to 7 transformation parameters), all with respect to the current **IGSyyPww SINEX** solution. This step **can** be viewed as an approximation of a back substitution adjustment process for the (IGS Final) satellite orbit solutions. Due to annual

and semiannual effects for some stations in most current AC solutions (see the AC poster presentations at this workshop), it is mandatory that, until these effects are removed or mitigated, that the new **ITRF** realization use only the **IGSyyPww** solutions that are only derived from an exact multiple of years.

REFERENCES

Altamimi, Z. , 1998, IGS Reference Station Classification Based on **ITRF96** Residual Analysis, *1998 IGS AC Workshop* held at ESOC Darmstadt, February 9-11.

Beutler, G., J. Kouba and T. Springer, 1995, Combining the orbits of the IGS Analysis Centers, *Bull. Geod.* **69**, pp. 200-222; also in the *Proceedings of the IGS Analysis Center Workshop*, held in Ottawa, Canada, October 12-14, 1993, pp. 20-56,

Blaha, G., 1971, Inner adjustment constraints with emphasis on range observations, *Depart. Of Geodetic Science Report 148*, The Ohio State University, Columbus, Oh., U.S.A.

Blewitt, G., Y. Bock and J. Kouba, 1994, Constructing the IGS Polyhedron by Distributed Processing, *Proceedings of the IGS workshop on the ITRF densification*, held at JPL, Pasadena, Cal., Nov. 30-Dec 2, pp.21-36.

Blewitt, G., C. Boucher and J. Kouba, 1997, Procedure for **ITRF** continuous realization, the report to the IGS GB, a draft dated Sep. 15, 1997, distributed to all ACS on November 14, and presented to The IGS Governing Board Meeting held in San Francisco, Cal on Dec. 11.

Boucher, C, 1990, definition and realization of terrestrial reference systems for monitoring Earth rotation, in *variation in Earth rotation*, D.D. McCarthy and W.E. Carter(eds.), pp. 197-201.

Boucher,C, Z. Altamimi and L. Duhem, 1994, Results and Analysis of the **ITRF93**, *IERS Technical Note 18*, Observatoire de Paris, October,

Boucher, C, Z. Altamimi, M. Feissel and P. Sillard, 1996, Results and Analysis of the **ITRF94**, *IERS Technical Note 20*, Observatoire de Paris, March,

Davies, P. and G. Blewitt, 1997, Newcastle-upon-Tyne IGS GNAAC Annual Report 1996, *International GPS Service for Geodynamics (IGS) 1996 Annual Report*, pp. 237-252.

Gendt, G., 1996, Comparison of IGS Tropospheric Estimations, *IGS AC Workshop Proceedings*, Silver Spring, Md, March 19-21, pp.151-164.

Gendt, G., 1998, IGS Combination of Tropospheric Estimates – Experience From Pilot Experiment, *1998 IGS AC Workshop* held at ESOC Darmstadt, February 9-11.

- Heflin, M.B., D.C. Jefferson, M.M. Watkins, F.H. Webb and J.F. Zumberge**, 1997, Comparison of Coordinates, Geocenter, and Scale from All IGS Analysis Centers: GNAAC Activities at the Jet Propulsion Laboratory, *International GPS Service for Geodynamics (IGS) 1996 Annual Report*, pp. 253-254.
- Herring, T.A.**, 1997, MIT T2 Associate Analysis Center Report, *International GPS Service for Geodynamics (IGS) 1996 Annual Report*, pp. 255-270.
- Huot, C., P. Tetreault, Y. Mireault, P. Heroux, R. Ferland, D. Hutchison and J. Kouba**, 1998, IGS Related Activities at the Geodetic Survey Division, Natural Resources Canada, "EMR" Analysis Center poster presentation, *1998 IGS AC Workshop* held at ESOC Darmstadt, February 9-11.
- Jefferson, D. C., M.B. Heflin, M.M. Watkins and F.H. Webb, J.F. Zumberge, Y.E. Bar-Saver**, 1997, Jet Propulsion Laboratory IGS Analysis Center Report, *International GPS Service for Geodynamics (IGS) 1996 Annual Report*, pp. 183-192.
- Kouba, J.**, 1997, Status of The IGS Pilot Project to Densify the ITRF, *International GPS Service for Geodynamics (IGS) 1996 Annual Report*, pp. 101-116.
- Kouba, J. and Y. Mireault**, 1997, Analysis Coordinator Report, *International GPS Service for Geodynamics (IGS) 1996 Annual Report*, pp. 55-100.
- McCarthy, D.D.** (cd.), 1996. IERS Conventions (1996), *IERS Technical Note 21*, Observatoire de Paris, July.
- Ray, J.**, 1997, IERS Geocenter Campaign /IERS Working Group on the ITRF Datum, see <http://maia.usno.navy.mil/geoc.html>.
- Ray, J.**, 1998, The IGS/BIPM time transfer project, *1998 IGS AC Workshop* held at ESOC Darmstadt, February 9-11.
- Reigber, C. and M. Feissel.** (cd.), 1997, IERS missions, present and future, Report on the 1996 IERS Workshop, *IERS Technical Note 22*, Observatoire de Paris, January.
- Schaer, S. and J. Feltens**, 1998, Position paper on IGS ionospheric delay products, 1998 *IGS AC Workshop* held at ESOC Darmstadt, February 9-11.
- Springer, T., J.F. Zumberge and J. Kouba**, 1998, The IGS Analysis Products and Consistency of Combination Solutions, 1998 *IGS AC Workshop* held at ESOC Darmstadt, February 9-11,
- Vaniček P. and Krakiwsky, E.J.**, 1982, *Geodesy - The Concept, The North* Holland Publishing Co., Amsterdam, New York, Oxford.

Zumberge, J. F., M.B. Heflin, D.C. Jefferson, M.M. Watkins and F.H. Webb, 1997, Precise point positioning for the efficient and robust analysis of GPS data from large networks, *Journal of Geophysical Research (JGR)*, Vol. 102, No. B3, pp. 5005-5017.

APPENDIX I

(August 15, 1997)

ITRF station selection criteria. (For fuller explanations, see the Remarks at the bottom of the table.)

- 1) Stable and permanent monumentation, possibly with local stability nets (not used, but see Remarks below)
- 2) ACS *not* including site in SINEX submissions
- 3) High quality and reliable station hardware
- 4) Performance including timely data communications; based on igsnet and G-SNX GCOMP Reports: >0 - above, <0 below average; (#)- # of inclusions in GCOMP (=22 max; 0- local or not operating station (wk 0878-900))
- 5) Favorable station data quality (RFI, multipath, etc.) based on igsnet includes phase/Code quality: >0- above; <0 below average.
- 6) Supportive and responsive station staff
- 7) Good quality ITRF94 position and velocity
- 8) Multi-techniques collocations (R=VLBI, L=SLR, D=DORIS G= absolute G)
- 9) Established GPS observing history (> 2 years) (not used)
- 10) Comments from CODE Analysis Center

CODE	1)	2)	3)	4)	5)	6)	7)	8)	9)	10)
	Used	Hrdw.	Perf.	Qual.	Staff	ITRF	Tech.			AC
----- ----- ----- ----- .---. ----- ----- ----- ----- -----										
[For explanation of notations, see Remarks below]										

Europe:

*KOSG			R12	1.0(22)	0.6		A	1		Move !
* MADR			R8	-.5(4)	-1.7	X	A	R		x
MATE	r,e,j,s		TR	-1.3(11)	-1.7		A	RL		
NYAL	r		R8	-5.6(7)	-3.1		B	R D		x
ONSA	r,j		TR	0.7(22)	0.5		A	R		
* TROM			R8	-3.0(13)	-3.0		B	E-V r		Rec.
VILL	c,r,g,j,n,s		TR	2.5(0)	0.7		NONE			x
*WTZR			TR	0.1(22)	0.0		A	RL		
GRAZ			TR	-1.7(2)	-1.7		A	L		
POTS			TR	1.9(16)	1.9		A	L		
ZWEN			TR	-4.7(16)	-0.8		NONE			

Asia:

KIT3			TR	-0.3(13)	0.2		CT	D		
SHAO	r,g		TR	0.3(15)	0.2		CT	RL		
TSKB			TR	2.3(19)	0.6		B	r		
IRKT			TR	-2.0(9)	0.5		NONE			
LHAS			TR	-1.3(16)	-0.5		NONE			

Africa/Arabia :

BAHR	r,e,n,s	Z12	0.9(5)	-0.2		NONE		New
* HART		TR	-0.7(18)	0.0		B	RLD	
MALI		RC	-4.3(8)	-3.7		NONE		Rec.
MAS1	r,n,j,s	TR	N/A (to be completed ASAP)			ASAP)		

N. America

*ALGO		TR	2.7(22)	0.6		B	R	
BRMU	r,j	TR	2.7(22)	0.6		CT	r	
DRAO	e,j	TR	2.6(15)	0.7		z	r	
*FAIR		R8	2.6(20)	0.6		B	R D	x
* GOLD		R8	-1.6(19)	-1.6	x	CT	RLD	x
MDO1	r,j,s	TR	2.3(20)	0.6		A	RL	
NLIB	r,e,j,s	TR	2.1(6)	0.7		B	R	
PIE1	r,e,g,n,s	TR	2.6(0)	0.7		B	R	
THU1	r,e,n	R12	-0.6(0)	0.7		NONE		
*YELL		TR	2.0(22)	0.1		B	R D	
GODE		TR	2.4(0)	0.6		A	rL	
WES2		TR	1.3(20)	0.3		dU=4cm	Rl	

S. America

AREQ		TR	-1.0(17)	0.4		B	L D	
FORT		TR	-0.5(18)	-0.5		B	R	
* SANT		TR	1.1(17)	-0.3		B	R D	
BRAZ		TR	-1.3(12)	-0.3		NONE		
KOUR		RC	0.1(14)	-1.9		B	D	Rec.

Astralia:

HOB2	r,e	TR	-2.0(18)	-0.2		CT	R	
*TID2		TR	2.2(21)	0.7	x	?	RLD	x
*YAR1		R8	-2.1(21)	-1.9		B	LD	Rec.
MAC1	r	TR	-1.4(12)	0.1		NONE		
PERT		TR	2.4(22)	0.6		NONE		
CHAT		TR	0.4(2)	-0.2		NONE		
AUCK		TR	1.3(0)	0.2		NONE		

Antarctica:

CAS1	r,e	TR	-1.1(20)	0.0		c		
DAV1		TR	-1.4(17)	-0.4		c		
KERG		RC	-2.5(19)	-2.3		B	D	Rec.
MCM4		TR	1.7(19)	0.4		c		
OHIG	r	TR	-2.3(18)	-1.0		z	R	

Pacific

* KOKB		TR	2.2(21)	0.5	B	R D	
KWJ1	r	TR	2.4(2)	0.6	NONE	r	New
GUAM		TR	1.0(12)	0.5	NONE	D	

* current fiducial stations

=====
Columns Remarks:

- 1) Some stations have large antenna heights (> 2m) eg, NYAL, TROM, BAHR HART and MATE is mounted on a roof.
- 2) This column lists the analysis centers not using the station. The Information was obtained from the AC's weekly analysis report. (Letter code represents first letter of AC's name except for EMR which is "r")
- 3) Hardware codes are:
 - r8 for big rogue,
 - RC for mini rogue,
 - TR for 8 channel turborogue
 - R12 for 12 channel turborogue
 - Z12 for 12 channel ashtech
 - TE for 8 channel Trimble SSE
- 4) and 5) The code used are the average of the "igsnet" latency and **quality** code respectively. The average was computed using 4 randomly selected weeks of 1997.
- 6) X = poor response, likely should not be recommended
- 7) A = Class A: collocated sites with quality <2 cm at 1988 and 1993
 B = Class B: collocated sites with quality <3 cm at 1993
 c = Class C: not Class A or B, with no large residuals
 Z = Class Z: sites with large residual (blunder or poor determination); DRAO & OHIG have large height discrepancies
 T = local tie to GPS not available
 ? = TID2 not in ITRF94 (although TIDB is) and no site log available
 NONE = not included in ITRF94
 E-V = East velocity inconsistency with VLBI
 dU=4cm = GPS vs. VLBI height discrepancy of -4 cm at WES2
- 8) R=VLBI, L=SLR, D=DORIS G=absolute G; lower case letters indicate mobile site, poor data quality, or discontinued operations
- 10) X-means : Do NOT use as fiducial station.
 - New Relatively new station
 - Rec. Receiver change necessary (big or mini rogue)
 - Move Site will be moved!
 KOSG will be moved to Westerbork (tens of kilometers away).

However there will be something like a year "overlap" using both receivers; the old one in KOSG and new one at new site Westerbork.

=====

NOTE BY JF Zumberege's performance & quality coefficient determination

Col. 4:

Based on 169 daily IGSnet reports spanning the period October 12, 1996 through April 11, 1997, we show in Table 1 a summary of statistics. Scores from each of the following three categories have been normalized to zero mean and unit sigma: (1) number of times the site occurred with non-trivial entry in the daily IGSnet reports; (2) the quality field from the daily report; and (3) the latency field from the daily report (only nonzero latencies are considered). The sum of the three normalized numbers is then averaged for each site. Roughly, positive scores are above average.

Col. 4 (xx) # of weeks station survived GCOMP's (max 22); see GCOMP for rejection criteria

Col.5 the same as Col 4. except that only IGSnet quality considered

APPENDIX 11

ITRF96 and combined (IGS97P05) station coordinates residuals for 52 RF stations at 1997.0 (IGS97P05-ITRF96) after 14-parameter transformation.

1997.0 IGS97P05-ITRF96	(nun)					
	Dx	Dy	Dz	dN	dE	dH
ALGO	-1.0	0.0	-2.2	-1.4	-1.0	-1.8
AREQ	-0.4	-6.7	1.1	2.8	-2.5	5.7
AUCK	13.7	4.6	8.6	-0.9	-5.8	-15.7
BAHR	-7.0	-7.1	-5.4	-0.5	0.9	-11.3
BRAZ	0.8	-1.7	1.9	2.3	-0.5	1.2
BRMU	-0.6	-0.3	-0.9	-0.8	-0.7	-0.5
CAS1	-3.1	4.8	-10.6	0.8	1.2	11.9
CHAT	3.9	8.9	3.1	-0.8	-8.7	-5.4
DAV1	-2.6	3.8	-1.6	2.4	3.3	2.6
DRAO	1.2	-0.8	-2.5	-1.7	1.4	-1.8
FAIR	3.7	1.3	-7.7	0.2	0.9	-8.6
FORT	-1.4	-0.5	1.5	1.4	-1.3	-0.9
GODE	5.5	-15.3	10.7	-1.8	1.8	19.2
GOL2	2.4	-5.1	1.9	-0.4	4.5	4.0
GRAZ	-13.3	-4.3	-14.3	0.4	-0.6	-20.0
GUAM	-1.1	-1.8	-1.2	-1.2	2.2	-0.4
HART	-0.1	-0.5	-3.5	-3.3	-0.4	1.3
HOB2	0.1	1.0	-3.5	-2.3	-0.9	2.7
IRKT	-1.6	0.8	1.2	-0.1	1.3	1.6
KERG	-4.7	0.4	3.0	1.1	4.6	-3.0
KIT3	1.2	-2.0	-1.1	0.0	-1.8	-1.7
KOKB	5.0	0.3	-3.9	-1.8	1.4	-5.9
KOSG	-1.1	-1.1	-1.3	0.2	-1.0	-1.8
KOUR	1.4	-9.8	1.9	1.1	-4.8	8.8
KWJ1	2.2	-2.8	-2.8	-2.4	2.3	-3.1
LHAS	0.4	19.6	9.6	-1.3	-0.7	21.8
MAC 1	0.1	3.5	-1.2	0.2	-3.3	1.7
MADR	-2.7	3.1	-9.9	-5.7	2.9	-8.7
MALI	-2.5	-0.1	-0.2	-0.3	1.6	-2.0
MAS1	-3.6	0.7	-2.6	-0.6	-0.3	-4.4
MATE	-0.4	-1.4	-1.1	-0.3	-1.2	-1.3
MCM4	1.2	0.9	5.9	0.3	-1.1	-4.9
MDO1	0.5	-2.3	1.7	0.4	1.0	2.7
NLIB	0.7	-1.7	0.4	-0.8	0.7	1.5
NYAL	1.8	-0.8	6.7	-0.3	-1.1	6.9
OHIG	0.3	-4.6	0.0	3.6	-2.2	1.8
ONSA	1.5	0.0	4.0	1.0	-0.3	4.2
PERT	2.8	1.1	-0.5	-0.6	-3.0	0.1
PIE1	-0.7	-6.7	5.5	0.9	1.5	8.5
POTS	-1.6	-1.0	-1.8	0.3	-0.6	-2.5
SANT	0.2	-0.8	4.2	4.0	-0.1	-1.6
SHAO	-0.5	-0.6	-0.6	-0.3	0.7	-0.6
THU1	0.9	-2.7	4.5	-1.8	-0.1	5.1
TID2	5.3	-3.4	3.4	-0.9	0.2	-7.1

TROM	1.4	0.8	6.4	0.8	0.3	6.5
TSKB	0.1	-0.7	-0.5	-0.1	0.5	-0.7
VILL	-3.7	0.4	-2.1	0.8	0.1	-4.2
WES2	-2.3	-3.0	2.6	0.5	-3.1	3.3
WTZR	-2.3	-1.2	-2.1	0.6	-0.6	-3.2
YAR1	-0.3	8.7	-4.3	0.1	-3.5	9.1
YELL	2.2	2.2	-7.0	-0.7	1.1	-7.6
ZWEN	-3.5	0.1	-3.3	0.4	2.2	-4.3

Mean	0.4	-0.7	0.1	-0.2	-0.3	0.0	Epoch Excluded 1997 none
Sig	4.9	5.2	5.5	1.6	2.3	7.2	
Mean	1.8	0.4	1.9	0.2	0.0	0.0	1998 AUCK, CHAT
Sig	7.0	7.8	11.3	3.7	4.2	10.8	dE, MCM4 dH
Mean	3.1	1.5	3.6	0.5	0.0	-0.1	1999 AUCK, CHAT
Sig	10.3	12.6	19.1	6.0	7.2	17.4	dE, MCM4 dH

APPENDIX III

ITRF96 and IGS97P05 differences from NNR NUVEL1 A for RF stations. (* stations excluded from the averages and sigmas below)

STATION PLATE		IGS97P05- NNR NUVEL1A			ITRF96 -NNR NUVEL1A		
		N (mm/y)	E (mm/y)	H (mm/y)	N (mm/y)	E (mm/y)	H (mm/y)
GRAZ	EURA	0.7	-1.7	22.9	1.1	1.5	0.8
KOSG	EURA	2.2	-4.1	-0.3	0.6	-0.4	0.8
MADR	EURA	-7.0	1.9	-1.6	-0.5	1.4	3.9
VILL	EURA	-1.8	-4.7	-9.1	-0.9	0.1	1.5
WTZR	EURA	1.5	-3.3	-2.3	-0.3	0.7	-2.4
POTS	EURA	1.8	-3.2	-1.1	0.5	0.7	4.2
ONSA	EURA	1.7	-3.7	3.6	-0.6	-0.7	0.1
MATE	EURA	7.1	-2.8	2.6	5.6	2.3	-0.7
TROM	EURA	4.8	-6.0	19.5	3.0	-3.8	-0.8
NYAL	EURA	1.5	-4.0	14.8	1.1	-1.4	-2.0
ZWEN	EURA	5.5	-0.7	3.7	2.4	-1.8	-0.5
IRKT	EURA	1.0	3.1	1.8	2.6	2.3	-0.1
KIT3	EURA	3.8	0.9	-5.0	3.3	4.0	1.8
SHAO *	EURA	0.9	6.9	1.4	-0.6	10.2	-1.0
TSKB*	EURA	5.8	-26.7	-4.1	4.6	-21.0	-5.3
Mean	EURA	1.75	-2.18	3.81	1.37	0.36	0.52
Sigma	EURA	3.50	2.74	9.53	1.89	2.05	1.98
ALGO	NOAM	-1.9	0.4	-1.1	-2.2	1.2	-0.5
DRAO	NOAM	0.0	0.3	0.5	1.5	2.7	1.2
FAIR	NOAM	-3.4	1.4	-8.1	-2.4	2.3	-0.1
GODE	NOAM	-2.5	0.8	-3.3	-0.4	-2.1	-3.8
MDO1	NOAM	-0.9	0.7	-5.2	-1.5	1.4	2.0
NLIB	NOAM	-0.6	-0.3	-3.7	-1.2	0.9	-3.7
THU1	NOAM	-2.6	-0.4	9.0	-0.7	-1.9	-3.8
PIE1	NOAM	0.4	0.0	0.1	-1.5	1.0	1.2
WES2	NOAM	1.4	-5.0	6.0	-1.9	1.2	-1.4
BRMU	NOAM	-1.6	0.9	0.3	-0.5	0.8	2.4
YELL	NOAM	-0.3	1.5	-1.4	-0.9	1.7	0.7
GOL2*	NOAM	5.8	-6.0	-9.7	6.8	-2.5	0.1
Mean	NOAM	-1.09	0.04	-0.63	-1.07	0.82	-0.52
Sigma	NOAM	1.45	1.80	4.85	1.07	1.52	2.34
HOB2	AUST	2.6	-5.1	-5.9	1.5	5.2	-1.1
PERT	AUST	2.0	-4.2	-3.8	-3.4	4.9	-0.1
TID2	AUST	5.7	-1.1	-6.8	2.3	5.1	-3.7
YAR1	AUST	-0.2	-5.3	1.5	-3.5	3.6	-0.6
AUCK*	AUST	2.9	-4.8	-8.8	2.3	17.1	-0.6
MAC1*	AUST	-16.0	-6.7	-6.6	-17.9	3.8	0.8
Mean	AUST	2.53	-3.93	-3.74	-0.75	4.70	-1.40

Sigma	AUST	2.43	1.91	3.72	3.10	0.74	1.60
CAS1	ANTA	-3.0	-0.1	29.7	-7.3	2.2	13.9
DAV1	ANTA	-1.9	-5.1	-3.9	-8.0	-4.0	1.3
MCM4	ANTA	1.7	3.1	-16.5	0.3	9.5	27.4
OHIG	ANTA	0.5	-6.3	-6.7	-1.1	-0.8	1.8
KERG	ANTA	-2.2	-7.5	1.1	-5.7	-6.5	6.9
Mean	ANTA	-0.98	-3.17	0.75	-4.36	0.05	10.27
Sigma	ANTA	1.97	4.49	17.40	3.77	6.21	10.84
BRAZ	SOAM	1.5	0.6	-2.2	-2.3	-0.9	-10.1
FORT	SOAM	0.5	0.1	7.6	-0.1	3.3	2.3
KOUR	SOAM	1.4	4.5	4.2	0.3	5.1	0.3
AREQ*	SOAM	7.7	10.4	1.3	3.1	14.6	-1.1
SANT*	SOAM	7.4	18.9	-1.1	4.2	19.1	8.1
Mean	SOAM	1.12	1.73	3.18	-0.70	2.53	-2.50
Sigma	SOAM	0.57	2.38	4.97	1.42	3.08	6.64
BAHR	AFRC	12.1	2.5	1.0	15.6	1.9	2.0
HART	AFRC	-5.2	-15.8	0.3	-1.2	-4.1	1.5
MAS1	AFRC	-1.6	-4.2	-1.3	-1.8	-0.1	3.1
KOKB	PCFC	3.6	-6.5	-8.9	0.9	-2.5	-1.6
KWJ1	PCFC	1.6	-11.3	-6.0	3.2	-7.7	-4.2
CHAT	PCFC	3.5	-3.7	-7.6	2.5	25.3	-0.4
MALI	INDI	-4.2	-9.8	2.4	-5.6	-4.2	2.7
LHAS	INDI	-28.1	8.4	-20.6	-25.2	6.5	1.8
GUAM	PHIL	7.2	28.5	3.0	4.7	32.1	-0.5

APPENDIX IV

PROPOSED SINEX 1.00 EXTENSION EXTENSIONS FOR DATUM CONSTRAINTS AND TRANSFORMATION PARAMETER SOLUTION

By

Remi Ferland, NRCan

(Nov 20, 1997)

Transformation parameters and inner constraints are routinely estimated/applied during coordinates computations. Currently, there is no explicit definition to incorporate those in SINEX. This is an attempt to correct this minor problem by proposing standard names and usage.

The transformation parameters may be estimated and/or applied or their sigmas used to constrain the solution

When the transformations parameters are estimated, they can appear in the ESTIMATE block and optionally in the APRIORI block as is currently done for the station parameters. The sign convention should follow IERS convention.

When the transformation parameter sigmas are used to provide the reference frame constraint with the inner constraints technique, those constraints are unfortunately not explicitly provided.

The general SINEX practice has been to have a one to one explicit correspondence between APRIORI and ESTIMATED parameters. For the inner constraints case, the transformation parameters would only appear in the SOLUTION/APRIORI and optionally in the SOLUTION/MATRIX_APRIORI blocks. This would provide the 7 (or less) constraints to apply and code explicitly in the SINEX format.

Names should be reserved for the transformation parameters and their rates (units) such as:

RX RY RZ TX TY TZ SC (mas mas mas m m m ppb)
RXR RYR RZR TXR TYR TZR SCR (ma/y ma/y ma/y m/y m/y m/y pb/y)

When used as inner constraints, the variables Code, Point and Solution could be respectively '-----' '---' '-----'
The apriori values would not be needed.

Example #1:

Minimum datum (rotational) constraints only:

```

*-----
+SOLUTION/APRIORI
*Index  _Type_  Code Pt Soln  _Ref_Epoch_  Unit S  _Apriori Value_____  _Std_Dev____
   1  RX  -----  -  00:000:00000  mas  O  .000000000000000E+00  .1000000E+0
   2  RY  -----  -  00:000:00000  mas  O  .000000000000000E+00  .1000000E+0
   3  RZ  -----  -  00:000:00000  mas  O  .000000000000000E+00  .1000000E+0
-SOLUTION/APRIORI
*-----

```

Example #2:

Transformation from ITRF94 to ITRF93:

```

*-----
+SOLUTION/APRIORI
*Index  _Type_  Code Pt Soln  _Ref_Epoch_  Unit S  _Apriori Value_____  _Std_Dev____
   1  RX  -----  -  88:000:00000  mas  O  -.390000000000000E+00  .1000000E-1
   2  RY  -----  -  88:000:00000  mas  O  .800000000000000E+00  .1000000E-1
   3  RZ  -----  -  88:000:00000  mas  O  -.960000000000000E+00  .1000000E-1
   4  TX  -----  -  88:000:00000  m    o  .006000000000000E+00  .1000000E-1
   5  TY  -----  -  88:000:00000  m    O  -.005000000000000E+00  .1000000E-1
   6  TZ  -----  -  88:000:00000  m    O  -.015000000000000E+00  .1000000E-1
   7  se  -----  -  88:000:00000  ppb  O  .400000000000000E+00  .1000000E-1
   8  RXR  -----  -  88:000:00000  ma/y  O  -.110000000000000E+00  .1000000E-1
   9  RYR  -----  -  88:000:00000  ma/y  O  -.190000000000000E+00  .1000000E-1
  10  RZR  -----  -  88:000:00000  ma/y  O  .050000000000000E+00  .1000000E-1
  11  TXR  -----  -  88:000:00000  m/y   O  -.002900000000000E+00  .1000000E-1
  12  TYR  -----  -  88:000:00000  m/y   O  .000400000000000E+00  .1000000E-1
  13  TZR  -----  -  88:000:00000  m/y   O  .000800000000000E+00  .1000000E-1
  14  SCR  -----  -  88:000:00000  pb/y  O  .000000000000000E+00  .1000000E-1
-SOLUTION/APRIORI
*-----

```

(The **Apriori** Values are real but the Std_Dev were made-up for this example)

APPENDIX V

SUGGESTIONS FOR AC SUBMISSIONS OF MINIMUM DATUM CONSTRAINT A- SINEX SOLUTIONS

As proposed in the paper it is recommended that the ACS final orbit/EOP/station/clock solutions be only minimally constrained and that they be consistent. More details on possible approaches and suggestions on how to make all the AC solutions consistent can be found in the Appendix VI. Here it is only suggested how a minimum constrained AC Final (A-SINEX) station/EOP solution can be coded in the SINEX format.

Although in principle unconstrained (consistent) solutions could be used, it is convenient or even necessary to constrain (i.e. attach a datum to) the AC solutions for several reasons. As already discussed in the paper, at least for the time being it is essential that the datum constraints be minimal in order to preserve the relative station/orbit precision and/or datum connections. In this way it is hoped that an efficient feedback on orbit/EOP/station consistency can result in significant consistency improvements .

Since only the three orientation parameters (Rx, Ry, Rz) are nearly singular (with sigmas of a few 10's of mas), by definition, the minimum datum constraints can only include the three rotational parameters. In fact the example #1 of the Appendix IV already demonstrates how such a minimum (datum) constraint A-SINEX submission could be coded. In this way, the important geocenter and scale information implied from the Global AC analysis is preserved. Note that in principle (due to near singularity) any values Rx, Ry, and Rz can be used, so they are of little significance and need not even be coded (i.e. zero values could be used instead) . However the apriori sigmas, or the apriori matrix used, must be coded properly in the apriori SINEX blocks, so that the original (unconstrained) matrix can be recovered. The apriori minimum (rotation) constraints are thus somewhat arbitrary and could be based on e.g. a transformation between the original unconstrained station solution and the IGSyyPww solutions of the 52 RF station set. Alternatively, until IGSyyPww becomes available, the new ITRF96 station set of 47 stations can be used instead.

Analogously for the GNAAC weekly combined SINEXes only the minimum (i.e. rotation) datum constraints could also used, or alternatively, a complete 7-parameter solution (and the corresponding apriori information) could be coded (see e.g. the example #2 of the Appendix IV). When the IGSyyPww RF set becomes available it could be used for the transformation solutions/apriori or alternatively it can be used directly as apriori information. The important consideration here is that all apriori (datum) constraints be fully removable and the original geocenter and scale information be retained.

APPENDIX VI

SUGGESTIONS AND DISCUSSIONS ON AC SOLUTION/PRODUCT CONSISTENCY

It is essential that the consistency of all AC solutions be maintained. This is true for the proposed new ITRF realization in particular. The consistency of the Final orbit, EOP, station, clock and tropospheric delay solutions are to be maintained regardless of whether minimum datum or no constraints are used. (Note that after June 28, 1998 it is proposed that only minimum or no constraints be used for all Final AC solutions; see the Appendix V for more details and the proposed coding in the SINEX format). Since ionospheric delays are not sensitive to reference frame changes and are only needed to connect the IGS clock solutions to external standards, they are not discussed here.

The fact that AC station solutions are currently accumulated and submitted to the IGS on a weekly basis somewhat complicates the product consistency. (Note that weekly-accumulated station solutions were adopted by IGS as a compromise between daily and yearly station submissions.) Depending on the degree of sophistication and the additional CPU time expense, there are at least three possible approaches available to ACS:

1. A rigorous adjustment for all products based on the whole weeklong period. Though preferable, for practical considerations and given the current submission and CPU limitations, this is difficult to realize.

2. A rigorous adjustment for a part of the AC products, e.g. station positions and EOP, accumulated over a one-week period. Then the remaining parameters are obtained by a rigorous back-substitution. This approach may already be feasible for some ACS; in fact, some ACS are already doing this. Note that the solutions for the remaining parameters, while fixing all the relevant parameters obtained from the above-accumulated rigorous (partial parameter) solution, are equivalent to rigorous back-substitution in terms of the parameter values only, but not in terms of the corresponding covariance matrix. So, if the matrix is not required (as is currently the case for the AC orbit/clock/tropo solutions), this back-substitution by parameter fixing could also be a practically viable alternative.

3. A rigorous adjustment for a part of the AC products, e.g. Station positions and EOP, accumulated over a one-week period. All the remaining parameters are then obtained by approximations of back-substitution. More specifically, approximate solutions consistent with the weekly-accumulated SINEX station/EOP solutions can be obtained by applying appropriate parameter transformations computed between the daily (minimum datum or no constraint) station solutions and the accumulated AC A-SINEX solution for the current week. Since this is relatively easy to implement and likely will be a choice for most ACS, below are more details for all the relevant AC product solutions.

EOP (erp-format): The EOP and sigmas from the A-SINEX solution are coded in the erp weekly file, which accompanies the sp3 daily orbit files.

Orbits (sp3 format): 7 parameter transformations between each daily (minimum or no constraint) station solutions and the weekly A-SINEX solution are applied to the corresponding (minimum or no datum constraint) daily orbits. In this way the daily transformed orbits approximate back-substitutions and are consistent with the A-SINEX.

Satellite clocks: The (minimum or no datum constraint) daily clocks are increased by the height corrections computed from the daily station dx , dy , dz shift and scale (Sc) transformations. I.e. the following consistency corrections are added to the daily satellite clock solutions:

$$Dt = ((dx.Xs + dy.Ys + dz.Zs)/Rs + Sc.Rs)/c;$$

where Xs , Ys , Zs , are the ITRF SV coordinates, Rs is the SV radius vector and c is the speed of light. Note this correction accounts for the origin changes of the daily station solutions. The second correction, based on the orbit height errors (with respect to the daily station origin) also needs to be applied but with the opposite sign (see the test below for more details), however this is already being done during the current IGS orbit/clock combinations.

Station clocks: the daily station clocks (to be submitted for some stations in the near future, in a yet to be specified format) need to be corrected only for relative height errors, i.e. the daily station height residuals after 7 parameter transformation between the daily and the A-SINEX station solution. The daily station height residuals with respect to the A-SINEX, expressed in time units, are subtracted from the corresponding daily (minimum or no datum constraint) station clock solutions. Note that the daily transformation parameters (shift and scale) should not be included in this correction.

Tropospheric delays: The tropospheric (tropo) delay corrections are completely analogous to the station daily clocks, i.e. the only difference is that the daily station height residuals are scaled by an empirical scaling factor of about .15 to .30. This factor is likely COntant for an AC, but could vary from AC to AC. It may be a function of the elevation cut-off and/or elevation dependent weighting used.

EXAMPLE : Consistency transformation between EMR sigma constrained and unconstrained solution for Feb 02, 1998 (wk 0943, day 01)

In addition to the regular EMR09431 Final solution, which uses the ITR94 position and sigmas of the 13 ITRF stations as apriori constraints, the second, unconstrained solution was generated with large (at least 10 m) apriori position sigmas for all stations. The Table 1 summarizes the parameter transformations between the corresponding orbit as well as between station solutions.

Table 1: 7 parameter orbit and station transformations for unconstrained -constrained solutions

Product	dx	dy	dz	Sc	R x	Ry	Rz	2D	H
	mm	mm	mm	ppb	mas	mas	mas	RMs(mm)	
Orbits	3	66	43	0.0	.48	-.36	.26	73	40
Stations	-4	140	84	-0.1	.76	-.42	.24	9	13
Difference	1	-74	-41	0.1	-.28	.06	.02		

As one can see, except for the shift parameters dy, dz and the rotation Rx, both the orbit and station transformations are quite consistent. The large and disturbing dy bias, typically also seen for the EMR unconstrained (weekly SINEX) solutions (see the weekly GNAAC summary reports by JPL, MIT and NCL) is also seen for this daily solution. The smaller dy, dz orbit shifts are likely due to orbit dynamics and gravity field which should mitigate (or resist to) any geocentre offset, more than for the station solution. For most ACS the geocentre offsets of unconstrained solutions are much better behaved and usually they are small, within 10-20 mm. This EMR example, in fact, could represent a worst scenario case. The differences in Table 1 also indicate the need for daily 7 parameter transformations in the IGS orbit combinations to account for larger variations in the shift and orientation biases for some AC (minimum or no constraint) solutions.

As outlined above, the approximate transformations/corrections were applied to the unconstrained clock and tropo delay solutions and then they were compared to the constrained solution. The results of comparisons are summarized in Table 2. **Note that** for the satellite clocks, the orbit height error (which includes the daily orbit offsets and scales) were subtracted in addition to adding the above height corrections based on the daily stations offsets and scale transformations. The first (orbit height error) correction, in fact **simulates** the orbit height corrections available and applied in the current IGS clock combinations. In other words the orbit height corrections applied here effectively only include the differential dx, dy, dz and scale offsets listed in the last row of Table 1.

As one can see the consistency transformations/corrections of step 3) seem to be quite acceptable with respect to the formal sigmas. Although the formal sigmas are likely rather pessimistic due to significant correlation amongst the above solution parameters.

Table 2. Comparisons of the unconstrained and constrained clock, tropo EMR Final solutions for Feb 02, 1998.

Solution	RMS (unconstrained - constrained)		Average formal sigma
	Original	transformed	
Sat. clocks	.195 ns	.061 ns	.123 ns
Sta. clocks	.056 ns	.040 ns	.087 ns
Tropo delays	2.7 mm	1.7 mm	4.6mm

A final note on the 7-parameter transformation between unconstrained **daily** solution and the minimally constrained **A-SINEX** solution: Due to the near rotational singularity of the daily unconstrained solutions one can only use the identity matrix weighting. Alternatively, if matrix weighting is desired, one should first "condition" the unconstrained matrix by applying minimum rotation datum constraints, with the daily rotation solution values unchanged (see the example #1 of Appendix IV) .

ITRF96 AND FOLLOW ON FOR 1998

Claude Boucher, Zuheir Altamimi, Patrick Sillard
Institut Géographique National
ENSG/LAREG

6-8 Avenue Blaise Pascal
Cite Descartes, Champs-sur-Marne
77455 Marne-la-Vallee, FRANCE

E-mail: boucher@ensg.ign.fr, altamimi@ensg.ign.fr, sillard@ensg.ign.fr

INTRODUCTION

The **ITRF96** solution represents a new generation of realization of the International Terrestrial Reference System (**ITRS**). It is achieved by combining simultaneously positions and velocities using full variance - **covariance** information provided, in **SINEX** format, by the IERS analysis centers. Moreover, a rigorous weighting scheme is used, based on the analysis and estimation of the variance components using **Helmert** method.

The reference frame definition (origin, scale, orientation and time evolution) is achieved in such away that **ITRF96** is in the same system as the **ITRF94**. In addition, station velocities are constrained to be the same for all points within each site.

INPUT DATA

Solutions from the IERS analysis centers

The solutions provided by the IERS analysis centers and selected for the **ITRF96** analysis are 4 VLBI, 2 SLR, 8 GPS and 3 DORIS solutions. These data are listed in Table 1.

Local ties

As an improvement of the use of the local ties, all the eccentricities of **colocated** sites were converted into a complete set of positions for each site, provided in **SINEX** format. Each **SINEX** file reflects correlations between the **cartesian** components of the points within each site.

ITRF96 DATA ANALYSIS

The current strategy adopted for Terrestrial Reference Frame comparison/combination analysis is twofold: simultaneous combination of positions and velocities using full variance/**covariance** matrices; rigorous weighting scheme based on the analysis and estimation of the variance components using **Helmert** method.

The data analysis performed in view of the **ITRF96** establishment are mainly: comparison of the individual solutions with **ITRF94**, combination of the solutions within each technique and a global combination of all the solutions together with the local ties of **co-located** stations.

Among those selected for the ITRF96 combination, each individual solution was compared to the ITRF94 in order in one hand to estimate the transformation parameters of the system attached to the solution with respect to ITRF94 and, on the other hand, the level of agreement with the ITRF94 values.

In order to assess the relative quality of the individual solutions, independently from the influence of local ties, a combination within each technique was also performed. Matrix Scaling Factors have been rigorously estimated during the combined adjustment of the solutions.

The ITRF96 global combination is achieved with the following properties:

- It includes the 17 selected space geodetic solutions provided by the IERS analysis centers and 70 SINEX files containing positions and covariances, computed from local ties.
- The reference frame definition (origin, scale, orientation and time evolution) of the combination is achieved in such a way that ITRF96 is in the same system as the ITRF94.
- Velocities are constrained to be the same for all points within each site.
- Matrix Scaling Factors have been rigorously estimated during this combined adjustment which was then iterated.

Figure 1 shows the coverage of the 290 sites of the ITRF96. The position formal errors at epoch 1993.0 plotted in Figure 2 demonstrate an improvement of the ITRF96 with respect to ITRF94. Table 1 gives the quality analysis of the ITRF96 results, based more specifically on global residuals per solution.

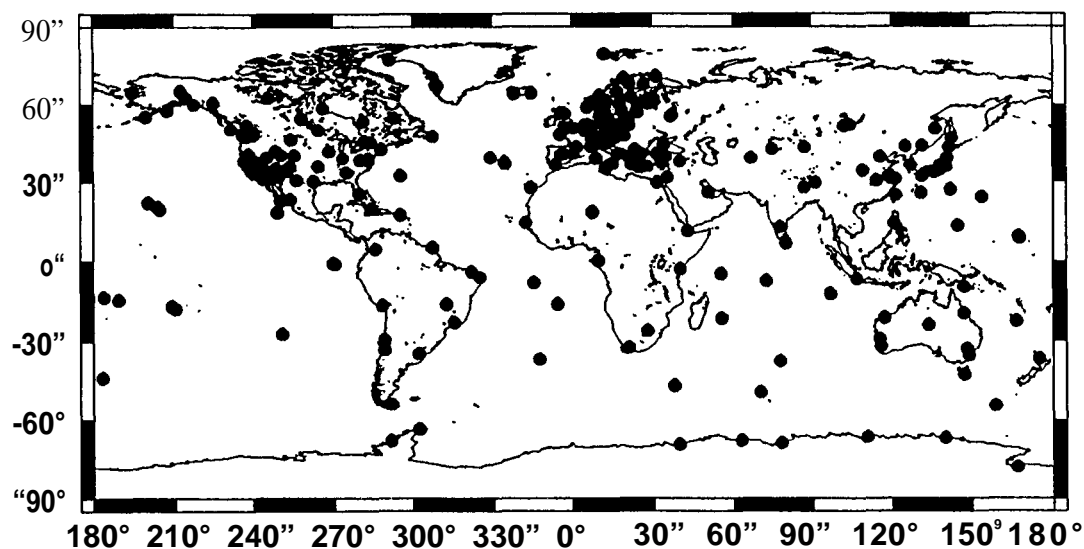


Fig. 1: ITRF96 Sites

Table 1. Global ITRF96 residuals per solution.

Solution	Number of points	Data Span YY-YY	Position RMS mm	Epoch yy:doy	Velocity RMS mm/y
<u>VLBI</u>					
SSC(GSFC) 97 R 01	120	79-97	5.80	93:001	1.90
SSC(GIUB) 97 R 01	43	84-96	13.60	93:001	.50
SSC(NOAA) 95 R 01	111	79-94	14.70	93:001	1.90
SSC(JPL) 97 R 01	8	91-96	20.70	93:001	
<u>SLR</u>					
SSC(CSR) 96 L 01	89	76-96	11.10	93:001	3.80
SSC(GSFC) 97 L 01	38	80-96	10.90	86:182	1.70
<u>GPS</u>					
SSC(EMR) 97 P 01	36	95-97	10.00	96:001	3.50
SSC(GFZ) 97 P 02	66	93-96	16.80	94:365	3.30
SSC(CODE) 97 P 02	100	93-97	7.10	95:076	1.90
SSC(EUR) 97 P 04	39	95-96	2.40	96:090	.30
SSC(EUR) 97 P 03	58	96-97	2.90	96:339	.30
SSC(MIT) 97 P 01	132	94-97	8.50	97:151	9.20
SSC(NCL) 97 P 01	114	95-97	5.40	96:001	6.30
SSC(JPL) 97 P 02	113	91-96	9.40	96:001	3.80
<u>DORIS</u>					
SSC(GRGS) 97 D 01	48	93-96	26.90	93:001	8.00
SSC(CSR) 96 D 01	54	93-96	26.10	93:001	10.60
SSC(IGN) 97 D 04	62	90-97	28.30	95:100	12.80

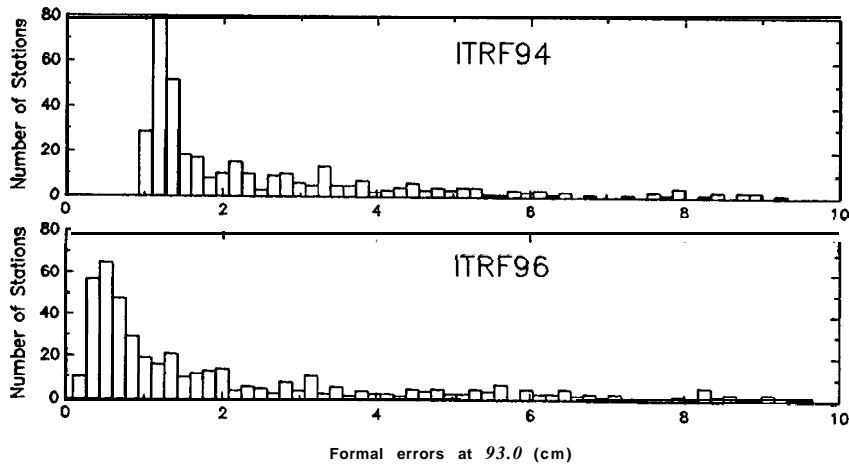


Fig. 2: Position formal errors

ITRF96 RESULTS

All the ITRF96 related files are available via Internet:

http: //lareg.ensg.ign.fr/ITRF/ITRF96.html

The SINEX files are available by anonymousftp:

ftp lareg.ensg.ign.fr (195.220.92. 14)

u sername: anonymous

password: e-mail address

move to the itr96 directory (cd pub/itr96)

compressed **ITRF96 SINEX** file (ITRF96.SNX.gz, about 52 Mbytes)

compressed **ITRF96_VLBI SINEX** file (ITRF96_VLBI.SNX. gz, about 3.7 Mb ytes)

compressed **ITRF96_SLR SINEX** file (ITRF96_SLR.SNX. gz, about 3.3 Mbytes)

compressed **ITRF96_GPS SINEX** file (ITRF96_GPS.SNX. gz, about 7.6 Mb ytes)

compressed **ITRF96_DORIS SINEX** file (ITRF96_DORIS.SNX.gz, about 0.8 Mbytes)

compressed **ITRF96_EUR_GPS_PERM SINEX** file (ITRF96_EUR_GPS_PERM. SNX.gz, about 0.6 Mbytes)

compressed **ITRF96_EUROPE SINEX** file (ITRF96_EUROPE. SNX.gz, about 4.1 Mbytes)

compressed **ITRF96_IGS_RS47 SINEX** file (ITRF96_IGS_RS47 .SNX.gz, about 0.5 Mbytes)

CONCLUSIONS

The IERS activities related to the Terrestrial Reference Systems will continue and be expanded in 1998. The main goals are:

to produce a new annual global solution (**ITRF97**) For that, detailed technical specifications will be issued in March 98.

to develop a pilot campaign to collect weekly solutions from the various techniques, in addition to GPS already organized in this way by IGS. A weekly combination in **ITRS** will then be determined. This will be a pilot experiment. The need and interests for such new IERS products should be investigated thanks to this campaign.

IGS REFERENCE STATIONS CLASSIFICATION BASED ON ITRF96 RESIDUAL ANALYSIS

Zuheir Altamimi
Institut Géographique National / ENSG/LAREG
6-8 Avenue Blaise Pascal
Cite Descartes, Champs-sur-Marne
77455 Marne-la-Vallee, FRANCE
E-mail: altamimi@ensg.ign.fr

INTRODUCTION

Using **ITRF96** results, we attempt in this report to classify and qualify the Provisional set of the IGS Reference Stations proposed by the IGS AC's which will replace the current 13 ITRF stations. **This provisional set contains 52 GPS stations, 32 of them are colocated with at least one of the 3 other IERS techniques (VLBI, SLR, DORIS).**

Position residuals of **all** the individual solutions included in the **ITRF96** are computed at **epoch 1997.0, taking into account velocity residuals. Based on 1997.0 position and velocity residuals, the provisional IGS Reference Stations were classified according to the 3 following criteria:**

- Agreement of GPS solutions for positions at epoch 1997.0
- Agreement of solutions for positions at epoch 1997.0 in the collocation sites
- Agreement of solutions for velocities

POSITION AGREEMENT OF THE GPS SOLUTIONS

If we consider **GPS_only** position estimates, disregarding if the GPS point is **colocated** with another technique or not, the 52 GPS proposed stations could be classified in the following classes:

Class A: Position residuals at epoch 97.0 below 1 cm over the 3 components for at least **THREE** individual solutions

Class B: Position residuals at epoch 97.0 below 2 cm over the 3 components for at least **THREE** individual solutions

Class C: Position residuals at epoch 1997.0 larger than 2 cm

POSITION AGREEMENT IN THE COLLOCATION SITES

Focusing on collocation sites, the following 4 classes could be distinguished:

Class A:

- **Site must contain a GPS class A station**
- The agreement between GPS and at least one **colocated** technique should be better than 2 cm over the 3 components.
- The local tie residuals should be below 2 cm

Class B:

- Site must contain at least a GPS class B station
- The agreement between GPS and at least one **colocated** technique should be better than 3 cm over the 3 components.
- The local tie residuals should be below 3 cm

Class C: Discrepancy between GPS and the **colocated** technique larger than 3 cm and less than 5 cm,

Class D: Poor collocation: discrepancy larger than 5 cm.

VELOCITY AGREEMENT

We Remind that in ITRF96, velocities were constrained to be the same for all points within each site. The analysis of the **ITRF96** velocity residuals for the 52 GPS stations leads to classify them into 4 classes:

Class A:

- For **GPS_only** sites, velocity residuals below 5 mm/y over the 3 components for at least **THREE** individual solutions
- For collocation sites, velocity residuals below 5 mm/y over the 3 components for at least **THREE** different solutions coming from at least 2 different techniques

Class B: Criteria as in Class A, but velocity residuals below 10 mm/y over the 3 components

Class C: Criteria as in Class A, but velocity residuals below 15 mm/y over the 3 components

Class D: Velocity residuals larger than 15 mm/y.

Table 1 summarizes the classification of the 52 GPS stations. For comparison, the ITRF94 classes are also listed in this table. A summary of the number of stations per class is given in Table 2, and illustrated on Figure 1. Figure 2 shows the coverage of the 52 sites.

Table 1, Classification of the IGS Reference Stations.

CODE	DOMES	nb.	Positions GPS	at 1997.0 Collocation	Velocities	ITRF94 class
ALGO	401	O4MOO2	A	A	A	B
AREQ	42202	MO05	A	A	B	B
AUCK	50209	MO01	c		c	
BAHR	24901	MO02	c		D	
B R A Z	41606	M001	B		B	
BRMU	42501	S004	A	m ¹	A	c
CAS1	66011	M001	B		c	c
CHAT	50207	MO01	B		D	
DAV1	6601	OMOO1	B		B	c
DRAO	401	O5MOO2	A	D	D	z
FAIR	40408	MO01	A	A	A	B
FORT	41602	M001	A	A	A	B
GODE	40451	M123	A	B	A	A
GOLD	40405	S031	A	m	A	c
GRAZ	11001	MOO2	A	A	A	A
GUAM	50501	M002	A	A	B	
HART	30302	MO02	B	B	A	B
HOB2	50116	M004	A	m	A	c
IRKT	123	13M001	B		B	
KERG	91201	M002	B	D	c	B
KIT3	12334	M001	A	B	A	c
KOKB	40424	MO04	A	A	A	B
KOSG	13504	MO03	A	c	D	A
KOUR	97301	M210	B	B	B	B
KWJ1	50506	M001	A		B	
LHAS	21613	M001	A		B	
MAC1	50135	M001	A		B	
MADR	13407	S012	A	A	A	A
MALI	33201	M001	B		B	
MAS 1	31303	MO02	A		A	c
MATE	12734	MO08	A	A	A	A
MCM 4	66001	M003	B		D	c
MDO1	40442	M012	A	A	A	A

m: missing local tie

Table 1. Classification of the IGS Reference Stations (continued).

CODE	DOMES nb.	Positions at 1997.0			Velocities	ITRF94 class
		GPS	Collocation			
NLIB	40465MO01	A	A	A	B	
NYAL	10317MO01	A	B	A	B	
OHIG	66008MO01	B	B	B	z	
ONSA	10402MO04	A	A	A	A	
PERT	50133M001	A		B		
PIE1	40456MO01	B	B	A	B	
POTS	14106MO03	A	c	B	A	
SANT	41705MO03	A	A	A	B	
SHAO	21605MO02	A	A	A	c	
THU1	43001MO01	A		B		
TIDB	501 03M108	A	A	B	B	
TROM	10302MO03	A	D	c	B	
TSKB	21730S005	A	A	B	B	
VILL	13406MO01	A		B	c	
WES2	40440S020	A	B	A	z	
WTZR	14201MO10	A	A	A	A	
YAR1	50107MO04	A	B	A	B	
YELL	40127MO03	A	A	A	B	
ZWEN	12330M001	A		B		

Table 2. Number of stations per class.

	Class A	Class B	Class C	Class D/Z
GPS_only	38	12	2	
Collocation	18	9	2	3
Velocity	25	18	4	5
ITRF94	9	17	10	3

CONCLUSION

-Based on this selection, it is suggested to exclude from the IGS Reference Stations list, stations having position or/and velocity class C or/and D. These stations are listed in Table 3 and are of two types:

- 5 pure GPS stations (not collocated with any other geodetic technique): (AUCK 50209MO01), (BAHR 24901 MO02), (CAS 16601 1M001), (CHAT 50207MO01),

(MCM466001M003). These stations should be rejected from IGS Reference Stations list.

5 colocated sites appear to have velocity or/and local tie problems: (DRAO 401 O5M002), (KERG 91201 M002), (KOSG13504M003), (POTS 14106M003), (TROM 10302M003). But if based on GPS-only estimates, they could be maintained in the IGS Reference Stations list.

Table 3. Class C or/and D stations.

CODE	DOMES nb.	Positions		at 1997.0 Velocities		ITRF94 class
		GPS	Collocation			
A U C K	50209M001	C			C	
B A H R	24901M002	C			D	
C A S 1	66011M001	B			c	c
C H A T	50207M001	B			D	
D R A O 401	O5M002	A	D		D	z
K E R G	91201M002	B	D		C	B
K O S G	13504M003	A	c		D	A
M C M 4	66001M003	B			D	c
P O T S	14106M003	A	C		B	A
T R O M	10302M003	A	D		c	B

(W13S240440S020) could be selected, but under a close watch, since the “best” position (at 1997.0) agreement between some GPS and VLBI solutions, **plus local tie, is estimated to be about 21 mm.** Meanwhile the “worst” agreement is about 51 mm.

ITRF96 demonstrates real improvement **for 14 GPS colocated sites with respect to ITRF94.**

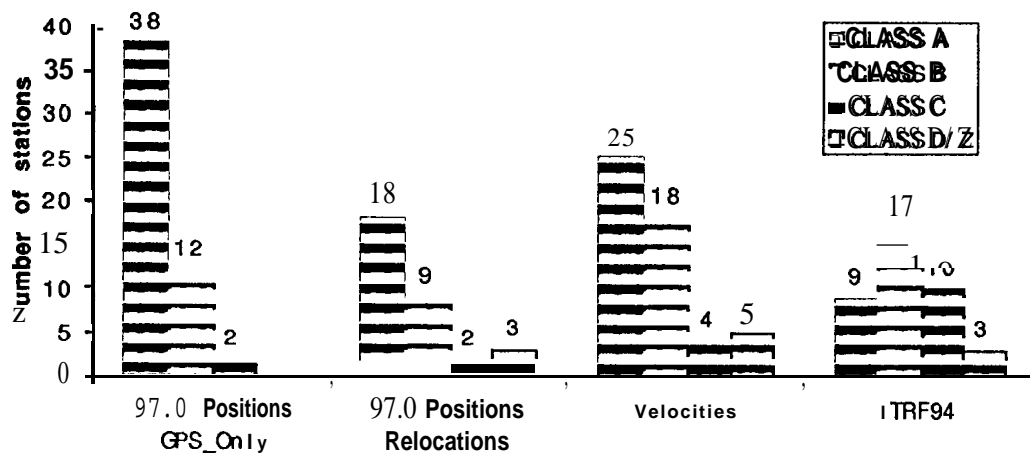


Fig. 1. Classification of the IGS reference stations.

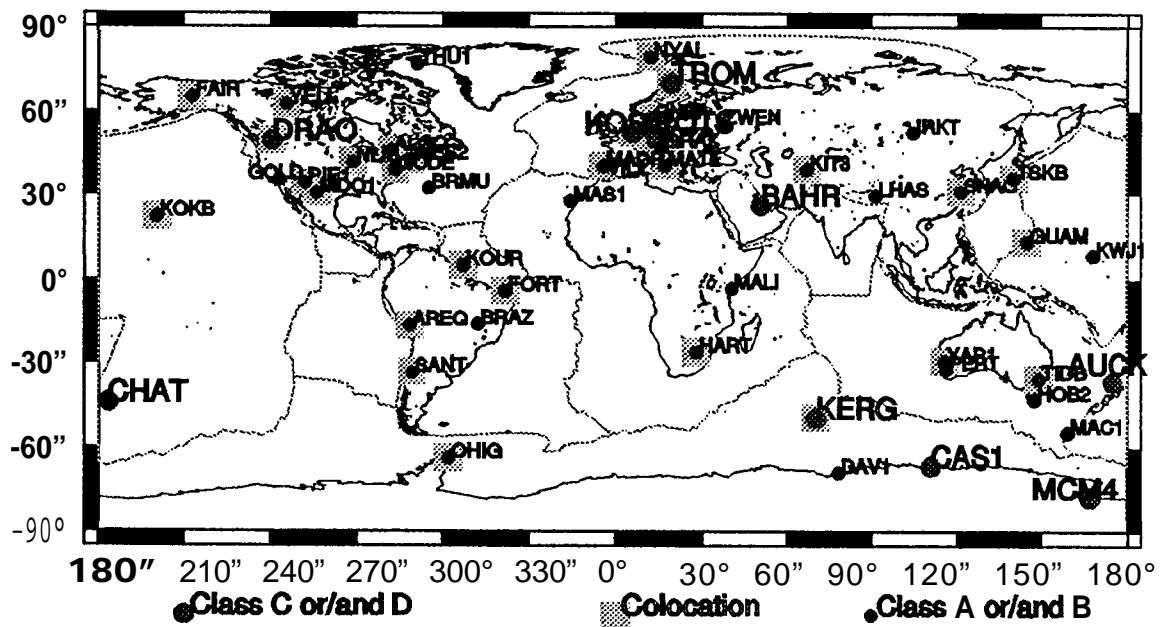


Fig. 2. Distribution of the IGS reference stations

References

Boucher C., Z. Altamimi, P. Sillard, 1998, Results and Analysis of the ITRF96, IERS Technical Note 24, Observatoire de Paris.

ESTIMATION OF **NUTATION** TERMS USING GPS

Markus Rothacher, Gerhard Beutler
Astronomical institute, University of Berne
CH-3012 Berne, Switzerland

ABSTRACT

Satellite space-geodetic measurements have been used since a long time to determine UT1-UTC rates (or length of day values). The estimation of nutation rates (in longitude and obliquity), however, was thought to be reserved to VLBI and LLR. It can be shown, that there is no fundamental difference between the estimation of UT1-UTC rates and nutation rates. Significant contributions to nutation by GPS may be expected in the high frequency domain, i.e., for periods below about 20 days.

CODE, the Center for Orbit Determination in Europe, started to estimate nutation rates in March 1994 using the data of the global IGS network. By now, the series of nutation rates from 3-day solutions has a length of about 3.5 years. From this series corrections to the coefficients of 34 nutation periods between 4 and 16 days have been determined. The resulting coefficients show an agreement of 10 μ as with the IERS 1996 nutation model. The GPS results are very consistent with the most recent model by Souchay and Kinoshita, too. GPS thus allows an independent verification of theoretical nutation models and results from VLBI and LLR. A thorough description and discussion of the estimation of nutation amplitudes using GPS may be found in [Rothacher et al., 1998].

INTRODUCTION

CODE, a cooperation of the Astronomical institute, University of Berne (Switzerland), the Swiss Federal Office of Topography, Wabern (Switzerland), the Bundesamt für Kartographie und Geodäsie, Frankfurt (Germany), and the Institut Géographique National, Paris (France), started to derive celestial pole offset parameters (nutation rates) in March 1994 in order to study whether GPS could be used to contribute to nutation theory.

From a mathematical point of view it can be shown [Rothacher et al., 1998] that the estimation of nutation rates in obliquity $\Delta\epsilon$ and longitude $\Delta\psi$ is very similar to the estimation of UT1-UTC rates: the offsets in all three components (Δt , $\Delta\psi$, and UT1-UTC) are fully

correlated with the orbital parameters describing the orientation of the orbital planes of the satellites (ascending node, inclination, and argument of latitude) and unmodeled orbit perturbations lead to systematic errors in the rate estimates. Major biases may be expected at a period of one revolution of the satellites or at annual and semi-annual periods (orientation of the orbital plane with respect to the sun) due to solar radiation pressure.

With a simple variance-covariance analysis it is possible to deduce in what frequency range corrections to nutation amplitudes may be computed with sufficient accuracy using GPS nutation rate estimates. Assuming a continuous nutation rate series of 1280 days and an RMS scatter of 0.27 mas/d for the nutation rate estimates – values taken from the actual GPS series produced at CODE – we find that the formal error $\sigma(A_T)$ of the nutation amplitude A_T at a nutation period T (in days) grows linearly with the period according to:

$$\sigma(A_T) \approx 0.0017 \cdot T \text{ mas} \quad (1)$$

When estimating nutation amplitude corrections from nutation *offsets*, as in the case of VLBI and LLR, the formal errors of the amplitudes are constant over a wide range of periods (i.e., for periods much longer than the typical spacing of the series and much shorter than the time interval covered by the series considered). From the literature ([Herring *et al.*, 1991], [Charlot *et al.*, 1995], [Souchay *et al.*, 1995], [Herring, 1997]) we obtain the formal errors of nutation amplitudes when using VLBI and LLR data. These formal errors are shown in Figure 1 together with those expected from GPS.

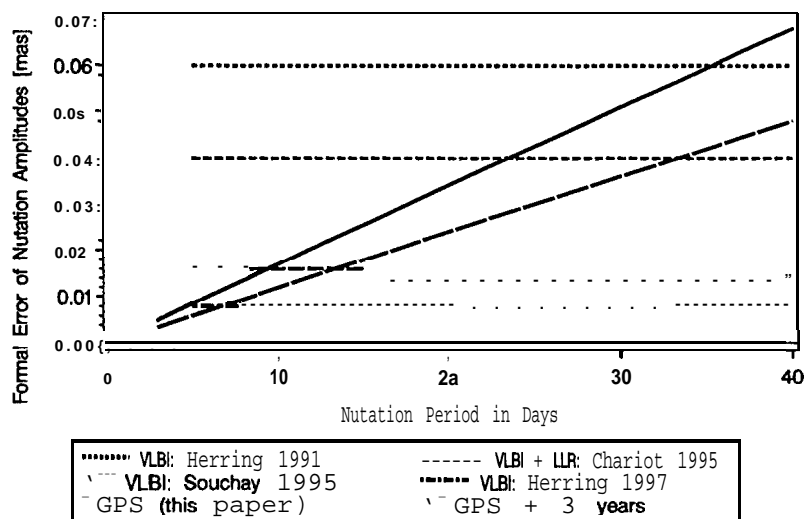


Figure 1. Precision of amplitude estimation from nutation offsets (VLBI and LLR) and from nutation rates (GPS) derived using a simple variance-covariance analysis.

Figure 1 clearly shows, that no major contributions to nutation theory may be expected from GPS for periods above about 20 days with the current orbit modeling. But GPS is in a good position to contribute at high frequencies (periods below 20 days). Let us mention

that the VLBI formal errors will only slowly improve from now on. Another 13 years of VLBI data will be needed to reduce the formal errors by $\sqrt{2}$, whereas for GPS, a factor of $\sqrt{2}$ can be gained with another 3 years of data even without modeling improvements.

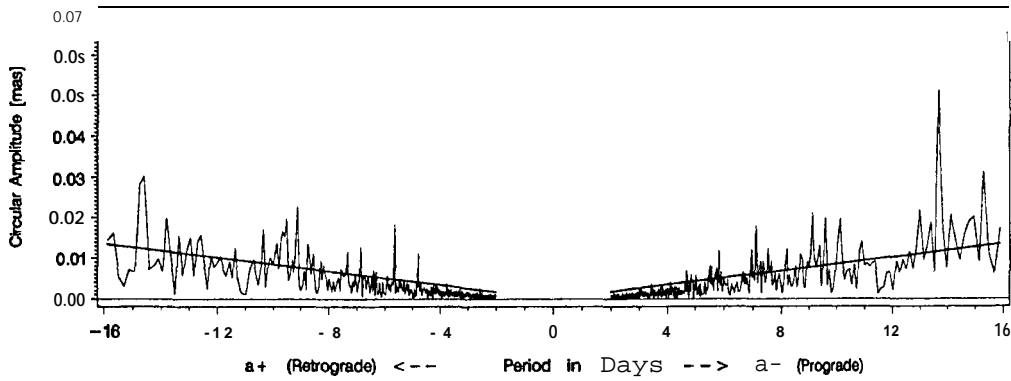
NUTATION RATE SERIES FROM GPS

The GPS nutation rate estimates were obtained from overlapping global 3-day solutions with 3-day satellite arcs using the data of up to 90 IGS sites. Over the three days one set of nutation rates was estimated in the two directions (obliquity and longitude) relative to the a priori nutation model, i.e. relative to the IAU 1980 Theory of Nutation (see [McCarthy, 1996]). It should be pointed out that rate estimates from 3-day solutions are more accurate than those from 1-day solution by about a factor of five. The reference frame was realized by heavily constraining 12 sites to their ITRF94 coordinates and velocities (see [Boucher et al., 1996]). All other site coordinates were freely estimated. Troposphere zenith delays were determined for each site with 6-hour intervals. During the 3.5 years covered by the nutation rate series (from March 1994 to November 1997) two important modeling changes took place. First, starting in January 1995, the ambiguities for baselines with a length below 2000 km were fixed to integers (80-90%) and secondly, end of September 1996, the satellite orbit parameterization was changed from the "classical" radiation pressure model with two parameters (direct radiation pressure coefficient and y-bias) to the extended CODE orbit model [Springer et al., 1998], where five parameters are routinely estimated in the 3-day solutions (constant radiation pressure coefficients in all three directions and periodic terms in X-direction). Both changes had an important effect on the nutation rate estimates. Whereas the ambiguity fixing improved the formal uncertainties of the rate estimates by almost a factor of three, the orbit model change deteriorated them by about the same factor. The worse formal uncertainties in the case of the new orbit parameterization is a consequence of the correlations between the nutation rates and the new radiation pressure parameters.

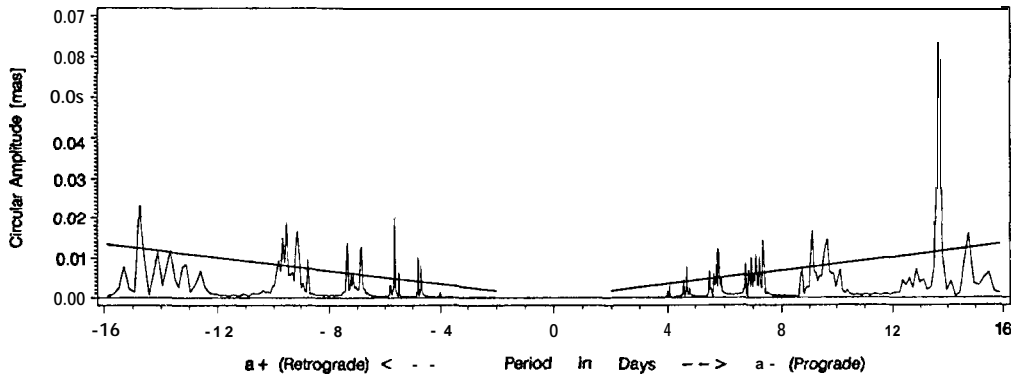
To give an impression of the type of signal contained in the GPS rate series, Figure 2a shows the high frequency spectrum derived from the nutation rate corrections relative to the IAU 1980 model. The *rate amplitudes* were thereby converted to actual amplitudes and transformed from $\Delta\epsilon$ and $\Delta\psi \cdot \sin \epsilon_0$ to amplitudes a^+ and a^- of *circular nutation* according to Eqn. (4) (see next section). For comparison the spectrum of the differences between the IAU 1980 and the IERS 1996 nutation model is depicted in Figure 2b. Many of the deficiencies of the IAU 1980 theory visible in Figure 2b, discovered by VLBI about a decade ago, are clearly seen by GPS, as well. The dashed lines in Figures 2 give the $1-\sigma$ uncertainties of the amplitudes estimates according to the Equation (1) (divided by a factor of 2 to account for the conversion to circular components of nutation).

ESTIMATION OF NUTATION AMPLITUDES

Starting with the GPS nutation rate corrections with respect to the IAU 1980 nutation model, a series of *total* nutation rates was generated by adding the rates given by the IAU 1980 model in order to obtain a series that is independent of the a priori model used.



(a) Spectrum of nutation corrections from GPS relative to the IAU80 model



(b) Spectrum of differences between the IERS96 and the IAU80 model

Figure 2. Spectrum of circular nutation amplitudes (see Eqn. (4) below) at low periods generated from (a) the GPS series of nutation rates converted to actual nutation amplitudes and (b) the differences between the IERS96 and the IAU80 model. The dashed lines indicate the $1\text{-}\sigma$ uncertainties of the amplitudes as expected according to Eqn. (1) (and (4)).

The nutation rate series was then used to estimate corrections to the nutation coefficients of a number of $n=34$ selected nutation periods relative to the more accurate IERS 1996 nutation model (IERS96) [McCarthy, 1996]. The corrections $\delta\Delta\epsilon$ and $\delta\Delta\psi$ in the nutation angles were thereby represented by

$$\delta\Delta\epsilon(t) = \sum_{j=1}^n (\delta\epsilon_{rj} \cos \theta_j(t) + \delta\epsilon_{ij} \sin \theta_j(t)) \quad (2a)$$

$$\delta\Delta\psi(t) = \sum_{j=1}^n (\delta\psi_{rj} \sin \theta_j(t) + \delta\psi_{ij} \cos \theta_j(t)) \quad (2b)$$

with θ_j denoting a combination of the fundamental nutation arguments, namely

$$\theta_j = \sum_{i=1}^5 N_{ij} \cdot F_i \quad (3)$$

where N_{ij} are integer multipliers of the fundamental arguments $F_i \in \{1, 1', F, D, \Omega\}$, also called Delaunay variables, and the angular frequency of the term j is given by $w := d\theta/dt$.

An alternative representation uses the circular components of nutation $a_{rj}^+, a_{rj}^-, a_{ij}^+$, and a_{ij}^- , which are related to the nutation coefficients in obliquity and longitude by

$$a_{rj}^+ = -(\delta\epsilon_{rj} + \delta\psi_{rj} \sin \epsilon_0)/2 \quad (4a)$$

$$a_{rj}^- = -(\delta\epsilon_{rj} - \delta\psi_{rj} \sin \epsilon_0)/2 \quad (4b)$$

$$a_{ij}^+ = -(\delta\epsilon_{ij} - \delta\psi_{ij} \sin \epsilon_0)/2 \quad (4c)$$

$$a_{ij}^- = +(\delta\epsilon_{ij} + \delta\psi_{ij} \sin \epsilon_0)/2 \quad (4d)$$

More details about the interpretation of the circular nutation components may be found in [Herring et al., 1991].

The coefficients $\delta\epsilon_{rj}$, $\delta\epsilon_{ij}$, $\delta\psi_{rj}$, and $\delta\psi_{ij}$ were determined with a least squares algorithm using the nut at ion rates from the GPS analysis as pseudo-observations. Figure 3 shows the differences between the nutation coefficients estimated from the GPS nutation rates and the coefficients of the IERS96 nutation model. The shaded area represents the 2σ error bars of the coefficients derived from GPS and shows the increase of these uncertainties with the nutation period.

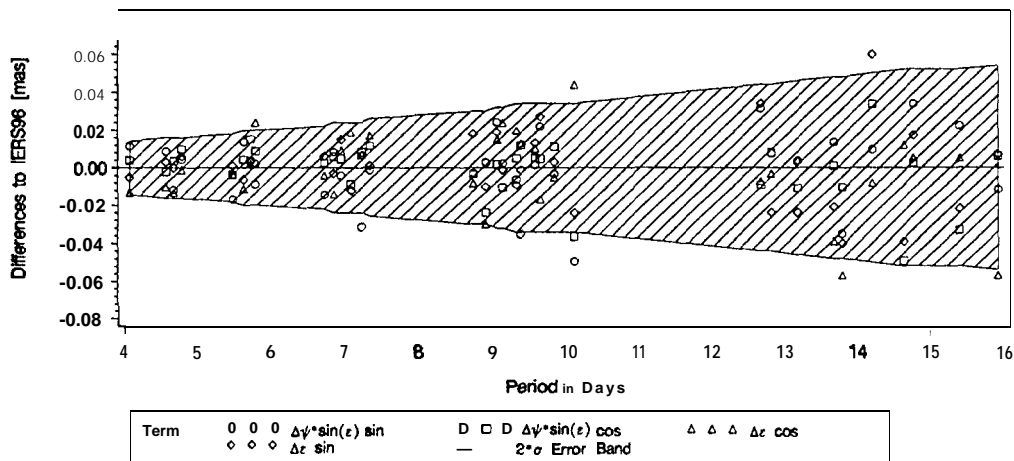


Figure 3. Nutation corrections relative to the IERS96 model for 34 periods estimated from the rate series obtained from GPS data. The shaded area represents the 95% confidence interval (20).

With a few exceptions all the nutation coefficients agree with the IERS96 nutation model at the level of twice the formal uncertainties (shaded area). The median agreement between

the GPS results and the IERS96 model over all 136 coefficients amounts to about 10 μ s. No major deviations from the IERS96 model can be detected by GPS. The actual values of the nutation coefficients from GPS for the 34 periods may be found in [Rothacher et al., 1998].

A more detailed comparison of various VLBI and LLR results given in the literature and the GPS results with the most recent model by Souchay and Kinoshita (SKV972) [Herring, 1997] may be seen in Figure 4.

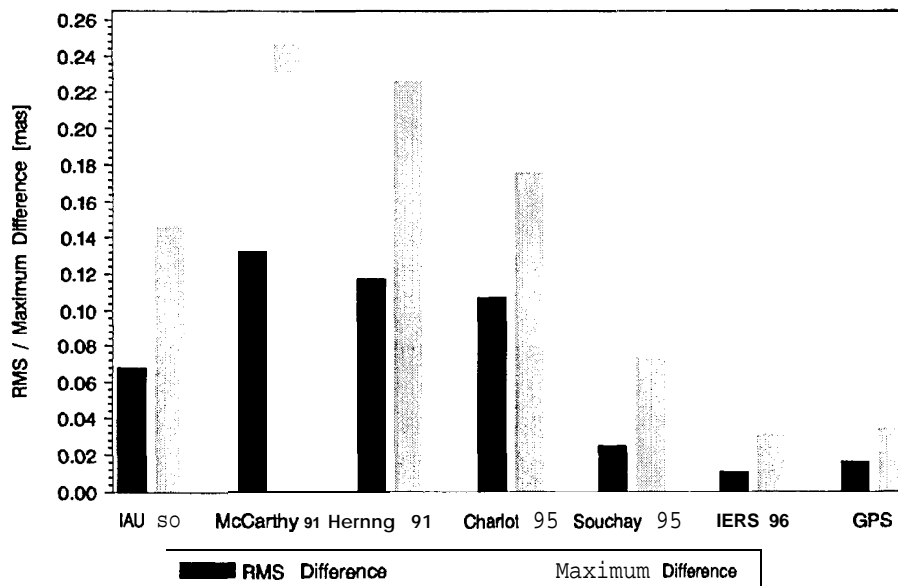


Figure 4. Rms difference and maximum difference over all terms of 4 major nutation periods, namely 13.66, 9.13, 14.77, 9.56 days, relative to the most recent model by Souchay/Kinoshita 1997.2.

Apart from the IAU 1980 (IAU 80), the IERS96 model and the GPS results, the comparison involves the results from [McCarthy and Luzum, 1991] (combined analysis of 10 years of VLBI and about 20 years of LLR data), [Herring et al., 1991] (9 years of VLBI data), [Charlot et al., 1995] (16 years of VLBI and 24 years of LLR data), and [Souchay et al., 1995] (14 years of VLBI data). Figure 4 depicts the rms differences as well as the maximum differences between these various results and SKV972 over all coefficients of the four major nutation periods at 13.66, 9.13, 14.77, 9.56 days (a total of 16 coefficients). We clearly see that the GPS results are in better agreement with the SKV972 model than most of the VLBI/LLR results.

A similar picture emerges when looking in detail at the coefficients of the 13.66 day period (see Figure 5), which is of special interest to geophysicists because of its large amplitudes. Again, the GPS results are very consistent with the results of the most recent model by Souchay and Kinoshita.

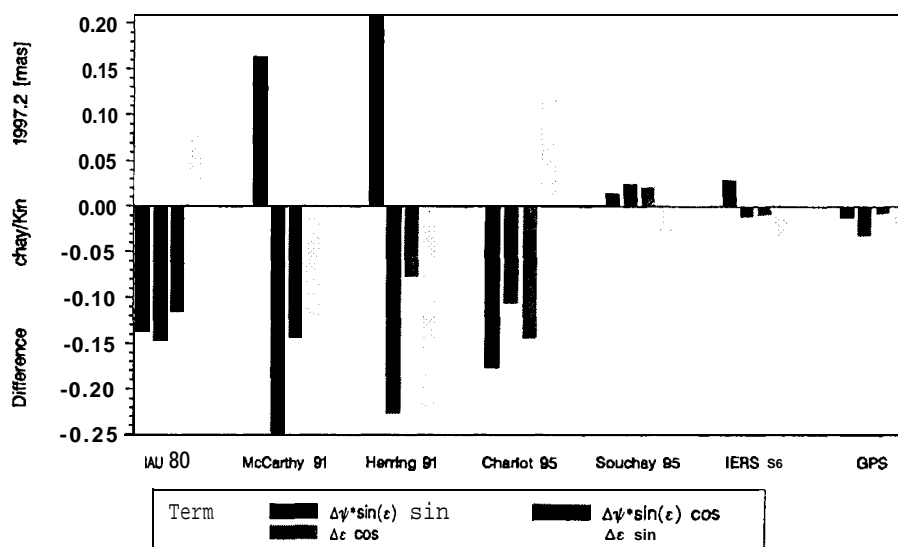


Figure 5. Comparison of the 13.66-day nutation coefficients from different sources with the most recent model by Souchay/Kinoshita 1997.2 .

CONCLUSIONS

Prom the above results we conclude that GPS may give a significant contribution to nutation in the high frequency range of the spectrum (periods below 20 days). The long term behavior is, however, reserved to VLBI and LLR. The nutation coefficients estimated from the GPS rate series show an overall agreement (median) of about $10 \mu\text{as}$ with the most recent nutation models by Souchay and Kinoshita. Using more refined orbit modeling techniques, carefully taking into consideration the correlations between the nutation rates and the orbital parameters, there is certainly much room for improvements. But already now GPS allows an independent check of present-day theoretical nutation models and VLBI/LLR results at the high frequency end of the spectrum. In future a combined analysis of VLBI, LLR, and GPS nutation series promises to give the most accurate nutation results.

REFERENCES

- Boucher, C., Z. Altamimi, M. Feissel, and P. Sillard (1996), Results and Analysis of the ITRF94, Central Bureau of IERS - Observatoire de Paris, Paris.
- Charlot, P., O. J. Severs, J. G. Williams, and X. X. Newhall (1995), Precession and Nutation From Joint Analysis of Radio Interferometric and Lunar Laser Ranging Observations, *The Astronomical Journal*, 109(1), 418-427.
- Herring, T. A. (1997), Most recent nutation model by Souchay and Kinoshita, Version 97.2 (private communication).
- Herring, T. A., B. A. Buffett, P. M. Mathews, and I. 1. Shapiro (1991), Forced Nutations of the Earth: Influence of Inner Core Dynamics, 3. Very Long Interferometry Data Analysis, *Journal of Geophysical Research*, 96(B5), 8259-8273.

- McCarthy, D. D., and B. J. Luzum (1991), Observations of Luni-Solar and Free Core Nutation, *The Astronomical Journal*, 102(5), 1889-1895.
- McCarthy, D.D. (1996), IERS conventions (1996), *IERS Technical Note 21*, Observatoire de Paris, Paris, July 1996.
- Rothacher, M., G. Beutler, T.A. Herring, and R. Weber (1998), Estimation of Nutation Using the Global Positioning System, *JGR*, submitted in March 1998.
- Souchay, J., M. Feissel, C. Bizouard, N. Capitaine, and M. Bougeard (1995), Precession and Nutation for a Non-Rigid Earth: Comparison Between Theory and VLBI Observations, *Astronomy and Astrophysics*, 299, 277-287.
- Springer, T. A., G. Beutler, and M. Rothacher (1998), Improving the Orbit Estimates of the GPS Satellites, *Journal of Geodesy*, January 1998, Submitted.

GLOBALY CONSISTENT RIGID PLATE MOTION: FIDUCIAL-FREE EULER VECTOR ESTIMATION

Geoffrey Blewitt, Ra'ed S. Kawar, and ¹Philip B.H. Davies

Department of Geomatics, University of Newcastle,
Newcastle upon Tyne, NE 7RU, UK

Abstract

IGS will begin in 1998 to routinely produce estimates of station velocities which will contribute to the definition of the terrestrial reference frame. The next logical step, is to use these velocities to estimate Euler vectors according to rigid plate tectonics theory. This will serve geophysicists who require kinematic boundary conditions to their regional analyses. Not only is IGS in the best position to do this (using GPS data), but also this type of analysis is important to IGS in terms of quality assessment of velocity products and station performance, and to enhance reference frame definition. We present some theoretical aspects of Euler vector determination, especially in the context of fiducial-free networks. We define and consider the "Chasles Effect," which must be considered due to imperfect realization of the Earth centre of mass. Preliminary results indicate that the weekly IGS polyhedron solutions provide an excellent dataset for the determination of plate motion. This provides one motivation for the IGS Analysis Centres to reprocesses data back to 1992.5 using today's models and standards.

1. Introduction

IGS Global Network Associate Analysis Centers (GNAACs) are now routinely producing weekly station coordinate solutions (with full covariance matrices) for over 100 stations worldwide [Blewitt *et al.*, 1995]. These weekly solutions can then be used to estimate station velocities and other types of motion (e.g., co-seismic displacement) [Blewitt *et al.*, 1998]. Unlike dense regional networks designed for the study of crustal deformation, the kinematics of the IGS polyhedron can be almost entirely explained in terms of angular velocities known as Euler vectors. The IGS is therefore in a position to estimate these Euler vectors in a globally self-consistent model, using full covariance information.

This paper explores how Euler vectors can be estimated using GNAAC solutions, and why IGS should be interested in this. Applying the philosophy underlying the IGS densification pilot project, the theory of rigid plate kinematics is first considered geometrically, so that the role of the reference frame can clearly be seen in contrast to the physical kinematics, which are necessarily frame-independent. This leads logically to a fiducial-free approach to the estimation of Euler vectors, similar to the situation with station coordinates and velocities. The

¹ Now at Royal Ordnance Survey, Southampton, UK

Newcastle **GNAAC** has undertaken a preliminary investigation to assess the feasibility of an operational estimation of Euler vectors and station velocity residuals, applying ideas presented here. Geodetic tools have been implemented to allow a more rigorous analysis, including generalized **outlier** detection, and variance component estimation.

This leads to our conclusion that IGS should routinely produce Euler vectors and station velocity residuals as a service to geophysicists and to IGS itself. Reprocessing of all past IGS data using current data processing models and strategies would strongly enhance the value of such products; therefore **IGS** should consider organizing such an activity, performed by IGS Analysis Centers.

2. Rigid Plate Kinematics

Introduction to Euler vectors

Rigid plate kinematics starts with the assumptions that (i) the plate does not deform, and (ii) the motion is constrained to the surface of a sphere. This is obviously equivalent to assuming rigid body motion with one point fixed at the **centre** of a sphere. Now Euler's theorem states that

“the general displacement of a rigid body with one point fixed is a rotation about some axis”
[e.g., Goldstein, p. 158, 1980]

Therefore, rigid plate motion at any instant in time is completely specified by an angular velocity vector, known as the “Euler vector” $\underline{\Omega}_i$ for each plate i (Fig. 1).

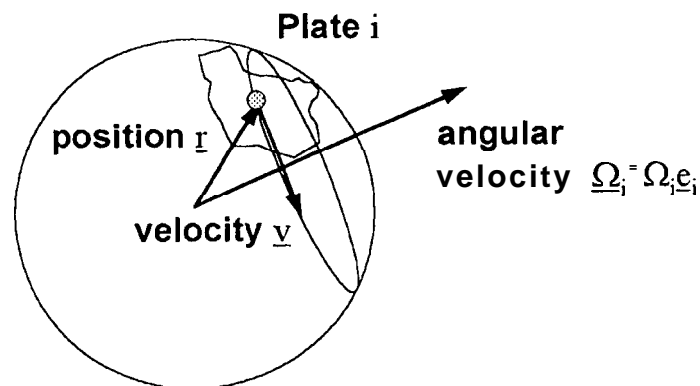


Fig. 1: Kinematics of a rigid plate as described by an angular velocity vector

The magnitude of this vector Ω_i represents the rate of rotation of the plate, often expressed in units of degrees per million years. The direction of this vector \underline{e}_i is known as the “Euler pole,” often expressed in terms of longitude λ_i and latitude ϕ_i computed on the sphere. The cartesian components of the Euler vector can be computed as follows:

$$\begin{aligned}\Omega_{ix} &= \underline{\Omega}_i \cdot \underline{e}_x = \Omega_i (\underline{e}_i \cdot \underline{e}_x) = \Omega_i \cos \phi_i \cos \lambda_i \\ \Omega_{iy} &= \underline{\Omega}_i \cdot \underline{e}_y = \Omega_i (\underline{e}_i \cdot \underline{e}_y) = \Omega_i \cos \phi_i \sin \lambda_i \\ \Omega_{iz} &= \underline{\Omega}_i \cdot \underline{e}_z = \Omega_i (\underline{e}_i \cdot \underline{e}_z) = \Omega_i \sin \phi_i\end{aligned}$$

The velocity of a point that is attached to plate i at position vector \underline{r} is given by the following vector cross product:

$$\underline{v} = \underline{\Omega}_i \times \underline{r}$$

Model Error due to Spherical Approximation

Note that the position vector should be expressed such that the origin is at the center of the sphere. The fact that the Earth is not exact] y spherical introduces the following problems: (i) rotation about an axis constrains a plate to the surface of a sphere, not the surface of an ellipsoid; and (ii) motion of an object constrained to an ellipsoidal surface generally introduces deformations, because the radius of curvature is a function of latitude. It can be shown that the velocity errors introduced by both these problems are of the order

$$\delta v \approx f v$$

where f is the ellipsoidal flattening factor, approximately $1/298$. Since plate velocities are limited to the order 100 mm/yr, the spherical approximation introduces errors at the level of a fraction of a millimetre per year (which is small, but not entirely insignificant as geodetic precision can approach this level).

Presumably due to the ambiguous nature of how to map ellipsoidal surface onto the sphere, the IERS [p. 15-16, 1996] publishes a standard FORTRAN subroutine (originally by Bernard **Minster**) which computes station velocities given the station coordinates, using Euler vectors from the geophysical model **NNR-NUVEL1 A** [DeMets et al. 1994]. It can be seen from the source code, that the cross product formula is applied using geocentric position vectors. As the **geocenter** does not generally coincide with the center of curvature for the surface of the ellipsoid, it can therefore be expected that very small but non-zero height velocities will be introduced. However, the IERS approximation does preserve plate rigidity. Alternatively, the user could ignore the height velocity and thus forego plate rigidity, Either way, the effects are fractions of a millimetre per year.

Reference Frame Dependence

Another problem with the model is that it is frame dependent. The geodetic results give velocity components which general] y include (i) relative rotational motion between the frame axes and the polyhedron, and (ii) relative translational motion between the origin of coordinate frame and the polyhedron. The adoption of frames which have a different evolution of origin or orientation will lead to different velocity results, and therefore different Euler vector results.

Reference Frame Dependence: Rotational Ambiguity

The first problem of frame dependence arises **because** we desire an Earth-fixed frame, yet **all points on the Earth's surface are in relative motion**, therefore **"Earth-fixed" is somewhat arbitrary**. Earth polar motion requires estimation, introducing an ambiguity as to whether the polyhedron is rotating, or the pole is moving. The data can only resolve the **relative rotation between the celestial ephemeris pole (CEP) and the polyhedron**. Moreover, a **global rotation of all plates around the CEP can be interpreted as either Earth rotation, or plate tectonic motion about the CEP - the data cannot separate the two effects, as the observations do not refer to the mantle (if indeed the mantle may be viewed as somehow absolute)**. The **velocity field from a fiducial-free solution therefore has a 3-rank deficiency**, which will propagate into the Euler vector estimates.

Euler vectors are therefore, strictly speaking, non-estimable, and require some form of datum constraints (which may be minimal). Velocity vectors determined by constraining a subset of station velocities to a specific frame will produce Euler vectors consistent with that frame. Therefore, Euler vectors determined in different frames will generally have a common angular velocity bias, which can itself be thought of as an Euler vector (Fig. 2).

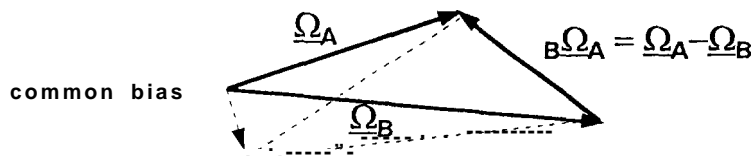


Fig. 2: Relative Euler vector, shown herein angular velocity space, is insensitive to a global reference frame rotation

In Fig. 2, it obvious that a common rotational bias does not affect the difference between two Euler vectors. This difference is known as the **"relative Euler vector."** The relative Euler vector has more physical significance than the absolute Euler vector, as it is independent of frame rotation, and is therefore estimable. The absolute version is, however, convenient, because it is far simpler (and better to ensure consistency) to specify a list of absolute Euler vectors rather than a 'much longer list of pairs.

Reference Frame Dependence: The Chasles Effect

M. Chasles (1 793-1 881) proved a stronger form of Euler's Theorem,

"the most general displacement of a rigid body is a translation plus a rotation"
 [e.g., Goldstein, p 63, 1980]

We define the "Chasles Effect" as the source of error introduced into Euler vectors due to net translational motion of the polyhedron with respect to the coordinate origin. Why is the Chasles Effect relevant, if we assume that rigid plates move effectively with one point fixed? The problem is that geodetic network solutions cannot perfectly realize the Earth centre of

mass (which we assume to be Euler's fixed point). GPS fiducial-free network solutions will have a small **drift** relative to the Earth **centre** of mass due to imperfect dynamic orbit models. This drift will cause a systematic error in the determination of plate rotations, which doesn't entirely cancel for relative Euler vectors. (The situation for VLBI is even more extreme, as there is no inherent dynamic origin.)

The essence of the problem is that we don't know the exact location of Euler's "fixed point" relative to the GPS stations. Under such circumstances we should instead assume Chasles' theorem is applicable rather than Euler's theorem. Therefore station motions relative to the coordinate origin can be modelled as a plate rotation about the coordinate origin, plus a global translational rate bias.

Frame Independent Analysis

Geodetic observable and estimable should only be a function of relative Euler vectors, not absolute Euler vectors. In fact, if an equation for a kinematic variable cannot be expressed in terms of relative Euler vectors, and if absolute Euler vectors are absolutely necessary in the formulation, then we can conclude that this kinematic variable is reference frame dependent. For example, it can be shown that baseline length rate between two points on arbitrary plates A and B can be written in terms of the relative Euler vector:

$$v_{L(A,B)} = {}_A\Omega_B \frac{(\underline{r}_A \times \underline{r}_B)}{\underline{r}_A - \underline{r}_B}$$

On the other hand, relative velocity cannot be written **only** in terms of relative Euler vectors, and is therefore frame dependent.

$$\begin{aligned} {}_B v_A &= v_A - v_B \\ &= (\Omega_A \times r_A) - (\Omega_B \times r_B) \\ &= (\Omega_A - \Omega_B) \times r_A + \Omega_B \times (r_A - r_B) \\ &= ({}_B\Omega_A \times r_A) + (\Omega_B \times {}_B r_A) \end{aligned}$$

It can be seen, however, that if the baseline is sufficient] y short, then the second term becomes negligible, and relative velocity is then only a function of relative Euler vector, and therefore frame independent. This is a logical result, considering the geophysics. Physical quantities, such as strain and stress buildup at plate boundaries must be a function of local kinematic quantities, such as relative velocity between two nearby points, either side of the plate boundary. The results of physical predictions can not be frame dependent, and therefore it is satisfying to see that the kinematic theory is consistent with this notion.

It therefore makes sense to talk unambiguously about relative velocity at a plate boundary, on the understanding that the limit of zero baseline length is taken. The predicted relative velocity at a plate boundary will determine the boundary's character: whether it be strike slip, spreading, or converging (and if so, at what angle relative to the boundary). Therefore, if we know where plate boundaries lie, the relative Euler vectors can be used to predict the nature of the plate boundary, and the integrated rate of strain accumulation as

we **move** across the boundary. This is the geophysical significance of relative Euler vectors. Conversely, one can therefore understand how it is that geophysicists can invert observations of plate boundary features to estimate relative Euler vectors.

Now that we have established the importance of relative Euler poles, and the rank-3 deficiency of absolute Euler poles, we are in a position to deduce a logical approach from geodesy. We propose that absolute Euler vectors be estimated from fiducial-free (loosely constrained) estimate of station velocities, taking adequate care to minimize the **Chasles** Effect. In the **preliminary** results presented in this paper, we have simply estimated and applied a 14-parameter transformation (i. e., the usual 7 **Helmert** parameters plus their 7 time derivatives) of our loose solution into **ITRF**. This effectively removes the global rotational bias as well as the global translational rate bias (and scale rate, although this may prove to be unnecessary). This is then followed by estimation of the Euler vectors. This is not the only scheme possible, but it is simple and appropriate to implement for an initial test, and it does ensure a good degree of consistency with the SLR realization of the **geocentre**. For **future** work, we intend to investigate the **Chasles** Effect, including the class of methods which do not rely on an externally supplied frame, but may rely on internal constraints and Earth models. We note that the estimation of all absolute Euler vectors is of course not strictly possible due to the 3-rank deficiency, however the application of loose constraints will ensure stability in relative Euler vector estimates, without distorting their values.

3. Why should IGS be interested in Euler vectors?

The horizontal motions of most stations of the IGS polyhedron can be almost completely explained in terms of the Euler vector model. The exceptions would be stations in zones of active **crustal** deformation, such as plate boundaries, and stations which, for whatever reason, are not representative of the plate (e.g., the monument is not anchored to bedrock).

The rigid plate motion model together with a map of plate boundaries provides us with a model of horizontal motion anywhere on the sphere. Any such model which covers the entire sphere allows us to overcome problems in reference frame definition arising from the fact that we do not monitor every possible point on the Earth's surface. If we were to define a frame independent of plate motion models, we would be forced to depend on internal constraints, such as no net rotation of stations; however, these types of constraints are strongly dependent on the selected network, and would have very different effects if applied to a future network with additional stations. The problem of sampling bias would be essentially insurmountable. Therefore, Euler vectors have an important role to play in the definition of a reference system, which is why they appear in the IERS Terrestrial Reference System.

Despite this, the link between the ITRF and plate motion models has in recent years become weaker in **favour** of internally consistent constraints. While internal consistency is **laudible**, there is no reason why a reference frame cannot be both internally consistent with itself, and externally consistent with a plate motion model. The external consistency would be on the evolution of the frame axes with respect to the polyhedron, whereas the internal consistency would be on the deformation of the polyhedron. The fact that ITRS is supposed to have no net plate rotation is explicitly realized when we consider that solutions are

rotated into ITRF using a 14-parameter transformation. It is therefore easy to see why the role of Euler vectors is often overlooked due to these procedures.

In principle, IGS could define its own frame, just as the geophysicists have done for geological models. IGS should investigate the polyhedron kinematics as far as possible prior to contributing to ITRF. From the point of view of potential users, IGS is in a position to produce Euler vector estimates, station velocity residuals, and to classify stations according to their kinematics.

4. Developments at NCL GNAAC

As part of the IGS ITRF Densification Pilot Project, global network solutions with **full covariance** matrices (in SINEX format) are produced every week by several IGS Analysis Centers (ACs). These are combined into a global polyhedron solution (GSINEX) by the IGS Global Network Associate Analysis Center (GNAAC) at Newcastle (NCL) every week, beginning September 1995 [Davies and Blewitt, 1997]. This global combination analysis features variance component estimation to optimize relative weighting, and **outlier** detection (which requires each station to be analyzed by a minimum of 3 ACs). Since July 1996, regional network solutions have been produced every week by several IGS Regional Network Associate Analysis Centers (RNAACs). NCL has attached these RNAAC solutions onto the global combination (so as not to perturb it), thus producing a **densified** IGS polyhedron solution (PSINEX).

NCL has also been conducting a second stream of analysis for research and development purposes, including reanalysis of past SINEX files using the latest combination software (TANYA), and producing "kinematic solutions" where station positions are parameterized as a **function** of epoch position and a velocity vector. Such a kinematic solution was submitted to IERS and has since been incorporated into ITRF96. The feedback from IERS has been that the NCL solution had one of the lowest WRMS statistics with respect to the final ITRF96 [Z. Altamimi, presented at this IGS workshop]. This may be expected, as a GNAAC solution already represents a combination of solutions which are being separately submitted to IERS.

Going beyond simple velocity solutions, NCL is moving towards interpretation and **modelling** of these velocities. The approach taken is to develop a geographical information system (GIS) that is **sufficiently** sophisticated to **identify** and **classify** tectonic zones according to the observed kinematics of geodetic stations. Specifically, we are developing a bootstrapping procedure identifies clusters of stations that, according to the data, appear to be co-rotating as if attached to the rigid plate interior. The idea is that clusters of stations are iteratively augmented while solving for Euler rotation vectors, and testing the plate rigidity hypothesis. Stations are classified as *regular* or *irregular*, depending on whether they are a cluster member (contributing to Euler vector estimation) The estimated rigid-plate velocity field with computed errors are then mapped onto the entire globe, and compared with regional geodetic data (e.g., data from the irregular stations) to investigate crustal deformation

The GIS under development would use object-oriented approach to defining a kinematic Earth model, which is based on a set of plates, with attributes including closed boundaries. These boundaries can be redefined by the user to test new hypotheses. The GIS would facilitate hypothesis testing using built in functions, and using any selection of geodetic data supplied to

it. Estimated relative Euler vectors could be mapped into relative plate velocities at respective plate boundaries, allowing us to objectively categorize boundary segments, and determine boundary parameters (e.g., rate and angle of convergence/spreading; rate of slip). This GIS could then allow for comparison of this geodetic classification with other geophysical data and geophysical interpretations.

While this GIS is under development, NCL has been testing the feasibility of some of these ideas, and has conducted preliminary research into appropriate tools to be incorporated as GIS **functions**. Such **functions** include variance component estimation when combining different geodetic data sets, **outlier** detection, and more importantly, generalized **outlier detection** (as applied to clusters of data suspected of not fitting the model) to allow more rigorous testing of hypotheses.

5. Preliminary Analysis and Results

Analysis

The input to this preliminary analysis are weekly **GSINEX** solutions, spanning 18 months, which include the coordinates and **full covariance** matrix of **IGS** stations that have been analyzed by a minimum of **3 ACS**. The union of all the input files contains 150 stations **satisfying** this criteria. The time series of coordinates were then scanned to ensure that obvious **step functions** (mainly due to equipment replacement) were detected and, if possible corrected.

This screening process has proved to be the most time consuming part of the analysis, which is why only 18 months of data have been processed here. We expect this problem to be mitigated in future due to the recent adoption of a central database at the IGS Central Bureau (the “**loghist**” file) with information on station configuration changes. In fact, this file is now the starting point of our routine **GNAAC** analysis, but the problem still remains until all ACS adopt this procedure.

These weekly coordinate solutions were then input to our processing software, **TANYA**, to **solve** for station velocities and epoch station positions, with a **full covariance** matrix. The solution at this point is fiducial-free, meaning that the reference frame is only loosely defined through loose station coordinate constraints (tight enough to prevent numerical instability, but loose enough not to influence internal **geometry**). A datum definition was then applied to this solution through a 14 parameter **Helmert** transformation to ITRF94 (which, as discussed, also mitigates the **Chasles** Effect).

This kinematic solution was then processed by **TANYA** to solve for Euler vectors and **full covariance** matrix. A manual iterative process (later to be automated) was applied to remove stations not fitting the Euler vector model. This is necessary, because some stations lie in zones of **crustal** deformation.

In addition to producing Euler vector estimates (in the ITRF96 frame) with **full covariance** matrix, station velocity residuals to the resulting estimated model were produced for subsequent analysis. Station velocity residuals can be interpreted in terms of random error, systematic error, or blunders. For example, residuals exceeding their computed 99% confidence ellipses may be interpreted **as** either systematic errors or blunders. Systematic error

can arise because the station actually is in a zone of **crustal** deformation, or because the station is **not** representative of the underlying rigid plate (e.g., due to monument instability). Errors due to change of instrumentation or monumentation can be classified as blunders.

Results

In contrast with station velocities, which in many cases are more than 5 cm/yr, the residual station velocities (after estimating Euler poles) are relatively small, typically several millimetres per year [Fig. 3.].

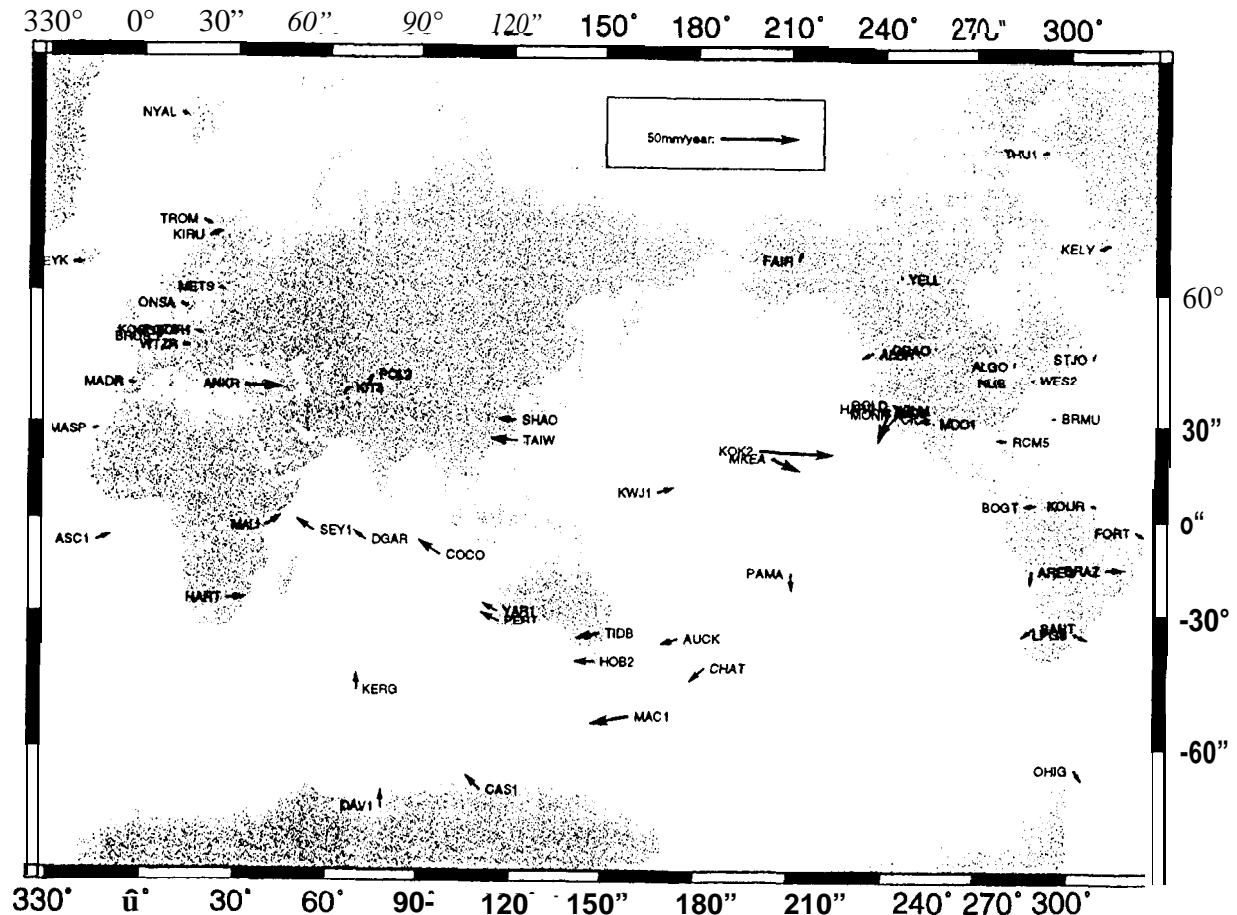


Fig. 3: Estimated station velocity residual vectors. (Note that the direction of the arrows should be reversed if these are to be interpreted as velocity relative to respective plates).

Clearly, the Euler vector model explains a significant proportion of the station velocities. Discrepancies from the Euler vector model can be seen at plate boundaries, and occasionally (e.g., Hawaii) within plate interiors. North America appears to be extremely stable, whereas Eurasia appears to be extended East-West, possibly as a result of the **extrusional** tectonics in Central Asia caused by the collision with the Indian subcontinent. The velocity residual of station **ANKR** in Turkey can be interpreted as that station moving due West relative to the Eurasian plate, which confirms that ANKR is actually on a different plate (namely, the

Anatolian block). The larger residuals in south west United States are due to regional deformation near the Pacific-North American plate boundary.

We emphasise that this analysis is preliminary and no checks have been made to reconcile discrepancies, for example, with misinformation on antenna configuration. Therefore, we should be **careful** in drawing conclusions about specific sites. Rather, we simply point out the potential of this approach at discriminating between sites which appear to behave as expected, and sites which require **further** investigation. (For example, we have not yet attempted to explain the discrepant behaviour of the two GPS stations on the Hawaiian Islands.)

Fig 4. shows that the estimated Euler poles largely agree within the expected errors with the NNR NUVEL- 1 A mode. (The one exception is the South American plate - a problem we are currently investigating). These preliminary results suggest that both the GNAAC solutions and estimated errors are reasonable.

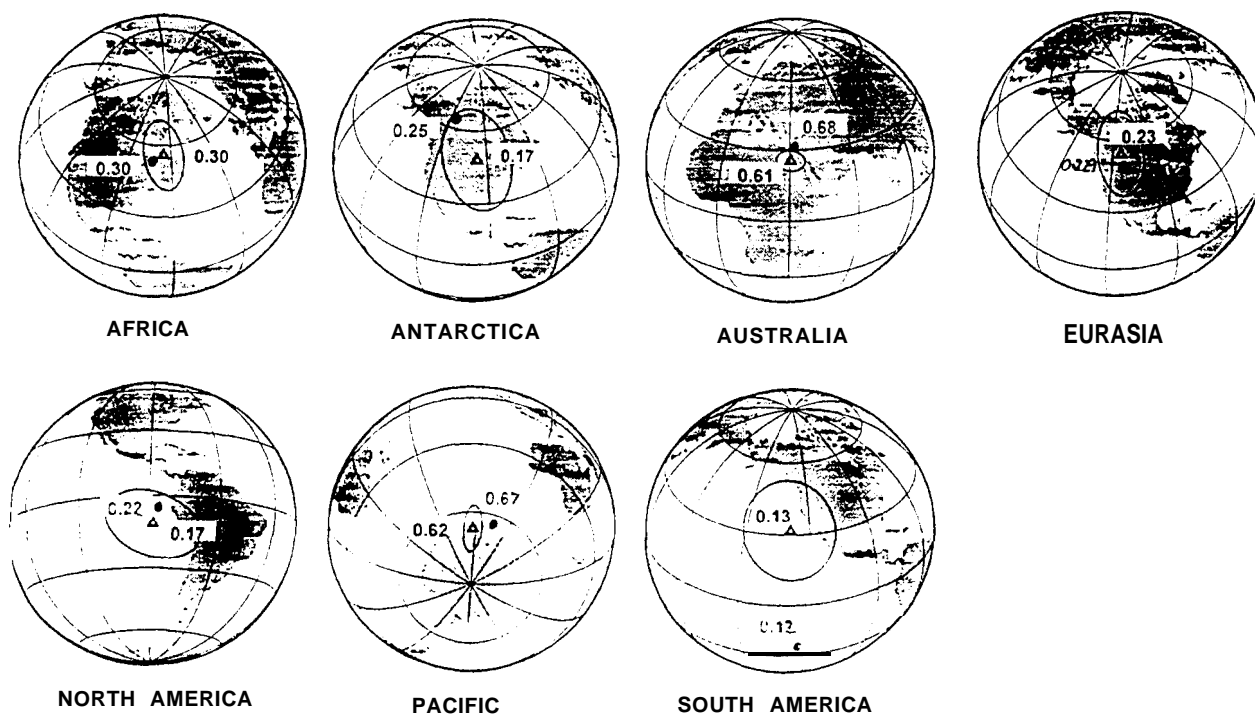


Fig. 5: Estimated Euler vectors and 1-standard deviation error ellipses

Africa-Eurasia kinematic boundary conditions

Certainly, more work is needed to provide results for serious geophysical interpretation, but the potential for this type of analysis is promising. The relative Euler vector solutions are particularly elucidating. For example, the estimated relative Euler vector between Eurasia and Africa can be used to compute relative plate motions at various points in the region of the plate boundary.

- . In northern Algeria, convergence of 5 mm/yr is computed with an azimuth of -310 (which happens to be normal to the general trend of the Atlas mountain range)
- . In northern **Italy**, convergence of 8 mm/yr is computed with direction -350 (which happens to be normal to the general trend of the Alps mountain range)
- . In the eastern **Mediterranean** around Cyprus, convergence of 11 mm/yr is computed precisely due North.

These computation are in close agreement with the **NUVEL- 1A** model, suggesting that current day collision of Africa and Europe has not changed significantly over recent geological time. Only regional measurements distributed around the plate boundary can locate where the convergence is being accommodated, but these types of computations do provide a "kinematic boundary condition" on the total path integral of relative motion across the boundary.

6. Conclusions

(1) We propose that **IGS** provide a service to geophysicists who are investigating **crustal** dynamics, by providing estimates of Euler vectors, station velocity residuals, and a classification of stations according to there observed kinematics. We argue that **IGS** is in the best position to do this (for GPS data), as **IGS** has and will continue to implement a very successful level of quality control, and adherence to standards. The alternative is for geophysicists to continue to derive their own Euler vectors, which due to limited resources, would tend to be limited to analyzing a subset of all data available to **IGS**. From the few examples given, station motions can in most cases be interpreted in simple geophysical terms. Much more **confidence** can be placed in geophysical interpretation if the Euler velocity residuals form a spatially recognizable pattern, rather than discrepant results which would be expected from station configuration problems.

(2) We also suggest that it is in **IGS'S** best interest to perform these type of activities. It is the logical progressive step after station velocity analysis, and allows for a new type of quality assessment of the station velocity products. Moreover, Euler vector analysis can be incorporated into processing schemes, and solutions can be easily updated on a weekly basis. The developments proposed here will allow **IGS** to gain better insight into reference frame realization, which is important for its own "reference system," for example, in the selection of core stations used in orbit production. As an example of where insight can be gained, we note that the "Chasles Effect" should be carefully considered when estimating plate motions.

(3) Finally, it is clear that a more robust and accurate analysis can be performed using data extending back to the beginning of the **IGS** pilot project, in mid 1992, This would require **ACS** to reprocess data using today's software and analysis strategies to produce a more homogeneous time series. It should also help eliminate some of the problems associated with station configuration information, which now exists at the Central Bureau,

Acknowledgments

The authors gratefully acknowledge financial support from the Natural Environment Research Council, including grant GR3/10041 and studentship GT4/94/386/G.

References

- Blewitt, G., C. Boucher, P.B.H. Davies, M.B. Heflin, T.A. Herring, and J. Kouba, "ITRF densification and continuous realization by the IGS," in *Proc. of the IAG General Assembly*, held in Rio de Janeiro, 1997 (in press 1998).
- Blewitt, G., Y. Bock, and J. Kouba, "Constructing the IGS polyhedron by distributed processing," in *Proc. of the IGS Workshop*, ed. by J. Zumberge, IGS Central Bureau, Pasadena, Calif., USA, p. 21-36 (1995)
- Davies, P.B.H. and G. Blewitt, "Newcastle upon Tyne Global Network Associate Analysis Centre Annual Report 1996," *IGS Annual Report 1996*, p. 237-252, IGS Central Bureau, Jet Propulsion Lab., Pasadena, California (1997)
- DeMets, C., R. Gordon, D. Argus, and S. Stein, "Effect of recent revisions to the geomagnetic reversal time scale on estimates of current plate motions," *Geophys. Res. Lett.*, 21, pp. 2191-2194 (1994)
- Goldstein, H., *Classical Mechanics (2nd Ed.)*, Addison-Wesley Pub. Co., Reading, Massachusetts (1980)
- IERS, *Technical Note 21: IERS Conventions (1996)*, Ed. Dennis D. McCarthy, Paris Observatory (1996).

Topic 4: IGS Products for Troposphere and Ionosphere

IGS COMBINATION OF TROPOSPHERIC ESTIMATES - EXPERIENCE FROM PILOT EXPERIMENT

Gerd Gendt
GeoForschungsZentrum Potsdam
D-14473 Potsdam, Telegrafenberg A17, Div. 1

INTRODUCTION

The existing global and regional networks of permanent GPS receivers installed for geodetic and navigational applications can be used with marginal additional cost for determination of atmospheric water vapor with high temporal and spatial resolution. In different countries projects are under way in which the impact of GPS derived water vapor on the improvement of weather forecast are studied. Within the IGS a network of 100 globally distributed sites are analyzed on a daily basis. The zenith path delay (ZPD) values obtained should be converted into **precipitable** water vapor (**PWV**) and should be made available to the scientific community.

This IGS product could meet the demands for **climatological** studies. Here a time resolution of 2 hours (this is what IGS will provide) is sufficient, because long-term characteristics are of interest only, and a time delay of a few weeks for product delivery is acceptable.

In the past some experiments had demonstrated the capability of IGS (Gendt, 1996, 1997) and on 26 January 1997 (GPS week 890) the Pilot Experiment for the determination of IGS Combined Tropospheric Estimates has started.

GENERATION OF THE COMBINED IGS TROP PRODUCT

Since the beginning of the Pilot Experiment six of the global IGS Analysis Centers (**ACs**) have regularly contributed. Different **mapping** functions and elevation cutoff angles of 10, 15 or 20 degrees are implemented (see Table 1.). Three of the ACS, CODE, GFZ and JPL, have made changes in these parameters during 1997. The number of sites per AC varies from 30 to 85, and we have **~100** sites in total (Fig. 1.). More than 60 sites are used by at least three ACS, so that sufficient statistical information about the quality of the tropospheric estimates can be gained. For the other sites poor or no quality checks are possible, only some conclusions from neighboring sites may be drawn.

Input to the weekly combination are seven daily files from each AC with the estimates of ZPD and station coordinates from all sites (in the format **TRO-SINEX**), as well as the weekly AC **SINEX** file from which the site description blocks are taken. The combination (details see Gendt 1997) starts with the derivations of 2h mean values for each AC. The mean is formed **epochwise** taking into account AC dependent biases not to get jumps by missing data. Additionally, the mean daily station coordinates are computed. Here a homogenization of all used antenna heights and types is performed, so

that all coordinates refer to the same physical point. **Vital to this step is that the daily coordinates from the AC TRO-SINEX files are based on the site descriptions given in the weekly SINEX file. Unfortunately, as checked by Helmert transformation residuals, this is not always the case. The product from the combination is a weekly file for each site containing the ZPD estimates and precipitable water vapor if conversion is possible. Additionally, a combination report will summarize some statistics on the differences to the IGS Mean (bias, standard deviation), for the global mean of each AC and separately for all sites.**

Table 1. Contributing Analysis Centers with some relevant parameters

	ZPD [minutes]	cutoff [deg]	Mapping Function	No. Sites	No. Sites 1 AC only
CODE (week 926)	120	20 10	Saastmoinen Dry Niell	85	14
EMR	60	15	Lanyi	30	2-4
ESA	120	20	Saastmoinen	50	
GFZ (week 929)	60	20	Saastmoinen Dry Niell	55	3-6
JPL (week 920)	5	15	Lanyi Niell	37	1-5
NGS	120	15	Niell	55	1-3

COMPARISONS, RESULTS

The results from 48 weeks in 1997 are used to estimate the achieved consistency. No information about the absolute accuracy could be obtained, with the exception of POTS - the only site for which water vapor radiometer (WVR) data were available.

In Figs. 3, 4 some statistics on the differences between individual AC estimates and the IGS Mean are shown. The information is given separately for about 60 sites, more or less classified into sites with smaller (left) and larger (right) standard deviation (stddev). For most sites and ACS the stddev is ± 6 mm ZPD (which corresponds to ± 1 mm PWV) and it approaches in many cases the ± 3 mm level. The magnitude of the stddev is of course highly correlated with the magnitude in the repeatability of the estimated station coordinates. In Fig. 2 the geographical distribution of the magnitude for the stddev is shown. The largest stddevs can be found in the equatorial region. The bias for most sites is below ± 3 mm. Even for sites with a larger bias its repeatability is very high.

In Fig. 5 global mean values (mean over all sites) of the difference to the IGS Mean are given. The mean stddev of the best ACS is at the 4 mm level. Only a small global

bias at the 1 mm ZPD level can be stated. However, significant effects of $\pm 1-2$ mm from AC to AC exist. The three ACS having changed their parameters (crop. Table 1) are extracted in the separate graph at the bottom. Only a slight indication for a bias shift of JPL is indicated at week 920. An more interesting effect can be noticed in the biases of CODE and GFZ. CODE has a large jump at week 926 where changes both from Saastamionen to Niell mapping function and from 20 to 10 degree cutoff angle were introduced (with elevation dependent weighting). Three weeks later GFZ also switches to Niell mapping function, leaving the elevation cutoff angle at 20 degrees. The resulting jump in the GFZ series brings the biases of CODE and GFZ to the same level again, but now 2 mm higher than before week 926. From this one may conclude that the influence of the mapping function on the bias seems to be higher than the influence of the elevation cutoff angle.

In Fig.6 the biases for all weeks and each AC for selected sites are shown. In the top typical examples for fiducial (or other well determined) sites are displayed. The biases are very small, and the repeatability is at the 2 mm ZPD level. Larger systematic effects can be found for some sites as given in the bottom. Here systematic effects of about ± 6 mm exist with single peak to peak differences in the weekly biases of 20 mm. The bias differences could be reduced by taking into account the well-known correlation between the station height and the ZPD estimates. This works rather good for some sites (see Fig. 7), but not for all. However, such a procedure will be not recommended because any corrections to the estimates are dangerous. It is better to reduce the scattering in the determined station heights. One step in this direction will be the enlarged set of 30 to 50 fiducials, which will be constrained to a certain extent by all the ACS. The introduction of a smaller elevation cutoff angle may also help to reduce the bias.

CONVERSION INTO PRECIPITABLE WATER VAPOR

The ZPD estimate must be converted into PWV. The directly estimated ZPD values are of interest for some special applications only, such as atmospheric corrections for collocated VLBI or two-color SLR instruments.

For the conversion meteorological surface measurements are needed. At the moment 19 sites report regularly their met data to the global data centers. Ten further sites have announced the installation of met packages, but the data are not yet available. The met data must be of high precision (1 mbar corresponds to 0.35 mm in PWV) and reliability (continuous time series). In Fig. 8 all sites with met sensors available in 1997 are given. For some sites too many missing days or larger gaps must be stated. In those cases no meaningful series of PWV could be produced. Unfortunately, only 10 to 15 reliable sites with met sensors exist at the moment (a small percentage of all analyzed sites).

The GPS derived PWV estimates can be compared with WVR measurements to get a measure for the absolute accuracy. Only at POTS measurements of a collocated WVR were available. A WVR-1100 of Radiometries Corporation is operated by Meteorological Observatory Potsdam of the German Weather Service, and is located 400m apart from the GPS receiver. In Fig. 10 the time series from WVR, CODE and

GFZ are extracted for 90 days at the end of 1997. Due to a lot of rainy days the WVR series has many gaps. The agreement of the GPS results (both CODE and GFZ) with the WVR is at the 1 mm level (**Fig. 9**). The stddev of the difference approaches ± 0.5 mm, the bias has a level of ± 1 mm and shows some long-periodic behavior for both GPS results. The difference between the two GPS solutions is smaller than their differences to the WVR measurements, The changes in the parameters of CODE (day 926.0 is 97/278) and GFZ (97/299) have obviously not caused any significant changes, neither in the difference between both solutions nor in their differences to WVR, although with 10 and 20 degrees rather different elevation cutoff angles are used.

SUMMARY

During the one year experiment all components involved in the combination have performed well and timely. Some small inconsistencies concerning the description of the station coordinate solutions must be avoided in future. It would be also more effective if the planned short **SINEX** version, containing no matrices, could be introduced soon.

The ZPD estimates have a high quality for all the weeks. The consistency is at the 4 to 5 mm level both for the bias and for the **stddev**. For sites in the equatorial region the quality is not as good - by a factor of 1.5 to 2 worse. The bias is highly correlated with the station height. A lower elevation cutoff angle and the enlarged set of **fiducials** can help to reduce the bias by smaller scattering in the daily station height solutions.

The importance of the IGS contribution to climate research will not only depend on the quality of the ZPD estimates but also on the number of sites which could be equipped with met packages. The number of instruments available now is not sufficient.

To get a better insight into the behavior of the bias more collocated WVR should be made available, either at existing IGS sites or at **non-IGS** sites which then should be analyzed by all **IGS ACS** for some test periods.

REFERENCES

- Gendt, G., 1996a, IGS Tropospheric Estimations - Summary, in *Proceedings Analysis Center Workshop Silver Spring 1996*, Eds. R E Neilan, P A Van Scoy, J F Zumberge, Pasadena, CA U. S. A., pp. 147-149
- Gendt, G., 1996b, Comparison of IGS Tropospheric Estimations, in *Proceedings Analysis Center Workshop Silver Spring 1996*, Eds. R E Neilan, P A Van Scoy, J F Zumberge, Pasadena, CA U.S. A., pp. 151-163
- Gendt, G., 1997, IGS Combination of Tropospheric Estimates (Status Report), in *Proceedings Analysis Center Workshop Pasadena 1997*, in press

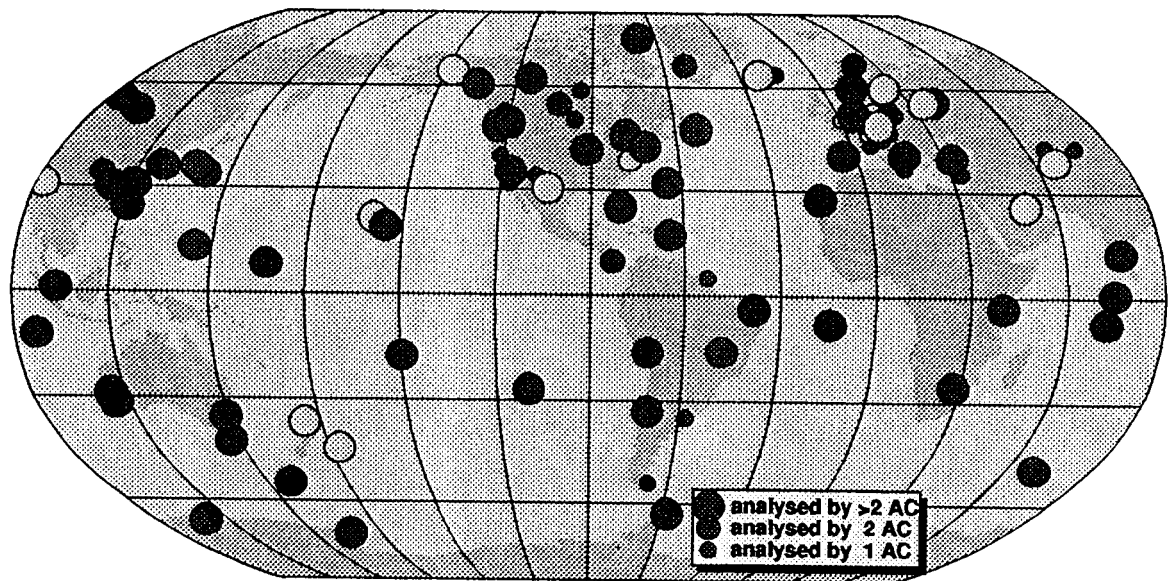


Fig. 1. IGS network with tropospheric estimates (Sites in gray have meteorological packages)

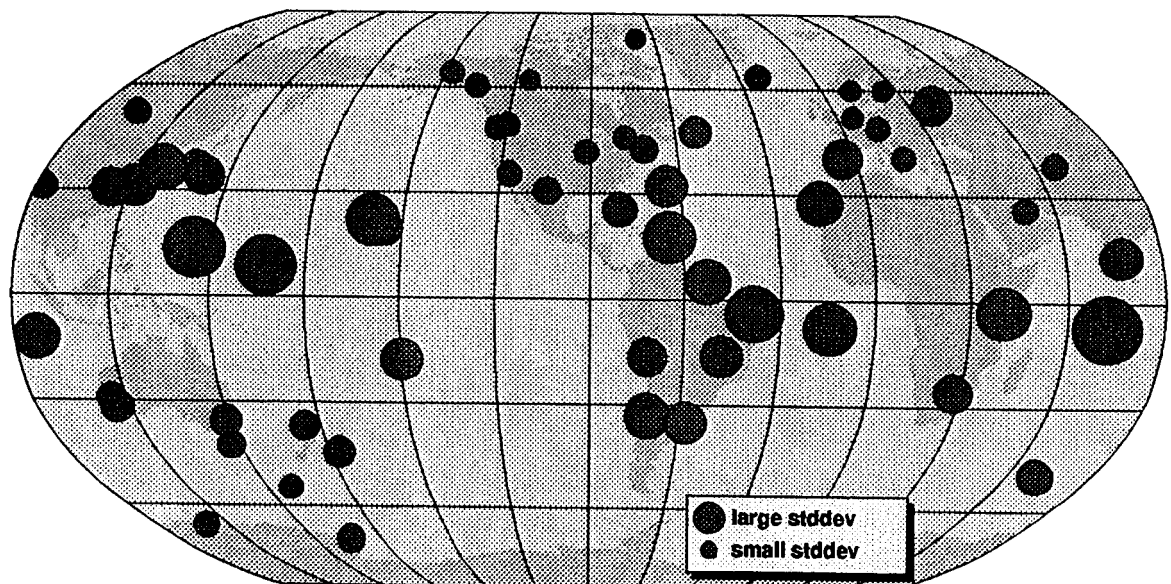


Fig.2. Geographical distribution for mean standard deviation of ZPD estimates

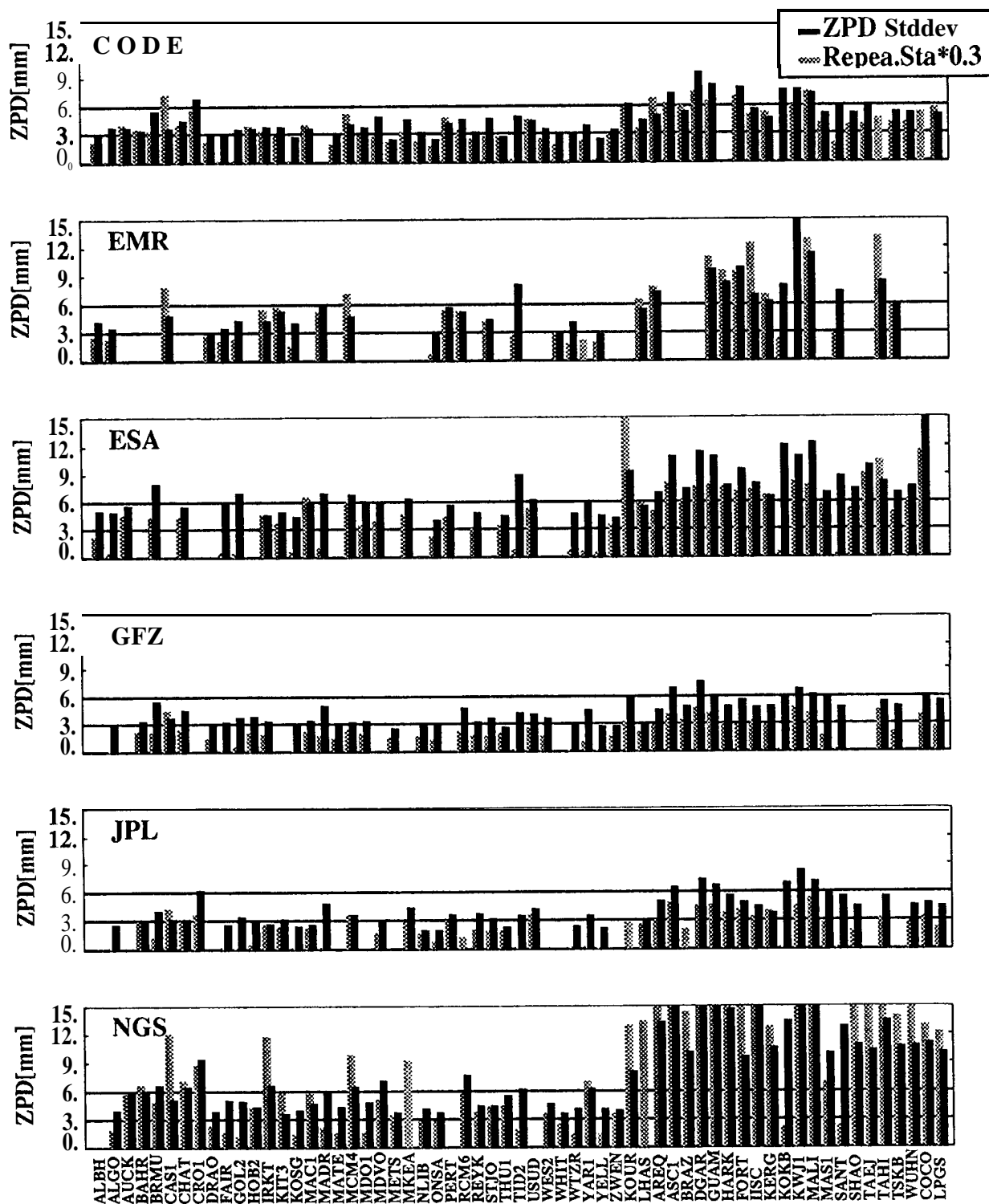


Fig.3. Difference between AC ZPD and IGSC Combined ZPD. Mean of weekly standard deviation for individual sites. Repeatability of station solutions (scaled by correlation factor 0.3) are given for comparison.

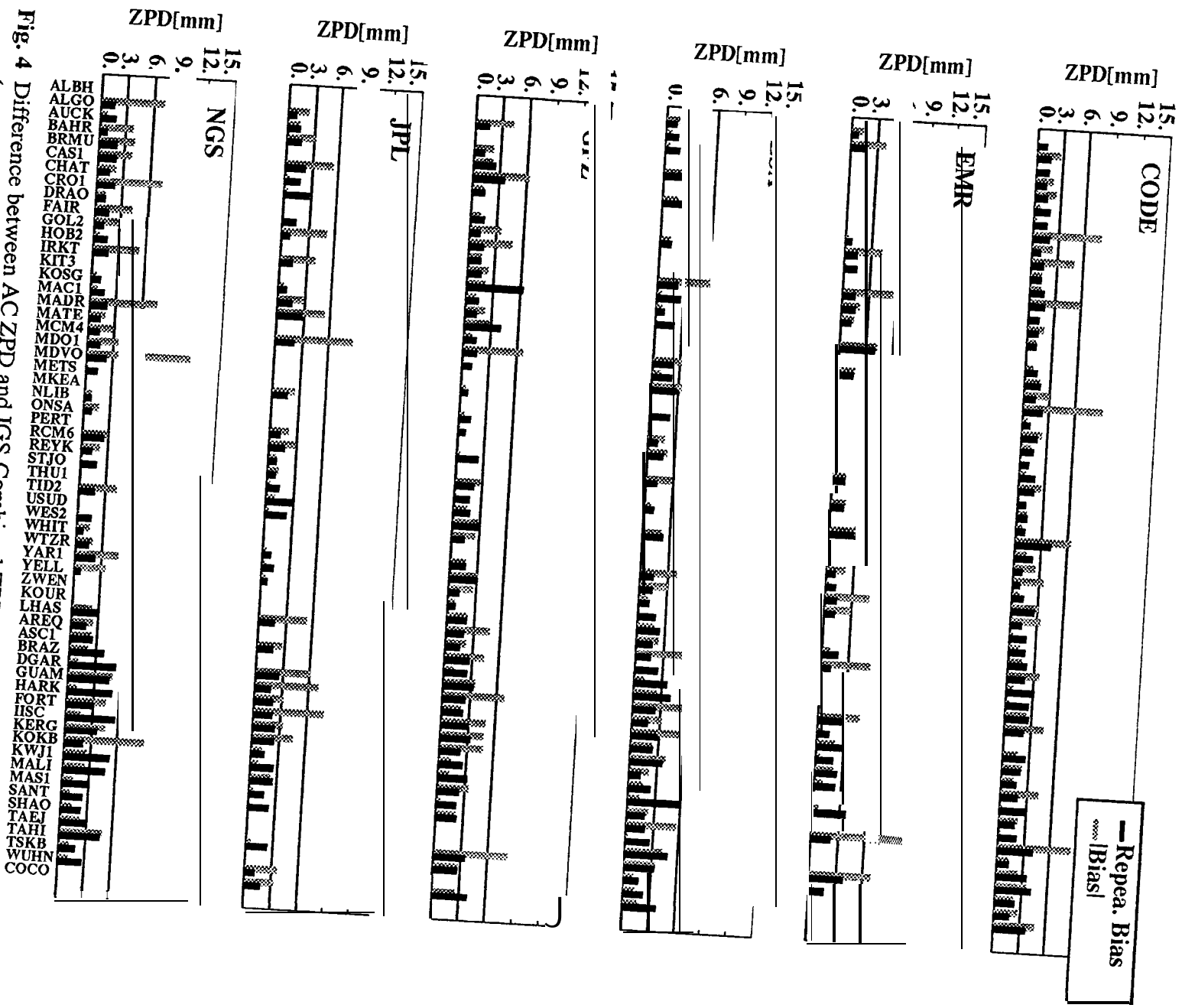


Fig. 4 Difference between AC ZPD and IGS Combined ZPD. Mean of weekly bias (magnitude of bias) and bias repeatability from week to week

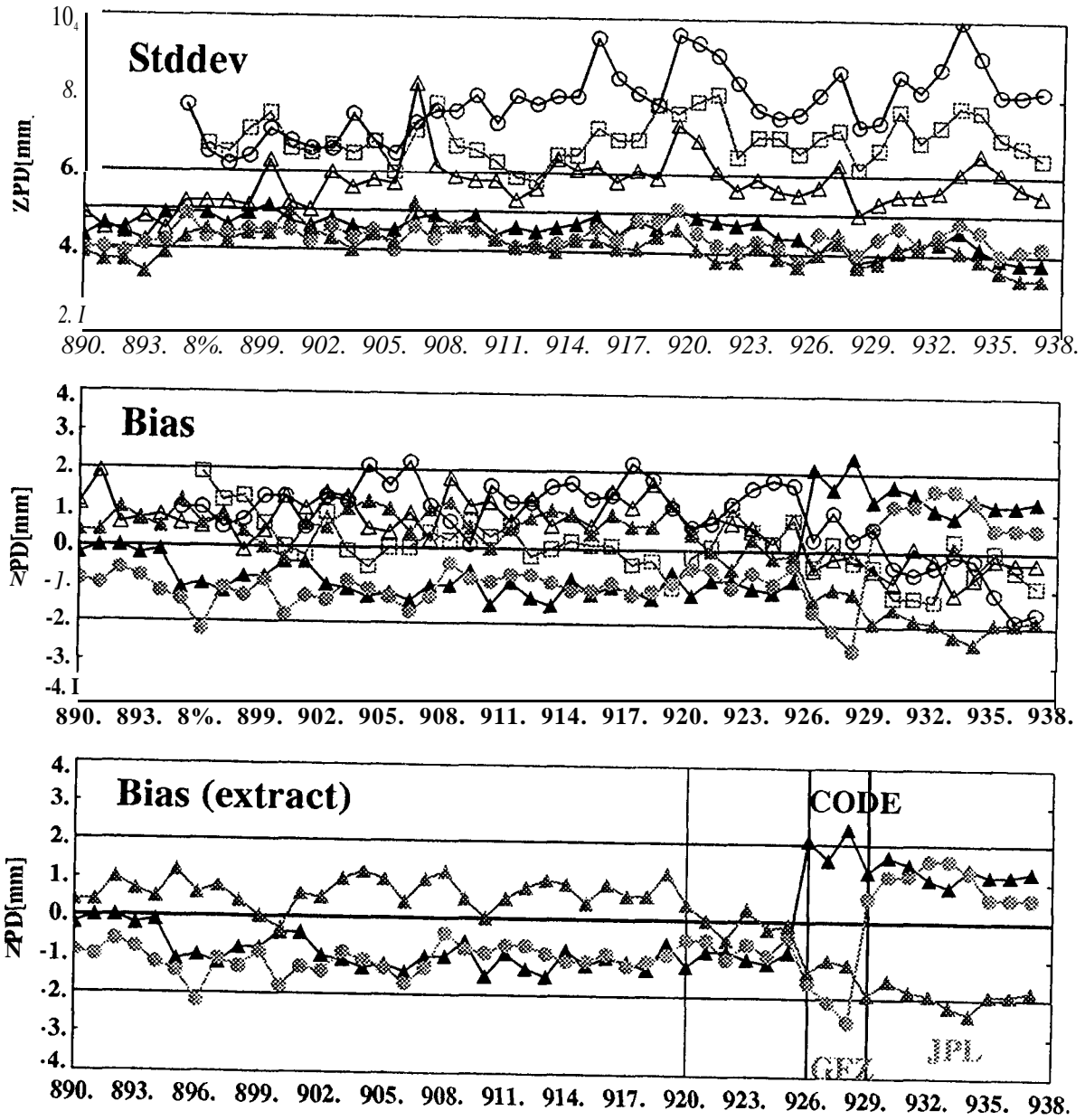


Fig. 5. Difference between AC ZPD and IGS Combined ZPD.
 Mean values (mean over all sites) per week and Analysis Center

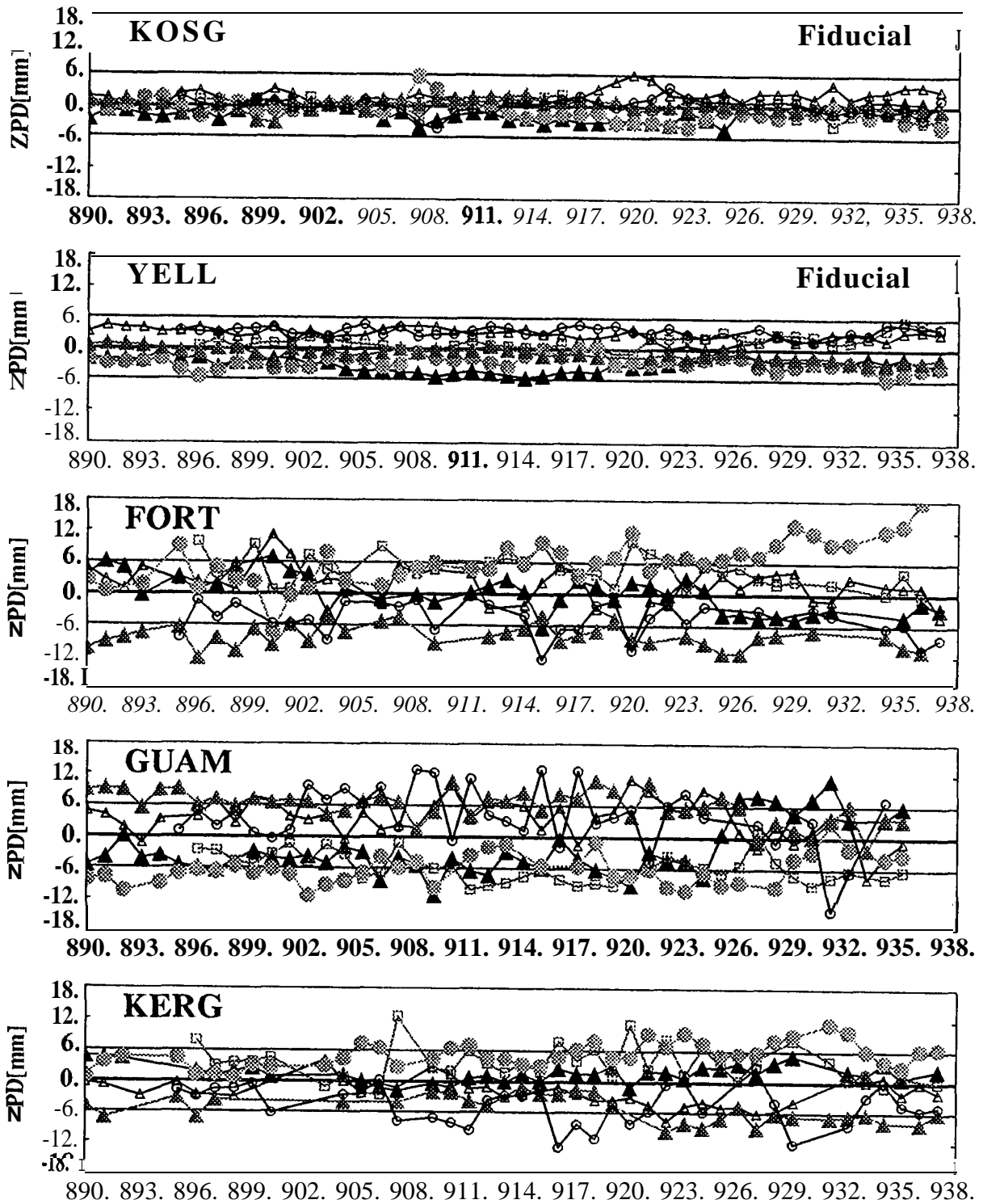


Fig. 6. Difference between AC ZPD and IGS Combined ZPD.
 Mean bias per week and Analysis Center

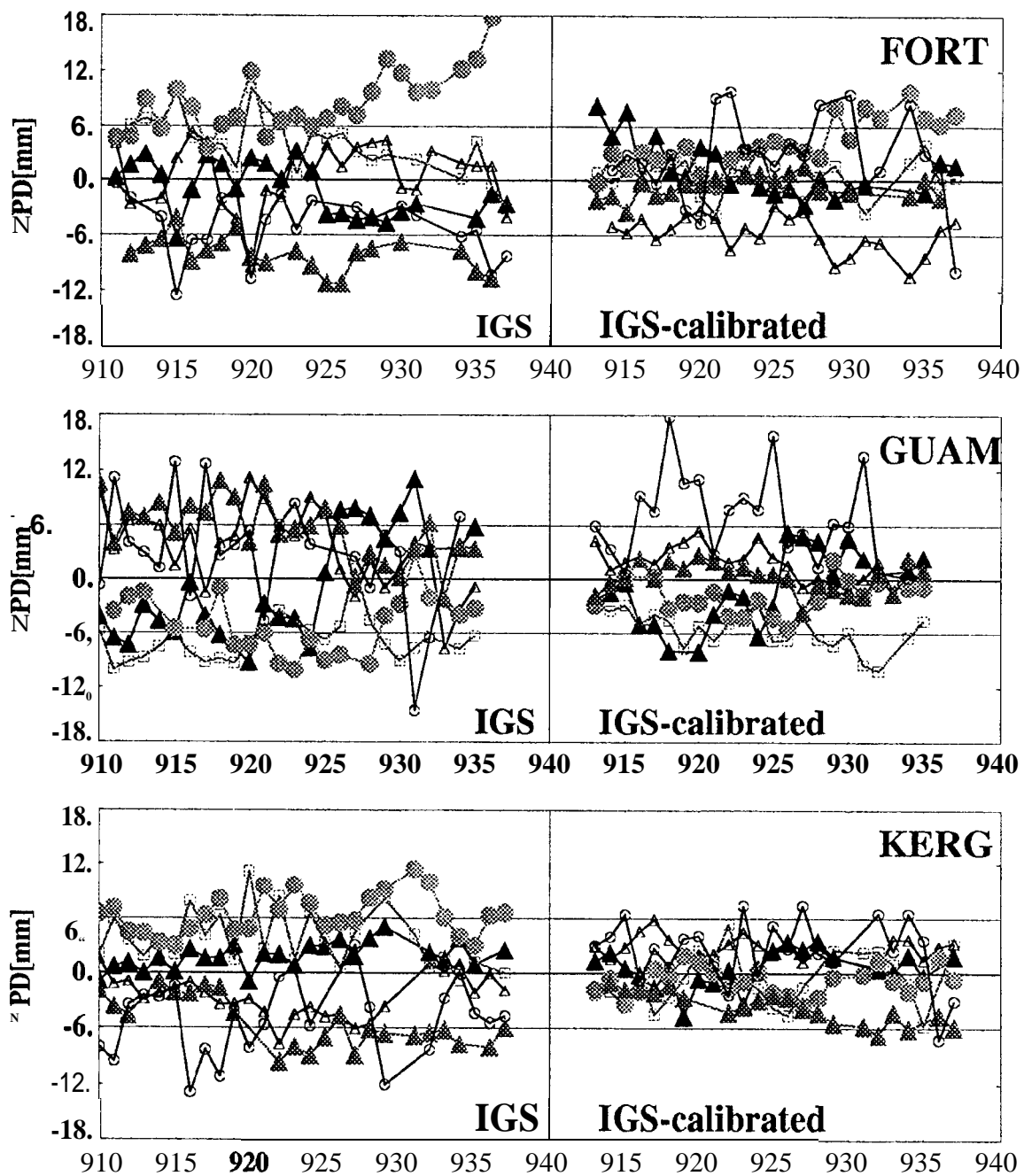


Fig. 7. Difference between AC ZPD and IGS Combined ZPD. Mean bias per week and Analysis Center. Left: Values from Fig. 6. Right: Results with bias corrections by correlation between station height and ZPD.

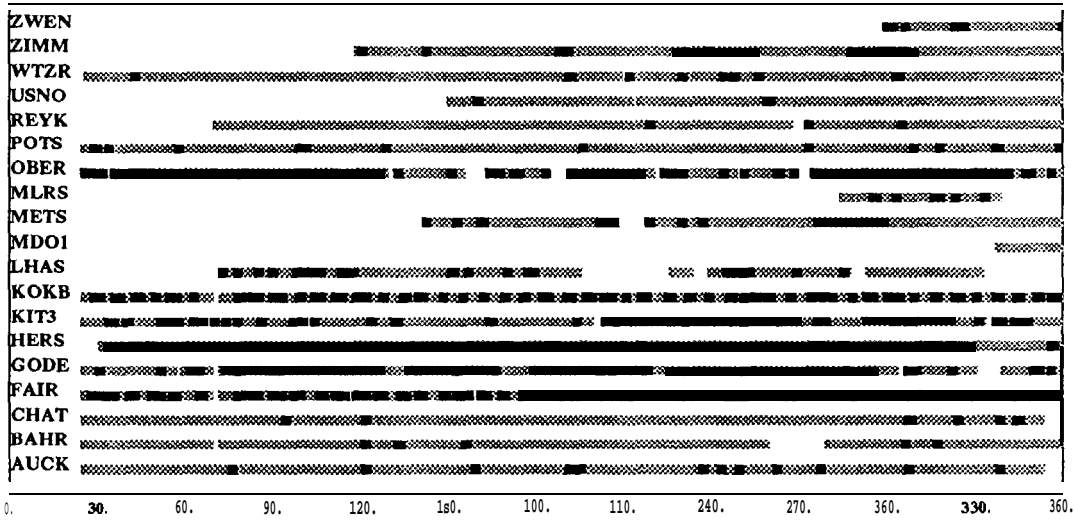


Fig.8. Statistics for existing RINEX Met Files at CDDIS.
Days with gaps >2 hours are marked with ■ .

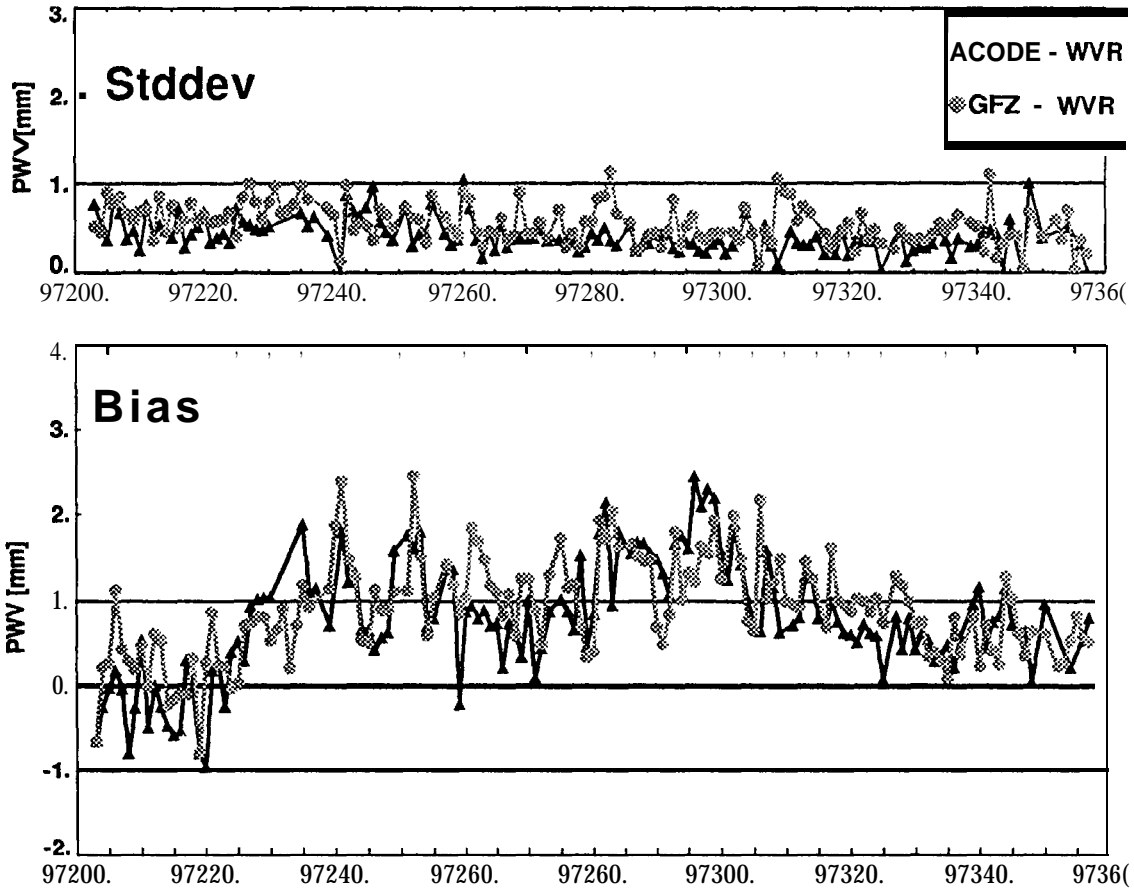


Fig. 9. Comparison of PWV estimates from GPS and WVR at POTS.
GPS results are from IGS site POTS (CODE and GFZ solutions) and WVR data are from the Meteorological Observatory Potsdam, 400m apart from GPS receiver

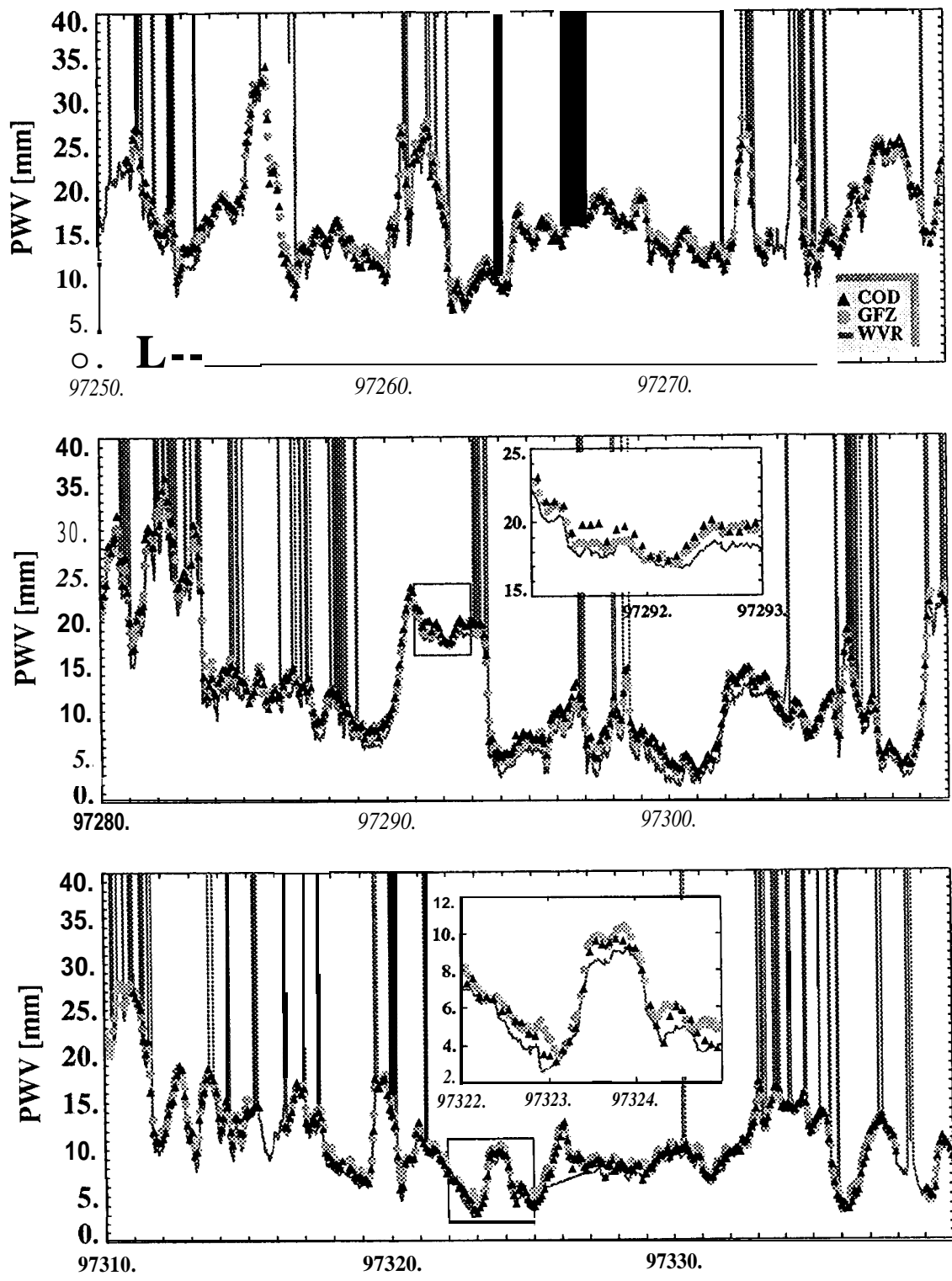


Fig.10. Comparison of PWV estimates from GPS and WVR at POTS.
 GPS results are from IGS site POTS (CODE and GFZ solutions) and WVR data are from the Meteorological Observatory Potsdam, 400m apart from GPS receiver